CHAEHO PAK
Application Of Electronic Structure Theory: Structures and Energetics Of Some Inorganic And Biochemical Molecules
(Under the direction of HENRY F. SCHAEFER III)

In recent years, density functional theory (DFT) has emerged as one of the most powerful tools to study the interested chemical systems due to their relatively low computational cost and high-quality accuracy. As part of the ongoing electron affinity studies at CCQC, I have examined molecules that are important in atmospheric chemistry, semiconductor industry, and biochemistry. For systems where many of the experimental electron affinities are available, particularly for silicon hydrides, the DFT B3LYP functional predicts the adiabatic electron affinity within an absolute error of only 0.06 eV. For systems where experimental electron affinities are not available due to their known volatile chemical nature, for example bromine fluorides, we predict the possible isomers of the neutral and the anion and their energy differences. We have also examined neutral and anion species of the amino acids arginine and glutamine due to their possible importance in biochemical recognition processes.

INDEX WORDS: quantum chemistry, *ab initio,* dft, bromine, silicon, arginine, glutamine, R, Q.

APPLICATION OF ELECTRONIC STRUCTURE THEORY: STRUCTURES AND ENERGETICS OF SOME INORGANIC AND BIOCHEMICAL MOLECULES

by

CHAEHO PAK

B.S., University of Washington, 1998

A Dissertation Submitted to the Graduate Faculty
of The University of Georgia in Partial Fulfillment
of the
Requirements for the Degree

DOCTOR OF PHILOSOPHY

ATHENS, GEORGIA

2002

APPLICATION OF ELECTRONIC STRUCTURE THEORY: STRUCTURES AND ENERGETICS OF SOME INORGANIC AND BIOCHEMICAL MOLECULES

by

CHAEHO PAK

Approved:

Major Professor: Henry F. Schaefer III

Committee: Paul von Rague Schleyer
Nigel G. Adams
Lucia M Babcock
Robert S. Phillips

Electronic Version Approved:

Gordhan L. Patel
Dean of the Graduate School
The University of Georgia
May 2002

To my parents,

ACKNOWLEDGEMENTS

Although it is an impossible task for me to thank everyone and elucidate every detail, my desire to do so is very strong. This makes this section, the most difficult part of the whole thesis. However, I will do my best to thank everyone, and I truly apologize to those who are not mentioned here explicitly.

When I look back my life, I have met many wonderful people who gave me much love, support, care and contributed to my life in many different ways. When I first came to America as a high school boy, my English teacher told us to write a diary in English. Through this diary I was able to communicate with her very well even though I probably knew less than 50 English words. She gave me much encouragement, patient, care, and education.

These qualities are shared by my adviser Professor Schaefer, and Dr. Yamaguchi, Dr. Xie, Dr. Allen and Professor Schleyer, all of whom have taught me a great deal either directly or indirectly. Their contribution to my scientific career is simply priceless.

I must also thank my sister for initiating my educational life, and my parents and fiance for their love and support. I am also grateful to all of the old, and current CCQC members for making CCQC a truly enjoyable work place, and to Mrs. Linda. and Dr. Richard for their unseen hard work, and to my committee members for going through this with me. Without all these people, both those I mentioned and those I did not, my life would have been very different. I sincerely thank everyone for their love and support.

TABLE OF CONTENTS

Page

CHAPTER 1

INTRODUCTION

When I was an undergraduate freshman, my biology teacher told us “if you want to know the meaning of life, know protein folding.”[1] His statement was so strong and convincing, I had to learn more about protein folding. I had to see what he meant. After all, it made sense. Every atom and molecule in nature follows certain rules and somehow with some magic, we exist. To understand perhaps God’s magic and certain rules in nature, we are constantly working and seeking for the truth. More than any other subject, quantum chemistry intrigued me the most because it seemed to deal with the basis of our nature, the natural rules.

There are many ways to appreciate our nature from philosophy to physics, psychology to biology, and sociology to chemistry. Although integration of all these subjects is essential in understanding many of the interesting problems, I choose Computational Quantum Chemistry because of its versatility in application to different molecular systems. As 1966 Nobel Prize winner R.S. Mulliken states, "the era of computing chemists, when hundreds if not thousands of chemists will go to the computing machines instead of the laboratory for increasingly many facets of information is already at hand." Computational Quantum Chemistry has emerged as one of the most powerful and essential tools in the chemical industry today.

In Computational Chemistry, there are many different ways to approach the chemical or biological systems depending on the size of the molecule and the accuracy desired. For example, one can calculate the electronic energy of the hydrogen atom by hand, whereas it becomes almost impossible for atoms bigger than hydrogen. This is where computers come in handy. Due to vast developments in the computer industry, it is an easy task for a computational chemist to compute the electronic energy of a molecule like water, in a split second. However, as the size of the molecule becomes larger, the computation becomes very complex, and therefore time consuming and possibly less accurate. For this reason, semi-empirical and empirical methods are used to study chemical and biological systems of interest.

Unlike *ab-initio* methods, empirical methods do not use the electronic Hamiltonian or wave functions. Instead they treat atoms and molecules as balls and springs and use algebraic equations with certain experimental or *ab-initio* parameters to describe the molecular systems. Therefore, they are not quantum-mechanical methods, and cannot accurately predict electronic energy, structures, and most of the spectroscopic parameters. However, they can be used as preliminary work for further more accurate studies, or a means to study large molecular systems that *ab-initio* methods cannot study. Semi-empirical methods can also study large molecules due to their simplified Hamilitonian.

In order to find accurate electronic energies, structures, and many of the spectroscopic parameters, one needs to employ *ab-initio* methods, which use correct Hamiltonians and wave functions. There are many different *ab-initio* methods available today: Configuration Interaction (CI), Coupled-Cluster (CC) methods to name a few.

Since all these theoretical methods treat electrons explicitly, they are said to include a correlational effect or energy. Besides the inclusion of correlational effect, one needs to provide sufficient number of basis functions (mathematical description of different molecular orbitals) in order to find accurate electronic structure or to describe the molecular systems better. In theory, when we have an infinite basis set with inclusion of full correlation effects, one can obtain the "exact" solution. However, this is not possible, as we cannot provide the infinite number of basis functions for any molecules.

Although *ab-initio* methods can give very accurate results, they can be applied only to small molecules, and they are very costly. For example, SCF roughly converges to N^4, CISD to N^6, and CCSD(T) to N^7, where N is the basis set size[2]. For this reason, Density Functional Theory (DFT) has been introduced, with its convergence roughly equal to N^3. DFT was first proposed by Kohn-Sham in 1965, however, it was not taken seriously until the mid 1980s because of its unexplainable functional. Due to this reason, DFT results cannot be improved systematically, as is the case for conventional *ab-initio* methods. However, current DFT methods can often reach "chemical accuracy," and can treat close to 30 atoms depending on the size of the basis sets. In recent years, we have studied more than 150 atoms and molecules using DFT at DZP^{++} basis sets, and found that DFT is a very reliable and effective method in studying many of the inorganic and organic molecules. As part of the ongoing electron affinity studies at CCQC, I have examined molecules that are important in atmosphere chemistry (Chapter 2), semiconductor industry (Chapter 3), and biochemistry (Chapter 4).

In preceding studies, all of the electron affinities are evaluated as differences in total energies in the following manner: the classical adiabatic electron affinities are determined by,

$$EA_{ad} = E_{(optimized\ neutral)} - E_{(optimized\ anion)}$$

zero-point corrected adiabatic electron affinities are determined by,

$$EA_{zero} = E_{(zero\text{-}point\ corrected\ neutral)} - E_{(zero\text{-}point\ corrected\ anion)}$$

the vertical electron affinities by,

$$EA_{vert} = E_{(optimized\ neutral)} - E_{(anion\ at\ neutral\ equilibrium\ geometry)}$$

and the vertical detachment energies by,

$$VDE = E_{(neutral\ at\ anion\ equilibrium\ geometry)} - E_{(optimized\ anion)}$$

Figure 1.1.

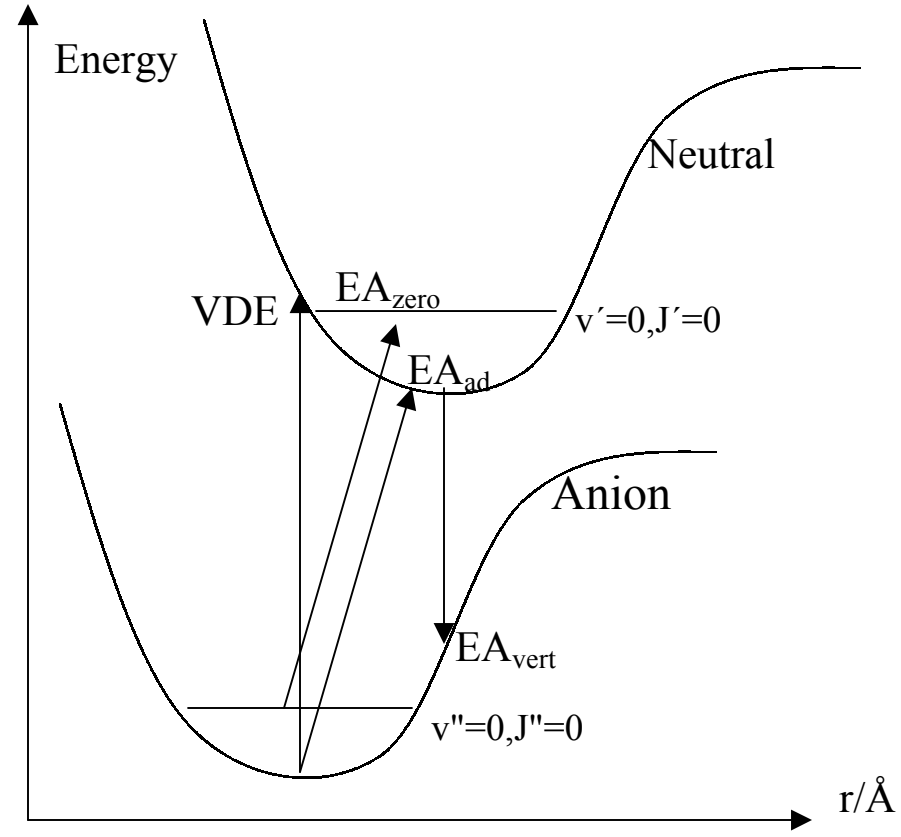

REFERENCES:

1. Biology 201 lecture from University of Washington.

2. DFT lecture from Dr. Yaoming Xie.

3. Rienstra-Kiracofe, J.C.; Tschumper, G.S.; Schaefer, H.F.; Nandi, S.; Ellison, G.B., *Chem. Rev*., **2002**, 102, 231.

CHAPTER 2

ELECTRON AFFINITIES OF BROMINE FLUORIDES, BrF_n (n = 1-7)[1]

[1]Pak, C.H., Y. Xie, T. J. Van Huis and H. F. Schaefer, J. Amer. Chem. Soc., 120, 11115 (1998). Reproduced in part with permission from American Chemical Society

Abstract

The molecular structures, electron affinities, and dissociation energies of the BrF_n/BrF_n^- (n = 1-7) molecules have been examined using hybrid Hartree-Fock/density functional theory (DFT). The three different types of electron affinities reported in this work are the adiabatic electron affinity (EA_{ad}), the vertical electron affinity (EA_{vert}), and the vertical detachment energy (VDE). The first Br-F dissociation energies of the BrF_n and BrF_n^- species have also been reported. The basis set used in this work is of double-ζ plus polarization quality with additional s- and p-type diffuse functions, and is denoted as DZP^{++}. Four different density functionals were used in this work. Among these, the best for predicting molecular structures and energies was found to be BHLYP, while other methods generally overestimated bond lengths. The most reliable adiabatic electron affinities, obtained at the DZP^{++} BHLYP level of theory, are 3.41 (Br), 2.64 (BrF), 4.78 (BrF_2), 3.77 (BrF_3), 5.58 (BrF_4), 4.24 (BrF_5), and 5.59 eV (BrF_6). The electron affinity of the Br atom predicted by this work is in good agreement with the experimental result, but not one of the molecular electron affinities (BrF_n, n = 1-7) is known. The neutral BrF_n bond distances range from 1.70 to 1.83 Å. However, the diatomic BrF^- distance and the axial Br-F distances in $BrF_3^-$and BrF_5^- are much longer, 2.25-2.30 Å, suggesting that the bonding in these three anions is quite different from that of their neutral counterparts.

Introduction

The BrF_n/BrF_n^- (n = 1-7) series of molecules, members of the interhalogen family, are all rather reactive. The bromine fluorides react vigorously with both organic and inorganic molecules. They are also very corrosive, oxidizing substances that have a

tendency to attack most other elements and hydrolyze rapidly.[1,2] While stable in comparison to the radical members of this series, the explosive reactions of (closed shell) BrF_3 and BrF_5 have made studies of even these species difficult.[3,4] Despite their violent chemical properties, these molecules have been studied extensively in connection with atmospheric chemistry;[5,6] bromine-containing molecules that are released to the atmosphere, primarily by fire extinguishers, may play a role in the depletion of the ozone layer.[7] Nevertheless, there seem to be no experimental or theoretical data for the electron affinities (EAs), a fundamental property, of the bromine fluorides. The possibility that the bromine fluoride anions could play a significant role in atmospheric chemistry makes their electron affinities attractive research targets.

In predicting molecular energies and structures, there are many theoretical approaches, but considering both reliability and computational expense, gradient corrected density functional theory (DFT) has been shown to be effective for many related inorganic species such as the SF_n/SF_n^-, PF_n/PF_n^-, ClF_n/ClF_n^-, SiF_n/SiF_n^-, and $C_2F_n/C_2F_n^-$ molecules.[8-12] In addition, while the prediction of an electron affinity is generally difficult due to being the result of a small difference between two very large energies, these previous works have shown that DFT can be a dependable source for EA predictions. For a recent systematic study of DFT with regards to EA determinations, one is referred to the 1996 work of Galbraith and Schaefer.[8b] The main objective of this study, therefore, is to provide theoretical data for the electron affinities of the bromine fluorides.

Theoretical Methods

The four different density functional or hybrid Hartree-Fock/density functional forms used are Becke's 1988 exchange functional[13] with Lee, Yang, and Parr's correlation functional[14] (BLYP), Becke's half-and-half exchange functional[15] with the LYP correlation functional (BHLYP), Becke's three-parameter semiempirical exchange functional[16] with the LYP correlation functional (B3LYP), and Becke's 1988 exchange functional with the Perdew correlation functional[17] (BP86). A restricted Hartree-Fock (RHF) reference was used for all closed shell systems, while an unrestricted (UHF) wave function was employed for open-shell species. All the electron affinities and molecular structures have been determined with the Gaussian 94[18] (for BLYP, B3LYP, and BP86) and the Gaussian 92[19] (for BHLYP) program suites. The default integration grid of Gaussian 94 was also applied in the Gaussian 92 work. The integrals that are evaluated in this study should be accurate to 1×10^{-5} E_h, the density was converged to 1×10^{-8} E_h, and Cartesian gradients were converged to at least 10^{-6} au.

The DZP^{++} basis set for bromine used herein was constructed with Ahlrichs' standard double-ζ *spd* set[20] with the addition of one set of *d*-like polarization functions [α_d(Br) = 0.389][20] as well as a single set of diffuse *s* [α_s(Br) = 0.0469096] and *p* [α_p(Br) = 0.0465342] functions. The corresponding basis on fluorine was comprised of the standard Huzinage-Dunning-Hay[21] double-ζ *sp* set with one set of *d* polarization functions [α_d(F) = 1.000] as well as a set of diffuse *s* [α_s(F) = 0.1049] and *p* [α_p(F) = 0.0826] functions. The diffuse function orbital exponents were determined in an "even tempered sense" as a mathematical extension of the primitive set, according to the formula of Lee and

Schaefer.[22] Pure angular momentum *d* functions were used throughout. The final contraction scheme for this basis is Br (15s12p6d/9s7p3d) and F (10s6p1d/5s3p1d).

The geometries reported in Figures 1-6 were found to be energy minima after determining the harmonic vibrational frequencies at the corresponding stationary point structures with the DZP^{++} B3LYP level of theory. Zero-point vibrational energies (ZPVE) evaluated at this level are presented in Table 1. The ZPVE differences between BrF_n and BrF_n^- (n = 1-6) are quite small, in the range of 0.003 to 0.097 eV. These differences could be used as a correction to the adiabatic electron affinities.

Results and Discussion

A. Br and Br^-.

The electron affinities of the $^2P_{3/2}$ state of the Br atom at various levels of theory, as well as experimental electron affinity data, are reported in Table 2. Values are determined from total energies of the Br atom and the Br^- ion. All four functionals predict the electron affinity of the Br atom to within 0.32 eV, and all values are larger than the experimental value of 3.36 eV given by Blondel, Cacciani, Delsart, and Trainham's laser-photodetachment threshold spectroscopy study of the Br anion.[23] The greatest correlation with experiment is achieved by DZP^{++} BHLYP, whose EA value is only 0.05 eV larger than experiment. The fact that BHLYP gives the best predictions for electron affinities was also noted in our earlier works on the second-row fluorides.[8-12] Since no experimental data are available for the BrF_n electron affinities, the comparison of the predicted EA at different levels of theory for the Br atom with experiment should be a

dependable calibrator. In the following discussions for the BrF_n molecules, we will mainly use the DZP^{++} BHLYP results unless otherwise indicated.

TABLE 2.1: The Electron Affinity of Br in eV (kcal/mol in parentheses).

Method	EA
BHLYP	3.41(78.7)
B3LYP	3.60(83.1)
BP86	3.68(85.0)
BLYP	3.46(79.9)
Expt.	3.36358 ± 0.00004

B. BrF and BrF^-.

Our optimized geometries for the ground $^1\Sigma^+$ state of BrF and the ground $^2\Sigma^+$ state of BrF^- are shown in Figure 1. All theoretical bond distances are longer than the experimental value for the neutral. The prediction closest to the experimental r_e of 1.759 Å obtained from Willis and Clark's microwave data[24a] for BrF came from the DZP^{++} BHLYP method, which gave a bond length of 1.756 Å. The bond lengths predicted by other functionals were overestimated by as much as 0.06 Å. Here we note the general trend for bond lengths yielded for the bromine fluorides as BLYP > BP86 > B3LYP > BHLYP. For the BrF^- ion, the DZP^{++} BHLYP bond length is 2.300 Å, longer by roughly 0.55 Å than that of the neutral species. We will discuss this large structural difference between neutral and anion later.

Table 3 contains the electron affinities for the adiabatic and vertical processes, as well as the vertical detachment energies for the BrF, BrF_2, BrF_3, BrF_4, BrF_5, and BrF_6 species. Note that the adiabatic values are not corrected for zero-point vibrational energy. Relying upon BHLYP, we report 2.64 eV as the most reliable adiabatic electron affinity

for BrF based on our data for the EA of the Br atom and previous work[8,10] on the sulfur and chlorine fluorides. One may note that the values for EA_{ad}, EA_{vert}, and VDE are significantly different due to the large bond length difference between the neutral and the anion (vide infra). The range for EA_{vert} is from 1.06 to 1.45 eV and the range for VDE is from 4.24 to 4.48 eV. Furthermore, from the positive values for EA_{vert} and VDE, one may readily see that the anion is thermodynamically stable.

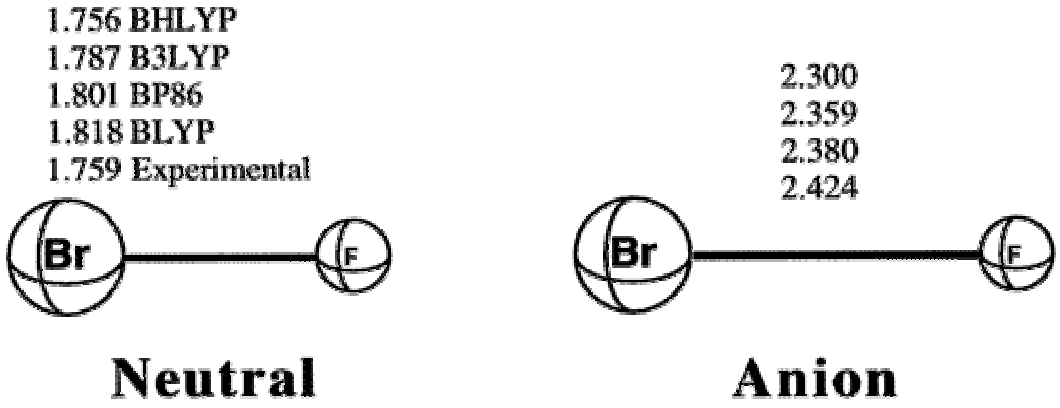

Figure 1 The molecular geometries of the $X^1\Sigma^+$ state of BrF and the $X^2\Sigma^+$ state of the anion, BrF^-. All bond lengths are in Å and all results were obtained with the DZP^{++} basis set.

C. BrF_2 and BrF_2^-.

The equilibrium geometries of the BrF_2 ground state ($^2A_1$) and the BrF_2^- ground state ($^1\Sigma_u^+$) are displayed in Figure 2. The BrF_2 radical has a bent structure with a bond angle of 154-169° as predicted by the four different functionals. The neutral Br-F bond length is in the range from 1.826 to 1.906 Å. As was the case for BrF, the DZP^{++} BHLYP method gives the shortest bond length for BrF_2. BrF_2^- is linear ($D_{\infty h}$), with Br-F bond distances predicted from 1.959 to 2.045 Å. These distances are only about 0.1 Å longer than their neutral counterparts, which is understandable as the BrF_2 radical's singly

occupied molecular orbital (SOMO) is a π-type orbital, thus having little overall effect on the bond length (vide infra).

The theoretical EA_{ad}, EA_{vert}, and VDE are listed in Table 3. The predicted range of EA_{ad} is from 4.34 to 4.78 eV, among which the DZP^{++} BHLYP method predicts the largest value (4.78 eV). The range of EA_{vert} is from 3.83 to 4.11 eV and the range of VDE is from 4.60 to 6.59 eV. Note that because the difference in the geometries of the neutral and the anion are not as great as that for BrF, there are smaller energy gaps between EA_{ad}, EA_{vert}, and VDE.

The theoretical EA_{ad}, EA_{vert}, and VDE are listed in Table 3. The predicted range of EA_{ad} is from 4.34 to 4.78 eV, among which the DZP^{++} BHLYP method predicts the largest value (4.78 eV). The range of EA_{vert} is from 3.83 to 4.11 eV and the range of VDE is from 4.60 to 6.59 eV. Note that because the difference in the geometries of the neutral and the anion are not as great as that for BrF, there are smaller energy gaps between EA_{ad}, EA_{vert}, and VDE.

D. BrF_3 and BrF_3^-.

The C_{2v} symmetry equilibrium geometries of the $\tilde{X}^1A_1$ state of BrF_3 and the $\tilde{X}^2A_1$ state of BrF_3^- are shown in Figure 3. The bond length predictions of the four functionals follow the same trends as above. Those predicted by the BHLYP method were again the closest to the experimental values. The gas-phase structure of BrF_3 was reported by Magnuson as 1.810 and 1.721 Å for the Br-F_{eq} and Br-F_{ax} bond distances and 86.2° for the F-Br-F bond angle, respectively,[25] while the DZP^{++} BHLYP method predicts them as 1.808 Å, 1.720 Å, and 85.7°. All four theoretical methods do a reasonable job in

predicting the important difference between the equatorial and axial Br-F bond distances. Our BrF_3 structure is also in qualitative agreement with an earlier theoretical study that employed the MP2/6-311+G* method and took into account the effects of relativity.[26]

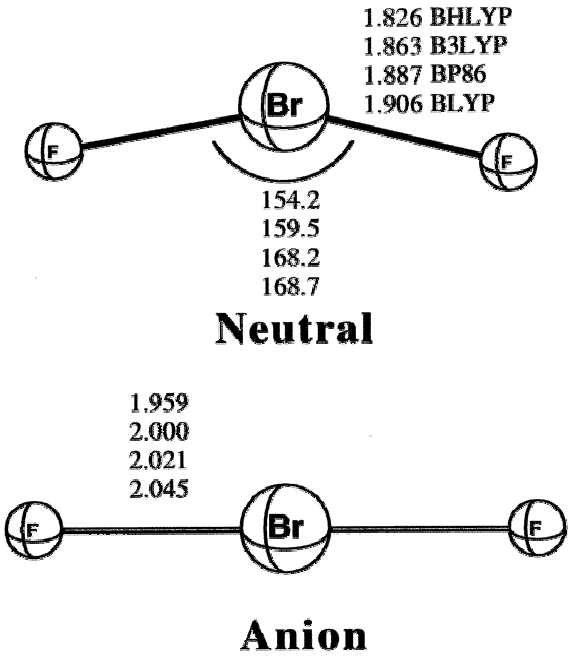

Figure 2 The molecular geometries of the $\tilde{X}^2A_1$ state of BrF_2 and the $\tilde{X}^1\Sigma_u^+$ state of the anion, BrF_2^-. Bond lengths and bond angles are in Å and deg, respectively. All results were obtained with the DZP^{++} basis set.

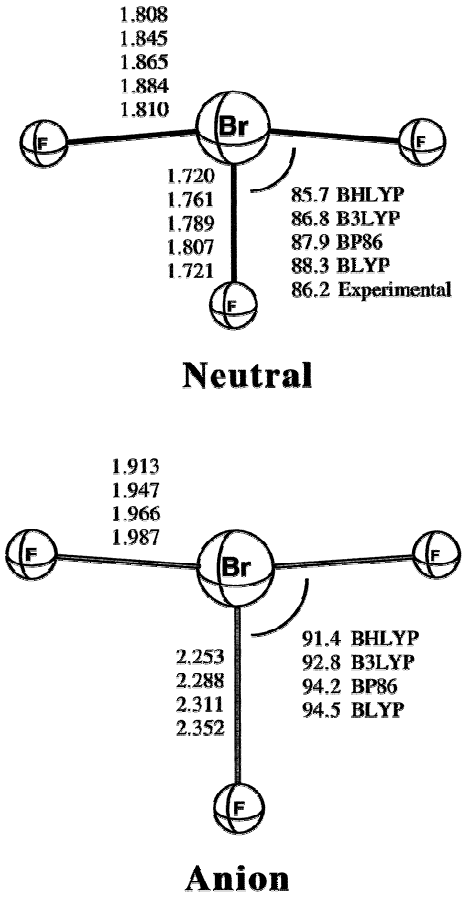

Figure 3 The molecular geometries of the $\tilde{X}^1A_1$ state of BrF_3 and the $\tilde{X}^2A_1$ state of the anion, BrF_3^-. Bond lengths and bond angles are in Å and deg, respectively. All results were obtained with the DZP^{++} basis set.

For the BrF_3^- ion, there are no experimental data with which to compare. The trend for the theoretical bond lengths is similar. The DZP^{++} BHLYP method predicts the geometrical parameters as 1.913 Å, 2.253 Å, and 91.4° for Br-F_{eq}, Br-F_{ax}, and ∠FBrF, respectively. Note that the Br-F_{ax} bond distance is nearly 0.5 Å longer than that of neutral BrF_3. Clearly the bonding in the radical anion, BrF_3^-, is quite different from that of the neutral. The reason for this will become clear in our discussion of the BrF_5 species below.

The most reliable adiabatic electron affinity is 3.77 eV from BHLYP. The substantial value of this EA is perhaps surprising given the fact that BrF_3 is a relatively

stable molecule, at least as far as bromine fluorides go. In previous work on the sulfur[8] analogues, for which many experimental EA values exist, it was found that DFT may slightly overestimate (<0.6 eV) the electron affinities of the larger species (SF_n; n = 5, 6); however the DZP^{++} BHLYP method provided excellent agreement for the n = 1-4 series and was usually within 0.2 eV of experiment. Therefore, the large EA_{ad} value for BrF_3 should be regarded as a dependable target for this molecule. The EA_{ad} values obtained for BrF_3 from the other functionals are in good agreement with BHLYP, showing deviations of about (or less than) 0.1 eV. The EA_{vert} range is from 1.78 to 2.30 eV, and the range for VDE is from 5.03 to 5.96 eV. Again, these large differences between EA_{ad}, EA_{vert}, and VDE are due to the large difference in geometry between BrF_3 and BrF_3^-.

E. BrF_4 and BrF_4^-.

The optimized C_{4v} geometry of the $\tilde{X}^2A_1$ state of BrF_4 and the D_{4h} symmetry structure of the $\tilde{X}^1A_1$ state of BrF_4^- are shown in Figure 4. DZP^{++} BHLYP predicts, an r_e of 1.793 and 1.893 Å for the neutral and anion, respectively. The only experimental structure data for the anion is provided by an X-ray crystal structure of $KBrF_4$.[27] The bond length according to this study was 1.890 Å, which differs by 0.03 Å from the DZP^{++} BHLYP result. However, as the BrF_4 anion was studied as an ionic complex with the potassium cation, this comparison may not be entirely valid; the agreement, though, between the gas-phase equilibrium geometry and the crystal structure is certainly satisfactory. The bond lengths provided by the other DFT functionals were longer by as much as 0.09 Å.

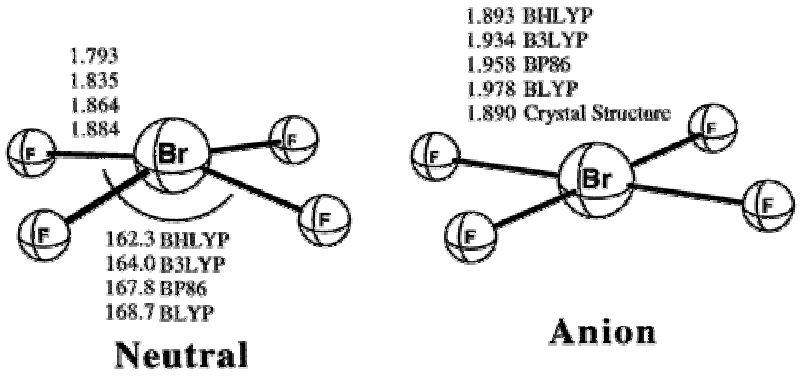

Figure 4 The molecular geometries of the $\tilde{X}^2A_1$ state of BrF_4 and the $\tilde{X}^1A_1$ state of the anion, BrF_4^-. Bond lengths and bond angles are in Å and deg, respectively. All results were obtained with the DZP^{++} basis set.

Our predicted adiabatic electron affinity for BrF_4 is 5.58 eV. The EA_{vert} ranges from 4.23 to 4.66 eV and the VDE ranges from 5.47 to 6.76 eV. Again, this is a very large electron affinity, strongly suggesting the observability of BrF_4^- in a carefully designed experiment. Like BrF_2, the EA_{ad}, EA_{vert}, and VDE values are similar due to the small difference in geometry between neutral and anion.

F. BrF_5 and BrF_5^-.

The C_{4v} equilibrium geometry of the $\tilde{X}^1A_1$ state of the BrF_5 and the C_{4v} geometry of the $\tilde{X}^2A_1$ state of BrF_5^- are shown in Figure 5. Once again, the DZP^{++} BHLYP method provides an equilibrium structure in good agreement with experiment, yielding values of 1.680 Å, 1.785 Å, and 83.5° for r_{ax}, r_{eq}, and $\angle F_{ax}$-Br-F_{eq}, respectively. X-ray crystal data,

reported by Burbank and Bensey in 1957, yielded the first look at this reactive species and gave an r_{ax} of 1.680 Å and an r_{eq} of 1.780 Å.[28] They also reported a slightly acute F_{ax}-Br-F_{eq} angle of 84.5°. More recent data[29] on the structure of this species are available; however, little has changed in the more than 40 years since Burbank and Bensey's study. Combining electron diffraction and microwave data in 1971, Robliette, Bradley, and Brier[29a] provided a gas-phase structure for BrF_5, obtaining r_{α} values of 1.69 and 1.77 Å for Br-F_{ax} and Br-F_{eq}, respectively. The F_{ax}-Br-F_{eq} angle was given as 84.8°. Similar to both BrF^- and BrF_3^-, the BrF_5^- ion has longer Br-F bond distances than the neutral, especially for Br-F_{ax}, which increases by about 0.5 Å. Again, as with BrF^- and BrF_3^- it is clear that the bonding in the anion (BrF_5^-) must be quite different from that for the closed-shell neutral species.

In Figure 6 we show the lowest unoccupied (BrF, BrF_3, and BrF_5) and singly occupied (BrF_2 and BrF_4) molecular orbitals. From these orbital plots, it is relatively easy to determine why the bond length differences between neutral and anionic bromine fluorides which contain an odd number of F atoms are so much greater than the corresponding differences in those bromine fluorides with even numbers of F atoms. Notice that the LUMO of BrF has a substantial amount of antibonding σ character. Adding electron density to this orbital should lower the bond order and substantially increase the Br-F bond length. This is also true in BrF_3 and BrF_5, in which the LUMOs again have substantial antibonding character along the axial Br-F bonds. The radicals, BrF_2 and BrF_4, do not suffer from this problem, as the anion can be formed by adding the additional electron in the π-type SOMOs which have little effect on the actual bond length. These orbitals do, on the other hand, have rather dramatic effects on the overall

symmetry of these species. Notice that in neutral BrF_4, the $12a_1$ orbital largely favors a square-planar geometry, and an additional electron in this orbital is going to force BrF_4^- to adopt this structure.

The adiabatic and vertical electron affinities and vertical detachment energies are reported in Table 3. The most reliable prediction of the adiabatic electron affinity of BrF_5 is 4.24 eV. The large magnitude of this EA suggests that BrF_5^- should be observable and could play a role in atmospheric chemistry. Even though it has been suggested that with these larger species (BrF_n; n = 5,6) DFT may overestimate EAs, the largest error observed for the SF_6 species was 0.56 eV.[8] The range 4.2-4.5 eV, then, engulfs our predicted EA_{ad} for BrF_5. The EA_{vert} values range from 1.68 to 2.82 eV and the range for VDE is from 5.65 to 6.99 eV.

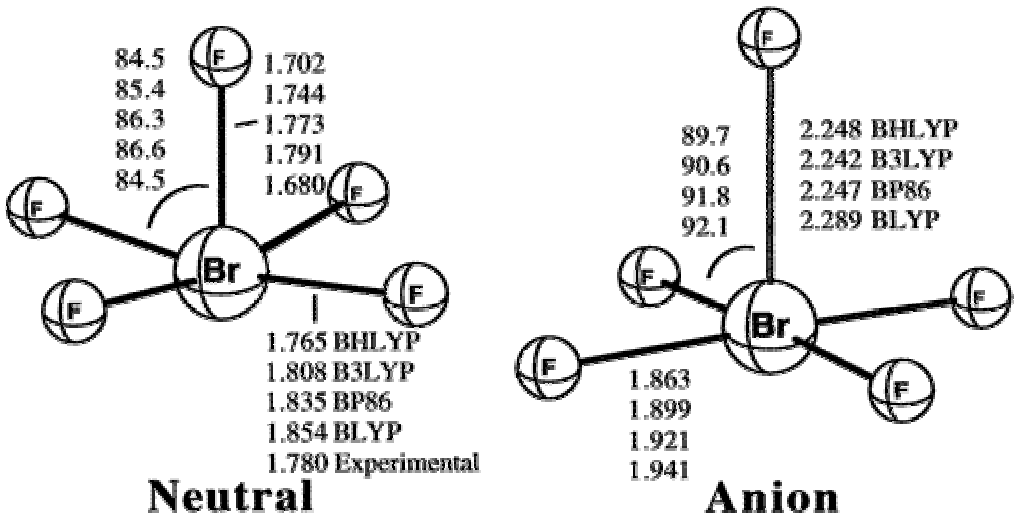

Figure 5 The molecular geometries of the $\tilde{X}^1A_1$ state of BrF_5 and the $\tilde{X}^2A_1$ state of the anion, BrF_5^-. Bond lengths and bond angles are in Å and deg, respectively. All results were obtained with the DZP^{++} basis set.

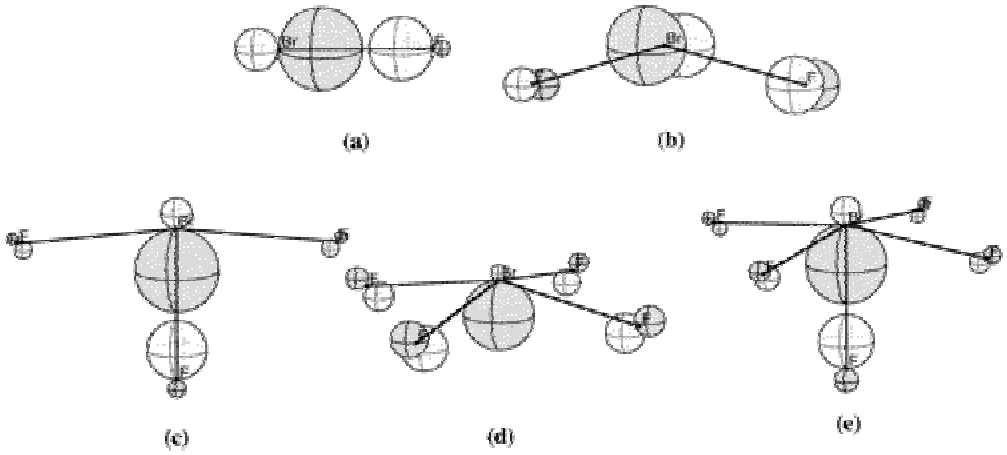

Figure 6 The lowest unoccupied (BrF, BrF_3, and BrF_5) and singly occupied (BrF_2 and BrF_4) molecular orbitals: (a) 11σ, LUMO of BrF; (b) $5b_1$, SOMO of BrF_2; (c) $16a_1$, LUMO of BrF_3; (d) $12a_1$, SOMO of BrF_4; and (e) $15a_1$, LUMO of BrF_5.

G. BrF_6 and BrF_6^-.

The equilibrium octahedral (O_h) structures of the X^2A_{1g} state of BrF_6 and the O_h structure of the X^1A_{1g} state of BrF_6^- are shown in Figure 7. Since there are no experimental data for these species, the most reliable Br-F bond distances are believed to be the BHLYP results, 1.773 Å for the neutral and 1.865 Å for the anion. For comparison with other theoretical work done on the BrF_6^- ion, the bond length obtained by MP2 theory conjoined with a basis set of triple-ζ plus polarization quality (referred to as TZVP) was 1.910 Å,[30] which is 0.045 Å larger than our DZP^{++} BHLYP (1.865 Å) result. This difference between theoretical methods is understandable due to the widely known fact that second-order perturbation theory almost always provides equilibrium bond lengths which are too long, even in the complete basis set limit.[31] The most reliable single prediction of the adiabatic electron affinity of BrF_6 is 5.59 eV, while the EA_{vert} range is from 4.84 to 5.68 eV and the range for the VDE is from 6.20 to 6.61 eV.

H. BrF_7 and BrF_7^-.

Since iodine heptafluoride is known to exist, we have investigated the D_{5h} structures of BrF_7 and BrF_7^-. The stationary points from the DZP^{++} BHLYP method have bond distances Br-F_{ax} = 1.689 Å and Br-F_{eq} = 1.793 Å for the neutral BrF_7 molecule and Br-F_{ax} = 1.789 Å and Br-F_{eq} = 1.890 Å for the BrF_7^- ion. The energy difference between them is 6.21 eV. However, neither of the D_{5h} structures are genuine minima, so this energy difference cannot be regarded as a true electron affinity. Due to the extreme multivalent nature of this species, perhaps the addition of *f*-like polarization functions would be important in locating the minima for both the neutral and its anion.

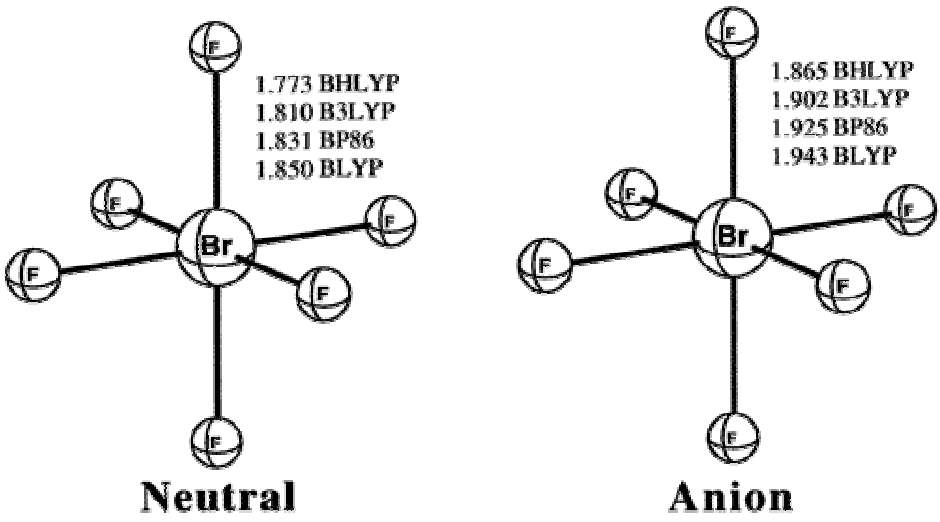

Figure 7 The molecular geometries of the $\tilde{X}^2A_{1g}$ state of BrF_6 and the $\tilde{X}^1A_{1g}$ state of the anion, BrF_6^-. Bond lengths and bond angles are in Å and deg, respectively. All results were obtained with the DZP^{++} basis set.

Dissociation Energies

The neutral and anionic bond dissociation energies for BrF_n/BrF_n^- (n = 1-6) are given in Tables 4 and 5. The DZP^{++} BHLYP dissociation energies are much lower than those from the other three methods. It was found in the previous studies of SF_n and ClF_n[8,11] that the DZP^{++} BHLYP predictions for dissociation energies were clearly the worst of the four functionals employed. As the DFT/HF hybrid BHLYP functional purports to include standard Hartree-Fock theory to the greatest degree of all the functionals used in this study, this finding is not surprising. It is well-known that Hartree-Fock theory (without the inclusion of dynamical or nondynamical correlation) performs dismally for bond-breaking processes.[32]

Table 4 shows the dissociation energies (for the process $BrF_n \rightarrow BrF_{n-1} + F$) of the neutral molecules. Excluding the DZP^{++} BHLYP results, the dissociation energy for BrF ranges from 2.54 to 2.97 eV. There is more than one experimental value for the dissociation energy of BrF. In the 1968 edition of his authoritative book on diatomic dissociation energies, Gaydon recommends D_o(BrF) = 2.384 eV (55.0 kcal/mol).[33] Huber and Herzberg, in their comprehensive 1979 book on diatomic molecules, recommend D_o(BrF) = 2.548 eV (58.76 kcal/mol).[24b] And from the heat of formation (0 K) as -50.8, 117.917, and 77.284 kJ/mol for BrF, Br, and F, respectively, in the 1985 JANAF tables,[34] the dissociation energy can be derived as 2.552 eV (58.9 kcal/mol). Best agreement with any of the experimental dissociation energies is provided by the B3LYP method.

The theoretical dissociation energies for BrF_2 decrease to the range of between 1.40 and 1.96 eV. The data of Table 4 show that this value increases for BrF_3 and decreases for BrF_4 again. The same trend continues for BrF_5 and BrF_6. In other words, the

dissociation energies become larger for BrF_n when *n* is an odd number, and smaller when *n* is an even number. This zigzag phenomenon can be readily explained. The BrF_n molecules with even number *n* are radicals, and are less stable than those with odd *n*, which have closed shell electronic structures. Another trend is that when the odd number *n* increases (i.e. from 1, to 3, to 5), the dissociation energy decreases. The molecules with even numbers follow the same trend. This indicates in a qualitative way that the larger BrF_n molecules are less stable than the smaller ones, which is understandable due to their increased hypervalency.

For the anions, BrF_n^-, there are two forms of dissociation: either to a neutral BrF_{n-1} plus an F^- ion, or to a BrF_{n-1}^- ion plus a neutral F atom. Excluding the DZP^{++} BHLYP dissociation energies, which are significantly smaller than the others, Table 5 shows that, for the dissociation to "BrF_{n-1}^- + F", the zigzag phenomenon is similar to that in Table 4. The amplitude of the zigzag is significant and the general trend is downward. The difference is that the molecules with even number *n* are more stable since they have closed shell electronic structures. This may also be related to the fact that when *n* is odd, the additional electron of the anions is residing in an antibonding orbital (primarily a σ* orbital), lengthening and destabilizing those σ bonds. However, for the dissociation to "BrF_{n-1} + F^-", the zigzag feature is not as obvious, and the general trend is upward. This indicates that when the size of the molecule increases, dissociation to a BrF_{n-1}^- ion plus a neutral F atom becomes preferable.

TABLE 2.2: Adiabatic and Vertical Electron Affinities of the Neutral and Vertical Detachment Energies of the Anionic Bromine Monofluoride (BrF), Bromine Difluoride (BrF_2), Bromine Trifluoride (BrF_3), Bromine Tetrafluoride (BrF_4), Bromine Pentafluoride (BrF_5), and Bromine Hexafluoride (BrF_6) in eV (kcal/mol in parentheses)[a]

Compd	Method	EA_{ad}	EA_{vert}	VDE
BrF	BHLYP	2.64 (60.8)	1.06 (24.3)	4.48 (103.4)
	B3LYP	2.80 (64.7)	1.36 (31.3)	4.47 (103.1)
	BP86	2.79 (64.3)	1.45 (33.4)	4.34 (100.0)
	BLYP	2.71 (62.5)	1.36 (31.3)	4.24 (97.7)
BrF_2	BHLYP	4.78 (110.2)	3.83 (88.3)	6.28 (145.0)
	B3LYP	4.71 (108.6)	4.07 (93.8)	6.59 (151.9)
	BP86	4.47 (103.0)	4.11 (94.8)	4.73 (109.0)
	BLYP	4.34 (100.2)	4.00 (92.3)	4.60 (106.1)
BrF_3	BHLYP	3.77 (87.0)	1.78 (40.9)	5.96 (137.5)
	B3LYP	3.89 (89.7)	2.18 (50.4)	5.53 (127.6)
	BP86	3.74 (86.3)	2.27 (52.4)	5.05 (116.6)
	BLYP	3.76 (86.8)	2.30 (52.9)	5.03 (116.0)
BrF_4	BHLYP	5.58 (128.7)	4.23 (97.5)	6.61 (152.5)
	B3LYP	5.58 (128.6)	4.58 (105.7)	6.76 (155.9)
	BP86	5.25 (121.2)	4.64 (107.0)	5.54 (127.7)
	BLYP	5.21 (120.1)	4.66 (107.6)	5.47 (126.1)
BrF_5	BHLYP	4.24 (97.7)	1.68 (38.8)	6.99 (161.2)
	B3LYP	4.48 (103.3)	2.45 (56.5)	6.30 (145.4)
	BP86	4.32 (99.6)	2.66 (61.3)	5.65 (130.2)
	BLYP	4.44 (102.5)	2.82 (65.0)	5.69 (131.2)
BrF_6	BHLYP	5.59 (129.0)	4.84 (111.6)	6.20 (142.9)
	B3LYP	6.10 (140.7)	5.48 (126.4)	6.61 (152.4)
	BP86	6.12 (141.1)	5.56 (128.1)	6.59 (151.9)
	BLYP	6.19 (142.7)	5.68 (130.9)	6.61 (152.5)

Table 2.4.: Dissociation Energies (D_{BrFn}) for the Neutral and Anion Members of the Series in eV (kcal/mol in parentheses)

dissociation	BHLYP	B3LYP	BP86	BLYP	exptl
$BrF \rightarrow Br + F$	1.93 (44.5)	2.54 (58.6)	2.97 (68.6)	2.87 (66.1)	2.55 (58.8)[b] 2.38 (54.9)[c]
$BrF_2 \rightarrow BrF + F$	0.64 (14.7)	1.40 (32.2)	2.02 (46.6)	1.96 (45.2)	
$BrF_3 \rightarrow BrF_2 + F$	1.67 (38.5)	2.10 (48.4)	2.44 (56.3)	2.29 (52.8)	
$BrF_4 \rightarrow BrF_3 + F$	0.40 (9.3)	1.18 (27.1)	1.85 (42.7)	1.77 (40.8)	
$BrF_5 \rightarrow BrF_4 + F$	1.70 (39.2)	2.03 (46.8)	2.34 (54.0)	2.13 (49.0)	
$BrF_6 \rightarrow BrF_5 + F$	-0.02 (-0.4)	0.69 (16.0)	1.19 (27.4)	1.07 (24.6)	

Dissociation Energies (D_{BrFn}^-) for the Anionic Members of the Series in eV (kcal/mol in parentheses)

dissociation	BHLYP	B3LYP	BP86	BLYP
$BrF^- \rightarrow Br^- + F$	1.15 (26.6)	1.74 (40.2)	2.08 (47.9)	2.12 (48.8)
$BrF_2^- \rightarrow BrF^- + F$	2.78 (64.1)	3.30 (76.1)	3.70 (85.3)	3.59 (82.8)
$BrF_3^- \rightarrow BrF_2^- + F$	0.66 (15.3)	1.28 (29.5)	1.72 (39.6)	1.71 (39.4)
$BrF_4^- \rightarrow BrF_3^- + F$	2.21 (51.0)	2.87 (66.1)	3.36 (77.5)	3.21 (74.0)
$BrF_5^- \rightarrow BrF_4^- + F$	0.35 (8.1)	0.93 (21.4)	1.41 (32.5)	1.36 (31.4)
$BrF_6^- \rightarrow BrF_5^- + F$	1.34 (30.9)	2.31 (53.4)	2.99 (68.8)	2.81 (64.8)
$BrF^- \rightarrow Br + F^-$	1.63 (37.5)	1.80 (41.5)	2.13 (49.0)	1.78 (41.0)
$BrF_2^- \rightarrow BrF + F^-$	2.47 (57.1)	2.56 (59.1)	2.85 (65.7)	2.50 (57.6)
$BrF_3^- \rightarrow BrF_2 + F^-$	2.50 (57.7)	2.45 (56.4)	2.55 (58.8)	2.25 (51.9)
$BrF_4^- \rightarrow BrF_3 + F^-$	3.04 (70.1)	3.21 (74.0)	3.47 (80.0)	3.17 (73.2)
$BrF_5^- \rightarrow BrF_4 + F^-$	2.99 (69.0)	2.96 (68.3)	3.03 (69.8)	2.77 (63.8)
$BrF_6^- \rightarrow BrF_5 + F^-$	2.63 (60.7)	3.25 (74.9)	3.67 (84.6)	3.45 (79.6)

Conclusions

On the basis of the experimental adiabatic electron affinity for the Br (3.36 eV) atom, and previous work on the SF_n/SF_n^-, PF_n/PF_n^- ClF_n/ClF_n^-, SiF_n/SiF_n^-, and $C_2F_n/C_2F_n^-$ molecules,[8-12] we have concluded that the DZP^{++} BHLYP method is the most reliable method for predicting the electron affinities [3.41 (Br), 2.64 (BrF), 4.78 (BrF_2), 3.78 (BrF_3), 5.58 (BrF_4), 4.24 (BrF_5), 5.59 eV (BrF_6)] and molecular structures of the bromine fluorides.

In predicting those structures for which experimental results were available (BrF, BrF_3, and BrF_5), the DZP^{++} BHLYP results were in closest agreement with the experimental structures, giving average bond distance errors for the four density functionals, BHLYP (0.009 Å), B3LYP (0.039 Å), BP86 (0.063 Å), and BLYP (0.081 Å).

Unlike predicting geometries and EAs for these molecules, the DZP^{++} BHLYP method is considered to yield the least reliable predictions of dissociation energies, as shown earlier for related molecules.[8-12] This may be correlated with the fact that the BHLYP functional incorporates the largest fraction of the ab initio Hartree-Fock method; thus similar to SCF, its performance for dissociation energies is less than desirable. The dissociation energy ranges for the neutral members of these interhalogens, excluding the DZP^{++} BHLYP values, are 2.54-2.97 (BrF), 1.40-2.02 (BrF_2), 2.10-2.44 (BrF_3), 1.18-1.85 (BrF_4), 2.03-2.34 (BrF_5), and 0.69-1.19 eV (BrF_6). Compared to the experimental dissociation energy for BrF (2.55 eV),[24b] our predictions are reasonable. The general trend in dissociation energy values is as follows: BP86 ~ BLYP > B3LYP ≫ BHLYP. The dissociation energy ranges for losing F from the BrF_n^- ions are 1.74-2.12 (BrF^-), 3.30-

3.70 (BrF_2^-), 1.28-1.72 (BrF_3^-), 2.87-3.36 (BrF_4^-), 0.93-1.41 eV (BrF_5^-), and 2.31-2.99 eV (BrF_6^-). The general trend in dissociation energy values for BrF_2^-, BrF_4^-, and BrF_6^- is BP86 > BLYP > B3LYP ≫BHLYP, and that for BrF^-, BrF_3^-, and BrF_5^- is BP86 = BLYP > B3LYP ≫BHLYP. The dissociation energy ranges for losing F^- from the anion member of these molecules are 1.78-2.13 (BrF^-), 2.50-2.85 (BrF_2^-), 2.25-2.55 (BrF_3^-), 3.17-3.47 (BrF_4^-), 2.77-3.03 (BrF_5^-), and 3.25-3.67 eV (BrF_6^-), and the general trend of dissociation energy values for BrF_2^-, and BrF_4^- and BrF_6^- is BP86 >B3LYP > BPYP ~ BHLYP, and that for BrF_3^- and BrF_5^- is BP86 > BHLYP > B3LYP > BLYP.

The range of bromine-fluorine bond distances predicted here is of special interest. For this purpose we consider only the BHLYP predictions. The neutral Br-F bond distances are 1.756 (BrF), 1.826 (BrF_2), 1.720 and 1.808 (BrF_3), 1.793 (BrF_4), and 1.702 and 1.765 (BrF_5), 1.773 Å (BrF_6). Thus the entire range, from 1.702 to 1.826, is 0.124 Å. For the anions, we predict a much broader range of bromine-fluorine bond distances. The negative ion Br-F bond distances are 2.300 (BrF^-), 1.959 (BrF_2^-), 1.913 and 2.253 (BrF_3^-), 1.893 (BrF_4^-), 1.863 and 2.248 (BrF_5^-), and 1.865 Å (BrF_6^-). We see that the closed shell species BrF_2^- and BrF_4^- have Br-F bond distances similar to the neutral bromine fluorides. However, the distance for diatomic BrF^- and the axial distances in BrF_3^- and BrF_5^- are all much longer than those observed for the neutral bromine fluorides.

One is tempted via ideas such as Badger's rule to suggest that unusually long bond distances might be associated with low electron affinities. Such an argument may be applied to the BrF system, which has by far the smallest EA of the bromine fluorides, and also a very long anion bond distance. However, the longest Br-F distance of all is that predicted for the axial BrF_5^- distance, while the BrF_5 species has a very large EA, namely

4.24 eV. This phenomenon is not readily explainable. Additionally, due to the existence of IF_7, it is desirable to locate the corresponding bromine analogue. Future theoretical work involving larger basis sets with the added directionality provided by *f* and perhaps even *g* functions is recommended. We hope that our theoretical predictions can provide inspiration for the further experimental study of these important interhalogen compounds and their anions.

Acknowledgment

This research was supported by the US National Science Foundation, Grant CHE-9527468.

BIBLIOGRAPHY

1. Pietro, W. J.; Francl, M. M.; Hehre, W. J.; Defrees, D. J.; Pople, J. A.; Binkley, J. S. *J. Am. Chem. Soc*. **1982**, *104*, 5039.

2. Cotton, F. A.; Wilkinson, G. *Advanced Inorganic Chemistry*, 5th ed.; Wiley: New York, 1988.

3. Gutzev, G. L.; Smolyar, A. E. *Chem. Phys. Lett.* **1980**, *71*, 296.

4. Shamir, J.; Yaroslavsky, I. *Israel J. Chem*. **1969**, *7*, 495.

5. Ko, M. K.; Sze, N. D. *Nature* **1994**, *367*, 505.

6. Monastersky, R. *Sci. News* **1996**, *149*, 151.

7. Butler, J. H.; Elkins, J. W.; Hall B. D. *Nature* **1992**, *359*, 403.

8. (a) King, R. A.; Galbraith, J. M.; Schaefer, H. F. *J. Phys. Chem*. **1996**, *100*, 6061. (b) Galbraith, J. M.; Schaefer, H. F. *J. Chem. Phys.* **1996**, *105*, 862.

9. Tschumper, G. S.; Fermann, J. T.; Schaefer, H. F. *J. Chem. Phys*. **1996**, *104*, 3676.

10. Van Huis, T. J.; Galbraith, J. M.; Schaefer, H. F. *Mol. Phys.* **1996**, *89*, 607.

11. King, R. A.; Mastryukov, V. S.; Schaefer, H. F. *J. Chem. Phys*. **1996**, *105* (16), 6880.

12. King, R. A.; Pettigrew, N. D.; Schaefer, H. F. *J. Chem. Phys.* **1997**, *107*, 8536.

13. Becke, A. D. *Phys. Rev*. *A* **1988**, *38*, 3098.

14. Lee, C.; Yang, W.; Parr, R. G. *Phys. Rev*. *B* **1988**, *37*, 785.

15. Becke, A. D. *J. Chem. Phys*. **1993**, *98*, 1372.

16. Becke, A. D. *J. Chem. Phys*. **1993**, *98*, 5648.

17. Perdew, J. P. *Phys. Rev*. *B* **1986**, *33*, 8822; *34*, 7046.

18. Gaussian 94 (Revision B. 3), Grisch, M. J., Trucks, G. W., Schlegel, H. B., Gill, P. M. W., Johnson, B. G., Robb, M. A., Cheeseman, J. R., Keith, T. A., Petersson, G. A., Montgomery, J. A., Raghavachari, K., Al-Laham, M. A., Zakrzewski, V. G., Ortiz, J. V., Foresman, J. B., Cioslowski, J., Stefanov, B. B., Nanayakkara, A., Challacombe, M., Peng, C. Y., Ayala, P. Y., Chen, W., Wong, M. W., Andres, J. L., Replogle, E. S.,

Gomperts, R., Martin, R. L., Fox, D. J., Binkely, J. S., Defrees, J. D., Baker, J., Stewart, J. P., Head-Gordon, M., Gonzalez, C., and Pople, J. A.; Gaussian, Inc.: Pittsburgh, PA, 1995.

19. Gaussian 92/DFT (Revision F.2), Frisch, M. J., Trucks, G. W., Schlegel, H. B., Gill, P. M. W., Johnson, B. G., Wong, M. W., Foresman, J. B., Robb, M. A., Head-Gordon, M., Replogle, E. S., Gomperts, R., Andres, J. L., Raghavachari, K., Binkley, J. S., Gonzalez, C., Martin, R. L., Fox, D. J., Defrees, D. J., Baker, J., Stewart, J. J. P., and Pople, J. A.; Gaussian, Inc.: Pittsburgh, PA, 1993.

20. Schäfer, A.; Horn, H.; Ahlrichs, R. *J. Chem. Phys.* **1992**, *97*, 2571.

21. Huzinaga, S. *J. Chem. Phys*. **1965**, *42*, 1293. Dunning, T. H. *J. Chem. Phys*. **1970**, *53*, 2823. Huzinaga, S. *Approximate Atomic Wave functions*; Department of Chemistry, University of Alberta; 1971; Vol. II. Dunning, T. H.; Hay, P. J. *Modern Theoretical Chemistry*; Schaefer, H. F., Ed.; Plenum Press: New York, 1977; pp 1-27.

22. Lee, T. J.; Schaefer, H. F. *J. Chem. Phys*. **1985**, *83*, 1784.

23. Blondel, C.; Cacciani, P.; Delsart, C.; Trainham, R. *Phys. Rev. A* **1989**, *40*, 3698.

24. (a) Willis, R. E.; Clark, W. W. *J. Chem. Phys.* **1980**, *72*, 4946. (b) Huber, K. P.; Herzberg, G. *Molecular Spectra and Molecular Structure*; Constants of Diatomic Molecules; Van Nostrand Reinhold: New York, 1979; Vol. 4.

25. Magnuson, D. W. *J. Chem. Phys.* **1957**, *27*, 223.

26. Schwerdtfeger, P. *J. Phys. Chem.* **1996**, *100*, 2968.

27. Edwards, A. J.; Jones, G. R. *J. Chem. Soc. A* **1969**, 1936.

28. Burbank, R. D.; Bensey, F. N. *J. Chem. Phys.* **1957**, *27*, 982.

29. (a) Robliette, A. G.; Bradley, R. H.; Brier, P. N. *Chem. Commun.* **1971**, *23*, 1567. (b) Georghiou, C.; Brier, P. N.; Baker, J. G.; Jones, S. R. *J. Mol. Spectrosc.* **1978**, *72*, 282. (c) Heenan, R. K.; Robliette, A. G. *J. Mol. Struct.* **1979**, *54*, 135.

30. Kaupp, M.; Van Willen, C.; Franke, R.; Schmitz, F.; Kutzelnigg, W. *J. Am. Chem. Soc*. **1996**, *118*, 11939.

31. Peterson, K. A.; Dunning, T. H. *J. Mol. Struct. (THEOCHEM)* **1997**, *400*, 93.

32. Roos, B. J. In *Ab Initio Methods in Quantum Chemistry*; Lawley, K. P., Ed.; John Wiley & Sons: New York, 1987; pp 399-445.

33. Gaydon, A. G. *Dissociation Energies and Spectra of Diatomic Molecules*; Chapman and Hall: London, 1968.

34. Chase, M. W.; Davies, J. R.; Downey, Jr.; Frurlp, D. J.; McDonald, R. A.; Syverud, A. N. *JANAF Thermochemical Tables*, 3rd ed.; *J. Phys. Chem. Ref. Data, Suppl. 1*, **1985**, *14*, 426.

CHAPTER 3

ELECTRON AFFINITIES OF SILICON HYDRIDES:

SiH_n (n = 0-4) and Si_2H_n (n = 0-6)[1]

[1]Pak, C. H., J. C. Rienstra-Kiracofe and H. F. Schaefer, *J. Phys. Chem. A,* **104** (47), 11232 -11242, 2000. Reproduced in part with permission from American Chemical Society.

Abstract

The molecular structures and electron affinities of the SiH_n/SiH_n^- (n = 1-4) and $Si_2H_n/Si_2H_n^-$ (n = 0-6) molecules, as well as the silicon atom, have been investigated using density functional theory (DFT) and hybrid Hartree-Fock/density functional theory. Specifically, four different types of electron affinities are reported in this work: the adiabatic electron affinity (EA_{ad}), zero-point corrected EA_{ad} (EA_{zero}), the vertical electron affinity (EA_{vert}), and vertical detachment energy (VDE). The basis set used in this work is of double-ζ plus polarization quality with additional s- and p-type diffuse functions, and is denoted as DZP^{++}. Of the six different density functionals used in this work, the BHLYP functional predicted the best molecular structures, and the B3LYP functional predicted the best electron affinities. When compared to the available six experimental electron affinities, the B3LYP functional has an average absolute error of just 0.06 eV. We predict the unknown electron affinities for Si_2H_2 (dibridged), Si_2H_3, Si_2H_4 (disilene), and Si_2H_5 (disilyl radical) to be 0.45, 2.21, 1.34, and 1.85 eV, respectively. These predictions assume that the (unknown) molecular structure of each anion is analogous to the known structure of the corresponding neutral molecule. The most interesting aspect of the present research is that for $Si_2H_2^-$ and $Si_2H_4^-$, the lowest energy structures are qualitatively different from those of the neutrals. For $Si_2H_2^-$ the disilavinylidene structure H_2SiSi^-, is predicted to lie 24 kcal/mol below the dibridged or "butterfly" anion. For $Si_2H_4^-$ the silylsilylene anion H_3SiSiH^-, is predicted to lie 3 kcal/mol below the disilene anion structure $H_2SiSiH_2^-$. The zero-point corrected adiabatic electron affinities of disilavinylidene, silylsilylidyne, and silylsilylene are 1.87, 1.01, and 1.71 eV,

respectively. The saturated closed shell systems SiH_4 and Si_2H_6 do not have conventional electron affinities.

Introduction

Silicon, like its first row counterpart, carbon, is a chemist's cornucopia.[1] The ability of silicon to make one, two, three, four, and even five-coordinate compounds is one of the primary reasons for its inexhaustible chemistry.[1] Among the simplest silicon species are the silicon hydrides, SiH_n (n = 0-4) and Si_2H_n (n = 0-6). Silicon hydrides play an important role in silicon chemical vapor deposition (CVD) processes,[2] which are of great significance to the semiconductor industry. Because of this significance, numerous experimental[3-17] and theoretical[18-36] studies have examined various chemical properties of the silicon hydrides, their corresponding ions, and other simple silicon-based compounds.

Silicon hydride systems are also of interest to chemists because of their sometimes unique bonding characteristics when compared to their simple hydrocarbon analogues. Although analogous carbon and silicon species are isovalent, the chemical properties of carbon and silicon congeners can be quite different. One of the reasons for these differences is that the relative orbital sizes of the valence s and p orbitals are different for the carbon and silicon atoms; silicon has a larger p orbital than carbon, and carbon has a larger *s* orbital than silicon.[37,38] Many properties of the species in the SiH_n/SiH_n^- (n = 0-4) and $Si_2H_n/Si_2H_n^-$ (n = 0-6) series may be compared to their carbon analogues, and some interesting differences may be found, for example, by comparing the adiabatic electron affinities of simple silicon hydrides to their hydrocarbon analogues.

In this work, we investigate the electron affinities (EA) of the silicon hydrides and the ability of density functional theory to predict accurate electron affinities for these species through comparisons to known experimental EAs and analogous hydrocarbon EAs. Experimental EAs[4,7,10,13,14] are available for Si, SiH, SiH_2, SiH_3, Si_2, and Si_2H.

When predicting molecular energies, structures, and electron affinities, there are many theoretical approaches, but considering both reliability and computational expense, gradient corrected density functional theory (DFT) has been shown to be effective for predicting EAs of many inorganic species such as the SiF_n/SiF_n^-, SF_n/SF_n^-, PF_n/PF_n^-, ClF_n/ClF_n^-, $C_2F_n/C_2F_n^-$, and BrF_n/BrF_n^- series.[31,39-43] In addition, while the theoretical prediction of an electron affinity is generally difficult due to the result being a small difference between two very large energies, our previous work has shown that DFT can be a dependable source for electron affinity predictions,[44-47] when used in a knowledgeable manner.

Method

Six different density functional or hybrid Hartree-Fock/density functional methods were used in this study. Five are gradient corrected functionals: Becke's 1988 exchange functional[48] (B) with Lee, Yang, and Parr's correlation functional[49] (LYP), BLYP; Becke's half-and-half exchange functional[50] (BH) with the LYP correlation functional, BHLYP; Becke's three-parameter exchange functional[51] (B3) with the LYP correlation functional, B3LYP; the B exchange functional with the Perdew correlation functional[52] (P86), BP86; and the B3 exchange functional with the P86 correlation functional B3P86. The sixth density functional scheme used in this study was the

standard local-spin-density approximation (LSDA) which employs the 1980 correlation functional of Vosko, Wilk, and Nusair[53] along with Slater's exchange functional.[54] The unrestricted Kohn-Sham method was used for all closed and open shell systems.[55] All computations have been evaluated with the Gaussian 94 program suite.[56] Using the default integration grid (75 302), the integrals that are evaluated in this study should be accurate to 1×10^{-5} E_h. The Kohn-Sham density was converged to $1 \times 10^{-8} E_h$ and Cartesian gradients were converged to at least 10^{-6} au.

A standard double-ζ plus polarization (DZP) basis set with the addition of diffuse functions was utilized. The DZ part of the basis set was constructed from the Huzinage-Dunning-Hay[57] set of contracted Gaussian functions. The DZP basis was formed by the addition of a set of five d-type polarization functions for Si and a set of *p*-type polarization functions for H [α_d(Si) = 0.50, α_p(H) = 0.75]. The DZP basis was augmented with diffuse functions; Si received one additional s-type and one additional set of p-type functions, and H received one additional s-type function. The diffuse function orbital exponents were determined in an "even-tempered sense" as a mathematical extension of the primitive set, according to the formula of Lee and Schaefer[58] [α_s(Si) = 0.02729, α_p(Si) = 0.02500, α_s(H) = 0.04415]. The final contraction scheme for this basis is Si (12s8p1d/7s5p1d) and H (5s1p/3s1p).

The geometries reported in Figures 1-14 were found to be minima after determining the harmonic vibrational frequencies via analytic gradients at the corresponding stationary point structures of each functional.

Finally, for SiH and SiH^-, we have performed coupled cluster studies with all single and double excitations and perturbative nonconnected triple excitations

[CCSD(T)],[59-61] to verify experimental data. The basis set used for the CCSD(T) computation was the correlation-consistent polarized valence quadruple-ζ set of Dunning[62,63] augmented with diffuse functions and is denoted aug-cc-pVQZ. An ROHF reference was used and core electrons for Si were frozen during CCSD(T) energy computations. These computations were done using ACES II ab initio program system.[64]

Results And Discussion

The electron affinity for the Si atom is given in Table 1. All four electron affinities for SiH_n (n = 1-4) and Si_2H_n (n = 0-6) are reported in Tables 2 and 3, respectively. Optimized geometries for each molecular species with all functionals are shown in Figures 1-14.

A. Si and Si^-.

The electron affinities of the Si (^3P) atom with various functionals, as well as the experimental electron affinity are reported in Table 1. All six functionals predict the electron affinity of the Si atom within a deviation of at most 0.62 eV (LSDA) from experiment. As is the case for most atomic systems,[47] B3LYP predicts the best electron affinity for Si. In this instance, the electron affinity was 0.03 eV lower than the experimental value, given by Scheer, Bilodeau, Brodie, and Haugen's single and multiphoton tunable infrared laser experiments.[14] We note here that carbon and silicon have similar electron affinities from experiment;[14] C = 1.262 eV, Si = 1.389 eV and that B3LYP and BLYP are within 0.15 eV for both silicon and carbon.[47]

Table 3.1.: Electron Affinity of Si in eV (kcal/mol in Parentheses)	
Method	EA
B3LYP	1.36(31.4)
B3P86	1.99(45.9)
BHLYP	1.18(27.1)
BLYP	1.24(28.6)
BP86	1.57(36.3)
LSDA	2.01(46.5)
exptl[a]	1.389521 ± 0.00002(32.0)

B. SiH and SiH^-.

Theoretical equilibrium geometries of silylidyne (silicon monohydride), SiH ($X\ ^2\Pi$), and its anion, SiH^- ($X\ ^3\Sigma^-$) are displayed in Figure 1. The experimental r_e of neutral silylidyne is 1.5201 Å. [65] Comparing with the experimental value, the most accurate bond length was predicted by BHLYP, being only 0.008 Å shorter than experiment. The hybrid functionals (B3LYP, B3P86, BHLYP) are within ± 0.013 Å of experiment, while the pure functionals (BLYP, BP86, LSDA) overestimate experiment by at least 0.026 Å. All functionals give a longer bond length for the anion than the neutral, by about 0.03 Å on average. In 1975, Kasdan, Herbst, and Lineberger[4] estimated the experimental r_e of the anion at 1.474 ± 0.004 Å which is 0.09 Å shorter than our average bond length of 1.565 Å. In 1978, Rosmus and Meyer[66] reinterpreted the laser photoelectron data of Kasdan et al. and found r_e (SiH^-) = 1.566 ± 0.004 Å with a ω_e (SiH^-) = 1804 cm^{-1}. Both the original and revised values are based on a Badger's rule estimate, and early theoretical results[66-68] supported the revised values. Our DFT results also predict r_e of the anion in good agreement with the revised experimental results.

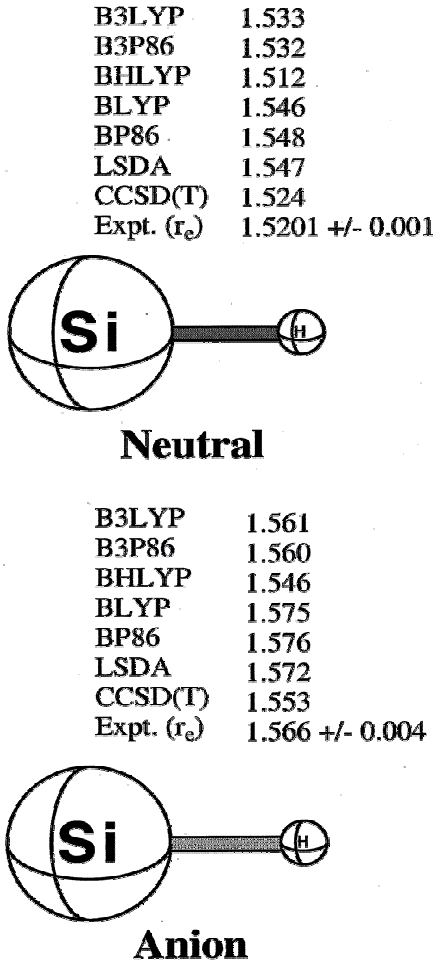

Figure 1 The molecular geometries for the X $^2\Pi$ state of SiH and the X $^3\Sigma^-$ state of SiH^-. Bond lengths are in angstroms. All results were obtained with the DZP^{++} basis set. Experimental r_e results for SiH and SiH^- are from refs 65 and 66, respectively.

To further investigate this matter, we performed CCSD(T)/aug-cc-pVQZ computations on SiH and SiH^-. We obtain r_e (SiH) = 1.524 Å and r_e (SiH^-) = 1.553 Å, along with ω_e (SiH) = 2043 cm^{-1} and ω_e (SiH^-) = 1860 cm^{-1}. The theoretical neutral bond length is just 0.004 Å longer than experiment and the harmonic frequency is only 1 cm^{-1} greater than the experimental ω_e = 2042 cm^{-1}. Furthermore, previous UCCSD(T)/aug-cc-

pV5Z calculations[34] predict r_e (SiH) = 1.522 Å. Our r_e (SiH^-) is 0.013 Å shorter than Rosmus and Meyer's revised value. Because the original experiment did not directly deduce ω_e, an error of ~50 cm^{-1} in the determination of ω_e can be expected.[4] We therefore suggest that the true r_e and ω_e for SiH^- are within ± 0.01 Å and ± 40 cm^{-1} of our CCSD(T)/aug-cc-pVQZ values. As with SiH, the hybrid functionals predict the best r_e for SiH^-, being within ± 0.008 Å of the CCSD(T) value, while the pure functionals overestimate the CCSD(T) result by at least 0.019 Å.

The EA_{ad} with CCSD(T) is 1.248 or 1.259 eV with ZPVE correction, and is only 0.029 or 0.018 (with ZPVE) eV lower than the experimental[4] laser photoelectron value of 1.277 ± 0.009 eV. As with Si, the best DFT electron affinity for SiH was predicted by B3LYP, which value is close (better than 0.03 eV) to experiment for both EA_{vert} and EA_{zero}. Other functionals gave electron affinity results within ± 0.2 eV, except for LSDA and B3P86. (See Table 2.)

The electron affinity[69] of CH is similar to the electron affinity of SiH,[4] 1.238 eV vs 1.277 eV. Density functional theory also describes EA_{ad} (CH) well,[47] though our results for EA_{ad} (SiH) are about 0.1 eV better on average.

C. SiH_2 and SiH_2^-.

Our optimized geometries for silylene, SiH_2 ($\tilde{X}\ ^1A_1$) and SiH_2^- ($\tilde{X}\ ^2B_1$) are shown in Figure 2. The three hybrid functionals are within ± 0.014 Å of the experimental[70] SiH_2 r_0 value, while the pure functionals overestimate experiment by at least 0.014 Å. All functionals are within 1.1° of the experimental angle, except LSDA. Our results for the neutral species are similar to the recent UCCSD(T)/aug-cc-pV6Z results of 1.516 Å and

92.3°.[34] We observe little change in the HSiH angle between SiH_2 and SiH_2^-, in accordance with the Walsh picture for the valence b_1 molecular orbital in XH_2 molecules. The bond lengths in SiH_2^- are about 0.02 Å longer than the neutral. Compared to methylene, CH_2, the electronic states for the anions ($^2B_1$) are the same, but states for the neutral species are different: the ground state for methylene is $^3B_1$ vs $^1A_1$ in silylene. Predicted geometries and electron affinities with DFT for SiH_2 and SiH_2^- should be more accurate than for CH_2,[47] which has large multireference character in its wave function due to the near degeneracy of the valence a_1 and b_1 molecular orbitals.

Our theoretical EA_{ad}, EA_{zero}, EA_{vert}, and VDE for SiH_2 are listed in Table 2. The predicted EA_{ad} ranges from 1.00 to 1.74 eV, among which BHLYP predicts the lowest EA_{ad}. The BHLYP EA_{ad} and EA_{vert} are often lower than those obtained with the other functionals, as is the case in many inorganic fluoride series.[39-43] Because there is not much difference in geometries between the neutral and the anion, the differences with a given functional between EA_{ad}, EA_{zer}, EA_{vert}, and VDE are small. From Leopold et al.[71] CH_2 has an experimental electron affinity of 0.652 eV compared to Kasdan, Herbst, and Lineberger's laser photoelectron spectrometry results for SiH_2 of 1.124 ± 0.020 eV.[4] The large difference in EAs for methylene and silylene is due to the fact that the extra electron must add to a singly occupied a_1 orbital in CH_2, but adds to a unoccupied, nonbonding b_1 orbital in SiH_2. For SiH_2, B3LYP, BLYP, and BHLYP EA_{zero} values are within ± 0.09 eV of experiment; remarkably in CH_2, B3LYP, BLYP, and BP86 are within 0.14 eV of experiment. However, BHLYP suffers from Hartree-Fock deficiencies, predicting an EA 0.35 eV lower for the multireference described CH_2.[47]

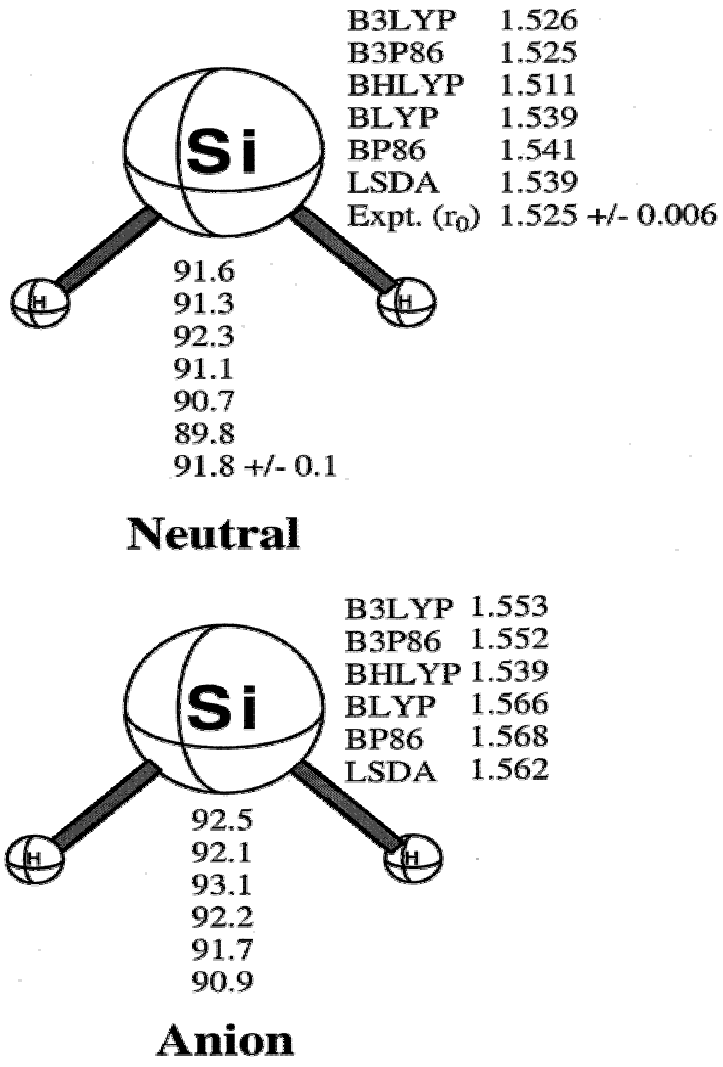

Figure 2 The molecular geometries for the $\tilde{X}\,^1A_1$ state of SiH_2 and the $\tilde{X}\,^2B_1$ state of SiH_2^-. Bond lengths and bond angles are in angstroms and degrees, respectively. All results were obtained with the DZP^{++} basis set. Experimental r_0 results are from ref 70.

D. SiH_3 and SiH_3^-.

The C_{3v} symmetry equilibrium geometries of the SiH_3 ($\tilde{X}\,^2A_1$) radical and SiH_3^- ($\tilde{X}\,^1A_1$) anion are shown in Figure 3. The neutral, silyl radical bond lengths ranged from 1.474 (BHLYP) to 1.496 (BP86) Å, and the bond angles from 111.1° to 111.4°. All

methods overestimate the experiment values[72] of 1.468 Å and 110.5°. However, our results are much closer to the UCCSD(T)/aug-cc-pVQZ values[34] of 1.482 and 111.3°. The anion bond distances are significantly longer, 1.532 to 1.558 Å, and the angles are tighter, 93.8° to 96.0°. This is in agreement with an experimentally observed tightening from ~112.5° to ~94.5° between the neutral species and the anion.[7] Our hybrid functional bond lengths for the anion are just ± 0.007 Å from the BS1 CCSD(T)-R12 results, $r_{(Si-H)}$ = 1.538 Å, obtained by Aarset et al.[36] The pure functionals overestimate the CCSD(T) result by at least 0.14 Å. All bond angles are in reasonable agreement with the BS1 CCSD(T)-R12 bond angles of 95.196°.

The best electron affinity result was from the B3LYP level of theory, EA_{ad} = 1.40 eV, which is 0.01 eV lower than that determined by photoelectron spectroscopy,[7] 1.406 ± 0.014 eV, though agreement is slightly worse with the ZPVE correction. The EA_{vert} ranged from 0.72 to 1.57 eV and the VDE ranged from 1.68 to 2.55 eV. It is interesting to note that the electron affinity of the methyl radical,[73] where the neutral species is D_{3h} ($^2A_2'$ '), is only 0.08 eV compared to 1.406 eV for the silyl radical.[7] B3LYP and BLYP both predict EA (CH_3) to within 0.05 eV.[74]

E. SiH_4 and SiH_4^-.

The optimized T_d geometries of silane, SiH_4 ($\tilde{X}\,^1A_1$) and SiH_4^- ($\tilde{X}\,^2A_1$) are shown in Figure 4. The three hybrid functionals predict a neutral Si-H bond length within 0.008 Å of the experimental value,[6] whereas the pure functionals overestimate experiment by nearly 0.02 Å. We also note that UCCSD(T)/aug-cc-pV5Z results give a bond length of 1.480 Å.[34]

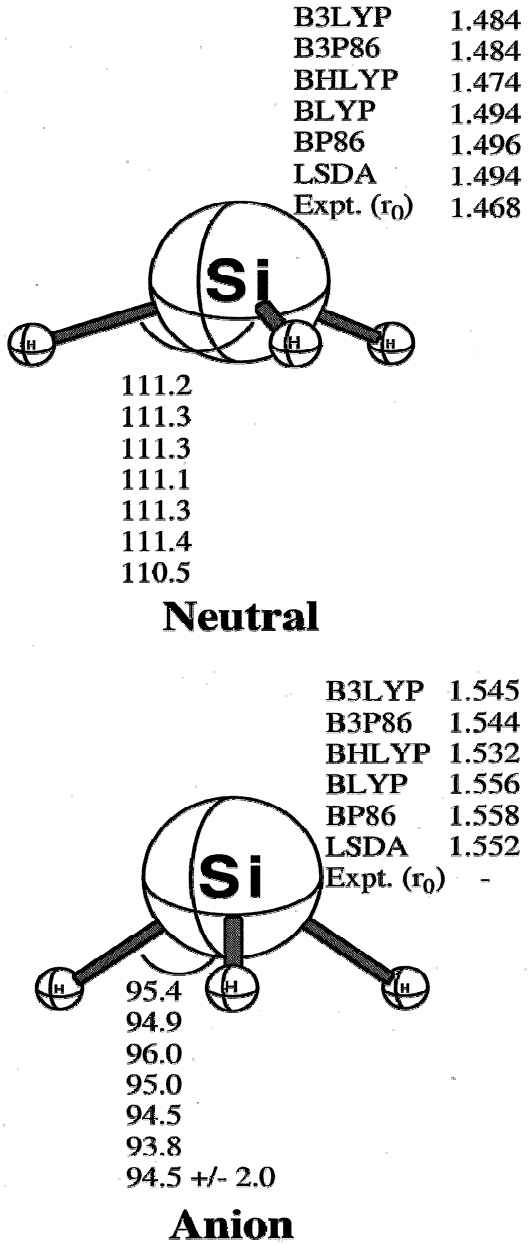

Figure 3 The molecular geometries for the $\tilde{X}^2A_1$ state of SiH_3 and the $\tilde{X}^1A_1$ state of SiH_3^-. Bond lengths and bond angles are in angstroms and degrees, respectively. All results were obtained with the DZP^{++} basis set. Experimental r_0 results for SiH_3 is from ref 72, and for SiH_3^- from ref 7.

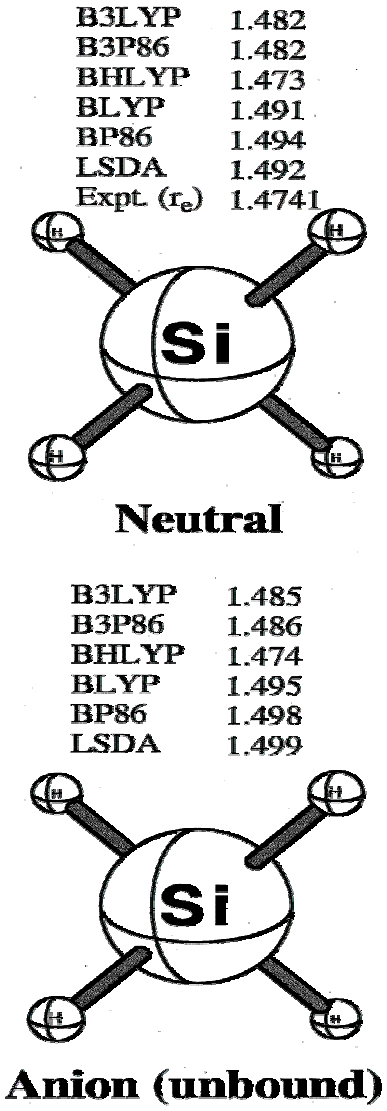

Figure 4 The molecular geometries for the $\tilde{X}^1A_1$ state of SiH_4 and the unbound $\tilde{X}^2A_1$ state of SiH_4^-. Bond lengths are in angstroms. All results were obtained with the DZP^{++} basis set. Experimental r_e results are from ref 6.

Although SiH_4^- is predicted to have an equilibrium geometry with each functional, all functionals predict the anion to be unbound with respect to neutral SiH_4. (See Table 2.) As both CH_4 and SiH_4 have filled (Ne, Ar-like) valences, neither displays a formal electron affinity. For SiH_4, only EA_{vert} has any physical meaning, as it represents the magnitude of the temporary (picosecond) electron resonant anion state.

F. Si_2 and Si_2^-.

Our optimized geometries for Si_2 ($X\ ^3\Sigma_g^-$) and Si_2^- ($X\ ^2\Sigma^+_g$) are shown in Figure 5. The geometry closest to experiment for the bond length was at the BHLYP level of theory, which was 0.003 Å longer than Huber and Herzberg's value.[65] Other functionals overestimate experiment by at least 0.025 Å, and even the UCCSD(T)/aug-cc-pV6Z result[34] overestimates by 0.006 Å. For the anion, the bond length shortens over that of the neutral as the electronic configuration changes from a $\sigma_g^2\Pi_u^2$ configuration to a $\Pi_u^4\sigma_g$ configuration, which corresponds to a $X\ ^2\Sigma_g^+$ state. The $^2\Pi_u$ state arising from a $\Pi_u^3\sigma_g^2$ configuration is known from experiment[10-12] to lie just 0.025 eV higher. Our predicted bond lengths for the anion are in reasonable agreement with experimental value r_e = 2.127 Å for $^2\Sigma_g^+$ as given by Nimlos, Harding and Ellison.[15] This is also similar to r_e = 2.1104 Å as derived by Liu and Davies.[11,12]

Our predicted EA_{ad} values for Si_2 ranged from 1.79 to 2.90 eV, among which the BHLYP predicts the smallest (1.79 eV). The EA_{zero} value predicted by BP86 was 0.07 eV larger than the experimental value: 2.202 ± 0.01 eV.[10,15,16] Our DFT results are within 0.23 eV of experiment for this system with BP86, BLYP, and B3LYP. We also note the QCISD(T)/17s,6p,3d,1f value EA = 2.09 eV as obtained by Raghavachari and Rohlfing.[18]

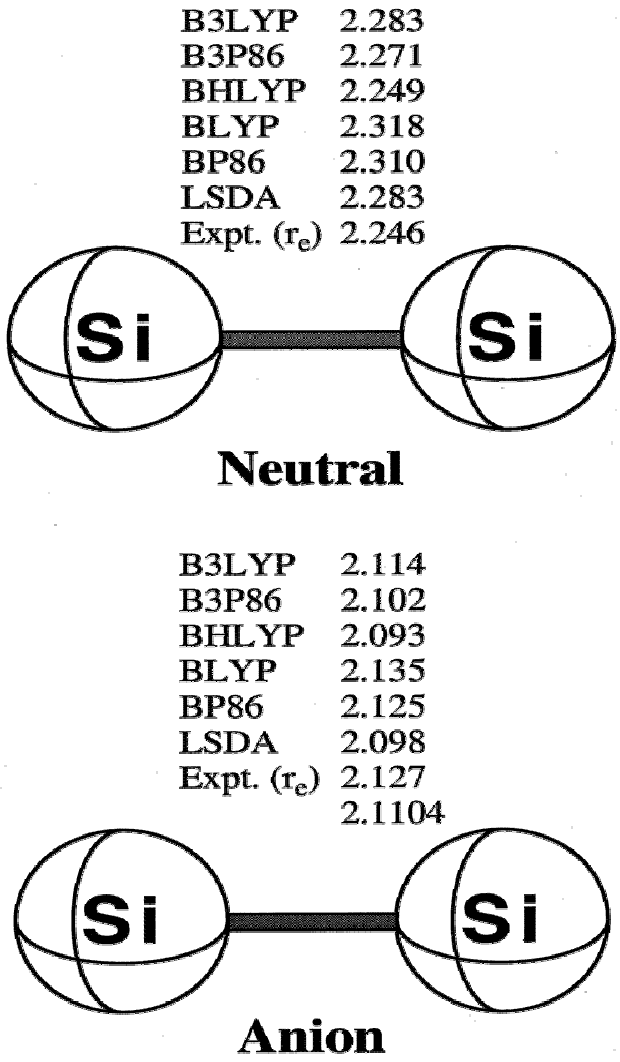

Figure 5 The molecular geometries for the X $^3\Sigma_g^-$ state of Si_2 and the X $^2\Sigma_g^-$ state of Si_2^-. Bond lengths are in Å. All results were obtained with the DZP^{++} basis set. Experimental r_e values for Si_2 and Si_2^- are from refs 65, 11, 12, and 15, respectively

The σ_g and σ_u molecular orbitals in the C_2 molecule are extremely close in energy and give rise to two nearly degenerate states: $^3\Pi_u$ and $^1\Sigma_g^+$, with the latter being the ground[65] state by only 716 cm^{-1}. Like many traditional ab initio methods, density functional theory has difficulties in describing ground-state C_2.[47,75-77] Indeed, most

functionals predict the triplet state to be the ground state and result in highly spin contaminated wave functions for the singlet state. However, if one examines the electron affinities for C_2 using the contaminated singlet state results, one finds that the B3LYP, BLYP, and BP86 functionals all predict EAs[78] within 0.3 eV of the experimental value 3.269 eV.[79]

In contrast, the highest occupied σ_u orbital is lower than the analogous σ_g orbital in Si_2, and gives a $^3\Sigma_g^-$ ground state in Si_2,[65] and the same three functionals give EA's within 0.23 eV of the experimental value, with wave functions that do not suffer from virtually any spin contamination effects for the neutral or anion species, despite the mere 0.025 eV X $^2\Sigma_g^+$ - A $^2\Pi_u$ splitting in the anion. Hence, despite the fact that DFT can predict EAs that are tolerable for both C_2 and Si_2, the DFT results for Si_2 appear to be more satisfying from a quantum mechanical point of view.

G. Si_2H and Si_2H^-.

There are three possible structures for neutral Si_2H: linear ($D_{\infty h}$), bent (C_s), and H-bridged (C_{2v}) structures. In 1996, at the CCSD/TZ2P(f,d) level, Ma, Allinger, and Schaefer[30] predicted the lowest energy structure to be C_{2v} (bridged) with a $\tilde{X}^2B_1$ state for neutral Si_2H.[30] The $\tilde{A}$ $^2A_1$ state was suggested to be just 0.07 eV higher than the $^2B_1$ state. These results were compared to the MRCI(D) results of Kalcher and Sax[27] which placed the $^2A_1$ state 0.02 eV lower than the $^2B_1$ state. Most recently, photoelectron spectroscopy experiments by Neumark and co-workers[13] and their QCISD(T)/6-31G* computations assigned the $\tilde{X}$ state to be $^2A_1$, with a 3° smaller Si-H-Si angle than the $\tilde{A}$ $^2B_1$ state, and

an $\tilde{X}$-$\tilde{A}$ splitting of only 0.01 eV by theory and 0.020 ± 0.005 eV by experiment. It is clear that the two electronic states are essentially degenerate.

Our DFT results all show the $^2A_1$ state to have a ~3° smaller Si-H-Si angle ~79° vs ~82° (See Figure 6). The three hybrid functionals place the $^2B_1$ state as the ground state, by 0.008 (B3P86), 0.04 (B3LYP), and 0.12 (BHLYP) eV. While the pure functionals have the $^2A_1$ state lower by 0.0007 (BLYP), 0.04 (BP86), and 0.13 (LSDA) eV. In this work, we report results for both states. Our geometries for the neutral $^2A_1$ state are in general agreement with the QCISD(T)/6-31G* results of Neumark:[13] R_{Si-H} = 1.690 Å, r_{Si-Si} = 2.182 Å, and Si-H-Si = 80.4°. The H-bridged anion has a $^1A_1$ ground state.[27,30] To ensure that the H-bridged anion is the lowest energy Si_2H^- isomer, we optimized linear $SiSiH^-$ ($^1\Sigma^+$), which unlike neutral, linear SiSiH, does not suffer from the Renner effect, and thus remains a linear species. At the B3LYP level, without zero-point correction, we find linear $SiSiH^-$ to be 8.9 kcal/mol (0.4 eV) higher than the H-bridged anion. This is similar to results reported by Kalcher and Sax[27] of 7.3 kcal/mol using MRCI(D). Thus, both the neutral and anion species of Si_2H adopt H-bridged structures.

The B3LYP zero-point corrected adiabatic electron affinities are 2.26 eV ($^2B_1 \leftarrow {}^1A_1$) and 2.31 ($^2A_1 \leftarrow {}^1A_1$) compared to the experimental 2.31 ± 0.01 eV ($^2A_1 \leftarrow {}^1A_1$), given by photoelectron spectroscopy.[13] BP86 and BHLYP ($^2A_1 \leftarrow {}^1A_1$) EA_{zero} values are within ± 0.1 eV of experiment. (See Table 3.) The EA (CCH), which in contrast to Si_2H involves linear neutral and anion species, is larger than that for Si_2H, the former being 2.97 eV.[79]

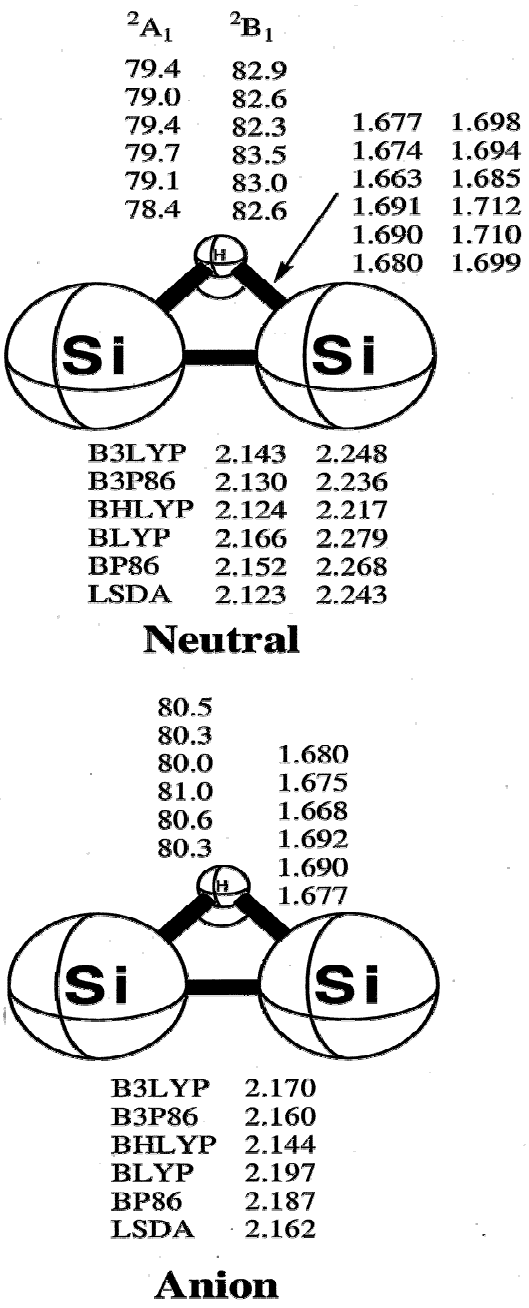

Figure 6 The molecular geometries for the $\tilde{X}^2A_1$ and $\tilde{A}\ ^2B_1$ states of Si_2H and the $\tilde{X}^1A_1$ state of Si_2H^-. Bond lengths and bond angles are in angstroms and degrees, respectively. All results were obtained with the DZP^{++} basis set.

H. Si_2H_2 and $Si_2H_2^-$.

The dibridged C_{2v} or "butterfly" equilibrium geometry of disilyne, Si_2H_2 ($\tilde{X}\,^1A_1$), and its anion, $Si_2H_2^-$ ($\tilde{X}\,^2A_2$) are shown in Figure 7. These molecules are good examples of silicon hydride molecules that show different bonding characteristics from their carbon analogues: linear acetylene, which has no formal EA. For the neutral Si_2H_2, the C_{2v} (dibridged) symmetry structure has been shown to be the most stable form.[21,26,80,81] Our hybrid DFT bond lengths for the neutral species slightly underestimate the experimental[82] Si-H distance but find good agreement for the Si-Si distance. The anion shows longer bond distances, ~0.13 Å for Si-Si, and a ~13° larger H-Si-Si-H torsion angle.

The predicted electron affinities for Si_2H_2 are small; our values ranged from 0.06 to 0.93 eV for the EA_{ad}. The B3LYP level of theory gives 0.45 eV for EA_{zero}, which may be representative of the true electron affinity. The experimental electron affinity is not known, as the anion ($Si_2H_2^-$) has never been detected. Our prediction of a small, but positive EA for Si_2H_2 is in contrast to the conclusion of Kalcher and Sax,[24] who state that "dibridged disilyne...is devoid of any propensity to bind an additional electron". Kalcher and Sax provide no theoretical computations to support this claim.

In Figure 8, we show four isomers of $Si_2H_2^-$. With B3LYP, we find that the disilavinylidene anion is 24.3 kcal/mol lower than the dibridged structure, and thus represents the global minimum for $Si_2H_2^-$. Detachment from the anion to neutral disilavinylidene has an EA_{ad} = 1.86 eV or EA_{zero} = 1.87 eV. This implies that, at the B3LYP level, neutral disilavinylidene lies 10.8 kcal/mol above dibridged Si_2H_2, in good agreement with the higher level 12.3 kcal/mol value reported by Grev and Schaefer.[81]

Our EA_{zero} for disiavinylidene compares well to that of Kalcher and Sax[24] who give a CEPA EA = 1.73 eV.

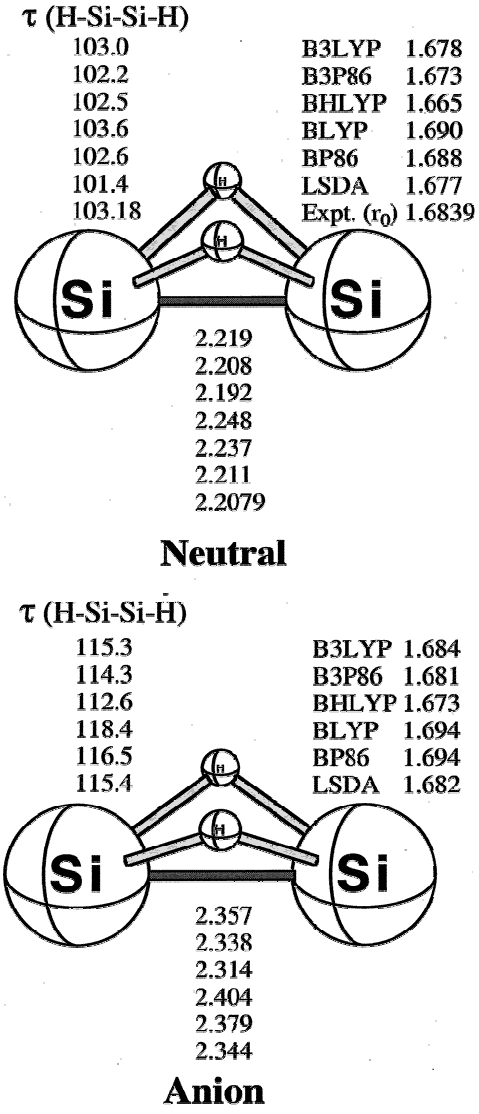

Figure 7 The molecular geometries for the $\tilde{X}^1A_1$ state of dibridged Si_2H_2 and the $\tilde{X}^2A_2$ state of dibridged $Si_2H_2^-$. Bond lengths and bond angles are in angstroms and degrees, respectively. All results were obtained with the DZP^{++} basis set. Experimental r_0 values are from ref 82.

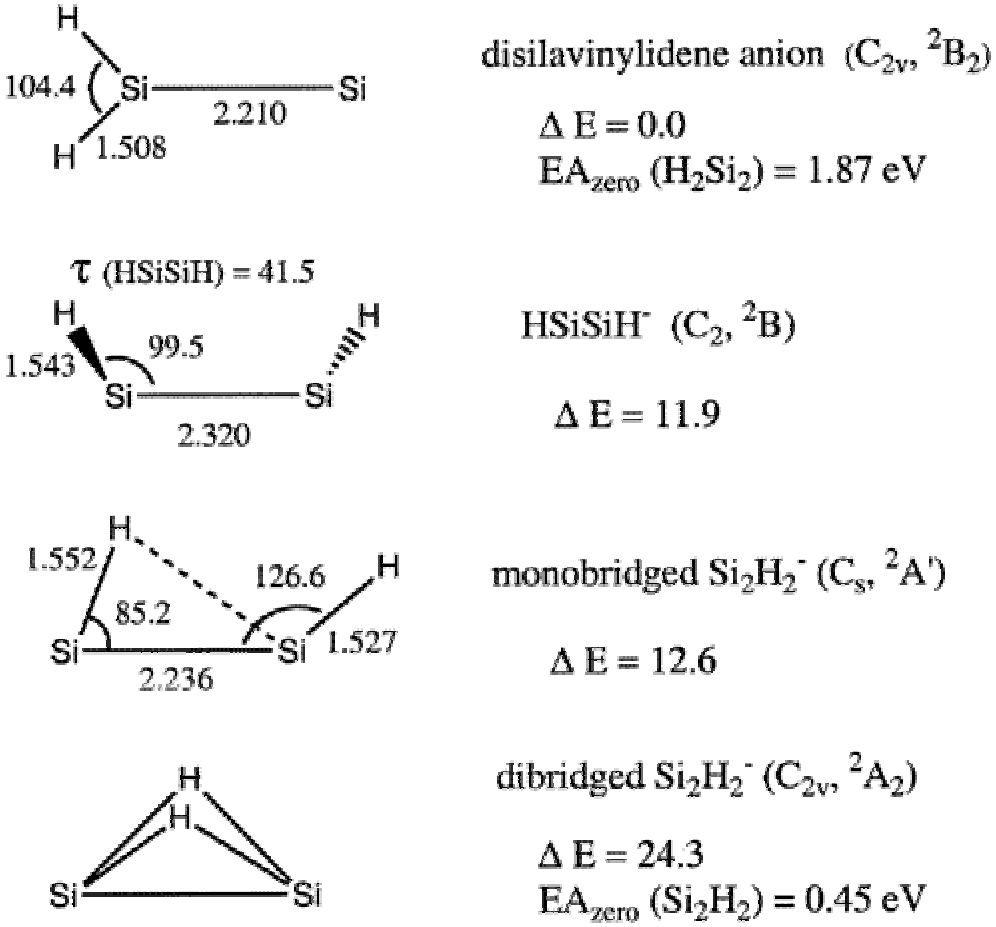

Figure 8 Four structural isomers of $Si_2H_2^-$. All results depicted are at the B3LYP level. For optimized geometries of the dibridged structure, see Figure 7. Relative energies are in kcal/mol and without ZPVE correction. Bond distances are in angstroms and angles in degrees.

Thus, we have two electron affinities for Si_2H_2: EA_{zero} = 0.45 eV, representing electron attachment to the dibridged neutral, and EA_{zero} = 1.87 eV representing electron detachment from the disilyinylidene anion. However, in examining the dibridged $Si_2H_2^-$ anion, we encountered wave function symmetry breaking problems: the UHF solution has

an imaginary b_2 harmonic frequency of 4839i cm^{-1}, with an IR intensity too large to be determined by Gaussian 94. Density functional theory is known to avoid artifactual symmetry breaking in many instances, especially when the exchange functional does not incorporate Hartree-Fock exchange. [83] Thus, it is no surprise that the magnitude of the b_2 mode changed from 4839i (UHF), 819i (BHLYP), 202i (B3LYP), to real values greater than 326 cm^{-1} for the remaining four functionals. Nonetheless, we suspect the B3LYP energetics to be relatively unaffected by the symmetry breaking and hence still recommend EA_{zero} = 0.45 eV for the dibridged neutral.

I. Si_2H_3 and $Si_2H_3^-$.

In 1997, Gong, Guenzburger, and Suitovitch[33] explored five neutral Si_2H_3 isomers: two monobridged isomers, HSiHSiH (C_2) and H_2SiHSi (C_s); a dibridged isomer; a tribridged isomer; and H_3SiSi (C_s). Their ab initio molecular dynamics method found the monobridged HSiHSiH (C_2) isomer to be the lowest energy isomer, just 0.04 eV below the other monobridged isomer, 0.09 eV below the dibridged isomer, and more than 0.39 eV below the remaining two isomers. However, they did not examine the near-planar H_2SiSiH isomer (C_1). G2 results for this isomer show it to be nearly equivalent in energy to the silylsilylidyne, H_3SiSi (C_s) isomer.[23] Kalcher and Sax,[24,85] report an EA of 2.20 eV using CEPA computations between the near-planar neutral H_2SiSiH isomer and a corresponding near-planar anion. They did not report results for other isomers.

It is beyond the scope of this paper to perform a complete investigation of all neutral and anion isomers. However, the previous results just discussed would indicate

that one of monobridged HSiHSiH (C_2), near-planar H_2SiSiH (C_1), or H_3SiSi (C_s) is likely to be the neutral global minimum. In Figure 9, we show neutral and anion results for these three isomers at the B3LYP level. The near-planar C_1 isomer becomes planar with the anion and more than 11 kcal/mol more stable than the other two anion isomers. For the neutral, as first noticed by Curtiss et al.,[23] we find that the near-planar H_2SiSiH and H_3SiSi isomers are nearly equivalent in energy, the former being more stable by just 0.02 kcal/mol. Although our results at the present level of theory cannot definitively conclude which isomer is the most stable, because of the strong preference for the anion to adopt a planar H_2SiSiH^- structure we report only EA results between the planar H_2SiSiH^- isomer and the near-planar H_2SiSiH isomer with all levels of theory. At the B3LYP level only, the EA_{zero} between neutral and anion silylsilylidyne (H_3SiSi) isomers is 1.01 eV.

The near-planar (C_1) structure of Si_2H_3 ($\tilde{X}\ ^2A$) and the planar $Si_2H_3^-$ ($\tilde{X}\ ^1A'$) structures are shown in Figure 10. The most accurate adiabatic electron affinity is likely to come from the B3LYP level of theory, which gives EA_{zero} of 2.21 eV (See Table 3). Note that C_2H_3 also has a C_s, H_2CCH structure for both the neutral and anion, but has a much smaller EA = 0.667 eV.[86]

J. Si_2H_4 and $Si_2H_4^-$.

From two possible C_s (silylsilylene) and C_{2h} (disilene) isomers, previous theoretical work[23,24,84] determined the lowest energy structure of neutral Si_2H_4 to be the C_{2h} isomer. Ernst, Sax, and Kalcher[84] predicted silysilylene to lie 9.1 kcal/mol above disilene with a 19.8 kcal/mol barrier for disilene to silysilylene isomerization. This is in

agreement with our B3LYP results which show that disilene is 6.5 kcal/mol more stable. In the anion, we find that the silylsilylene structure (H_3SiSiH^-, C_s, $^2A'$ ') is slightly lower in energy than the disilene structure ($H_2SiSiH_2^-$), specifically, 2.9 and 1.7 kcal/mol with B3LYP and BP86, respectively (See Figure 11). However, because of the strong preference for the neutral species to adopt the disilene structure, we consider only the EA of disilene at all levels of theory in this present work. Our optimized disilene structures, Si_2H_4 ($\tilde{X}\ ^1A_g$) and $Si_2H_4^-$ ($\tilde{X}\ ^2A_g$) are shown in Figure 12. The neutral and anion geometries differ significantly. In the anion, the Si-Si bond lengthens by ~0.16 Å and the Si-Si-H angle decreases from about 118° to 105°. The $Si_2H_4^-$ anion appears to be two SiH_2 units loosely bound (Si-Si ≈2.33 Å) by a single electron between two overlapping b_1 orbitals. (Recall that the b_1 orbital in SiH_2 is the LUMO and is oriented perpendicular to the molecular plane). On the other hand, neutral Si_2H_4 is bound by the overlap of two filled (in-plane) a_1 orbitals from each SiH_2 unit leaving Si_2H_4 nearly planar (Si-Si ≈2.17 Å). For Si_2H_4, our optimized geometries agree with Curtiss et al.'s[23] MP2/6-31G* results, which give Si-Si = 2.164 Å.

In contrast to Si_2H_4, ethylene has D_{2h} symmetry. Whereas planar ethylene has no electron affinity,[87] Si_2H_4 has a rather large electron affinity, specifically, EA_{ad} = 1.28 eV at the B3LYP level of theory (see Table 3). This is similar to the B3LYP EA_{ad} for a single SiH_2 unit, 1.17 eV. The EA_{ad} values for Si_2H_4 ranged from 1.13 to 1.68 eV, 0.28 to 1.08 eV for $EA_{vert,}$ and 1.59 to 2.37 eV for VDE, which agree well with previous CEPA predictions.[24] There are no experimental electron affinities available for Si_2H_4. We predict the Si_2H_4 (disilene) electron affinity to be 1.34 eV, using our B3LYP EA_{zero} result. The EA_{zero} between neutral and anion silylsilylene (H_3SiSiH) isomers is 1.71 eV.

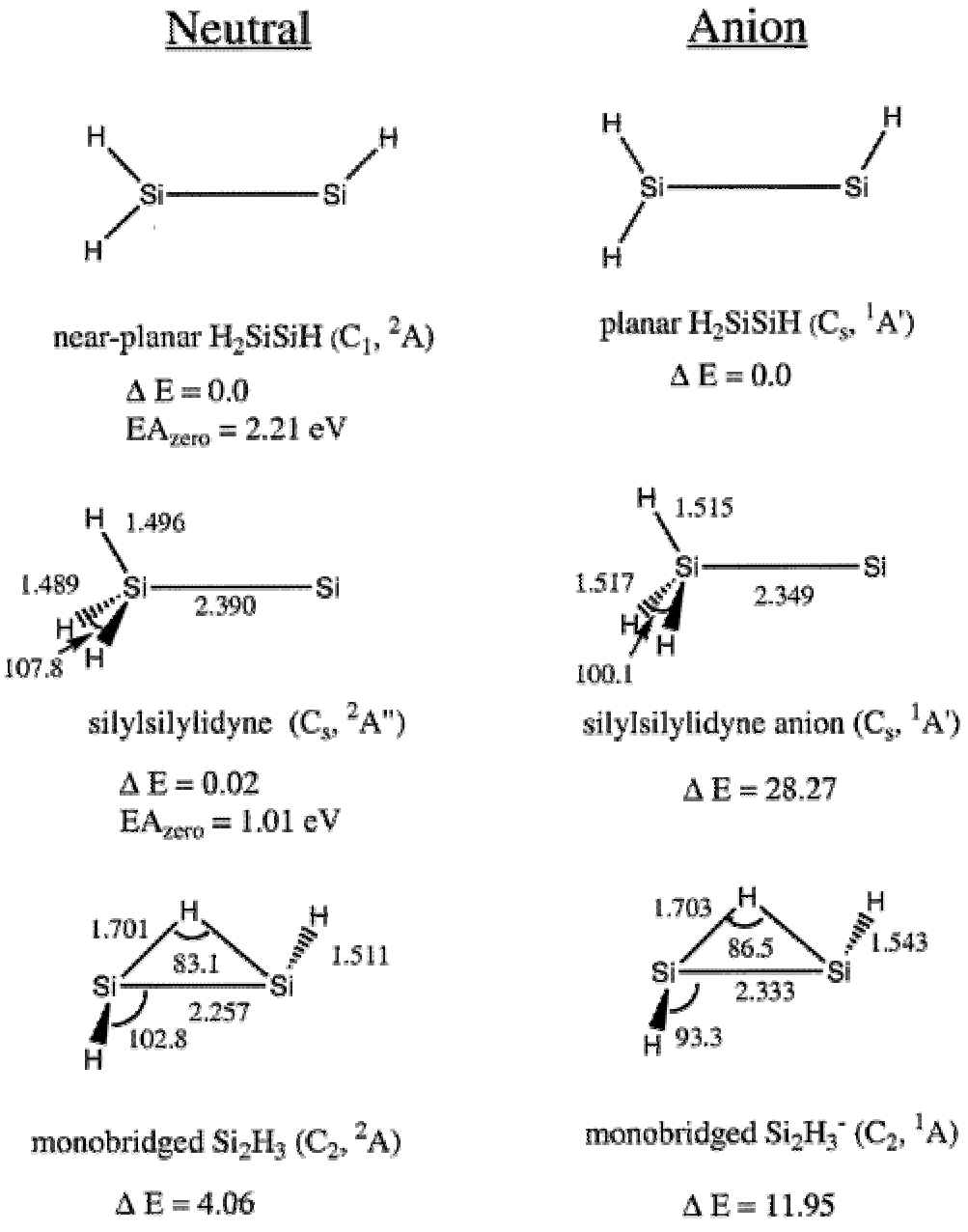

Figure 9 Three structural isomers of each Si_2H_3 and $Si_2H_3^-$. All results depicted are at the B3LYP level. For optimized geometries of the near-planar and planar H_2SiSiH/H_2SiSiH^- isomers, see Figure 10. Relative energies are in kcal/mol and without ZPVE correction. Bond distances are in angstroms and angles in degrees.

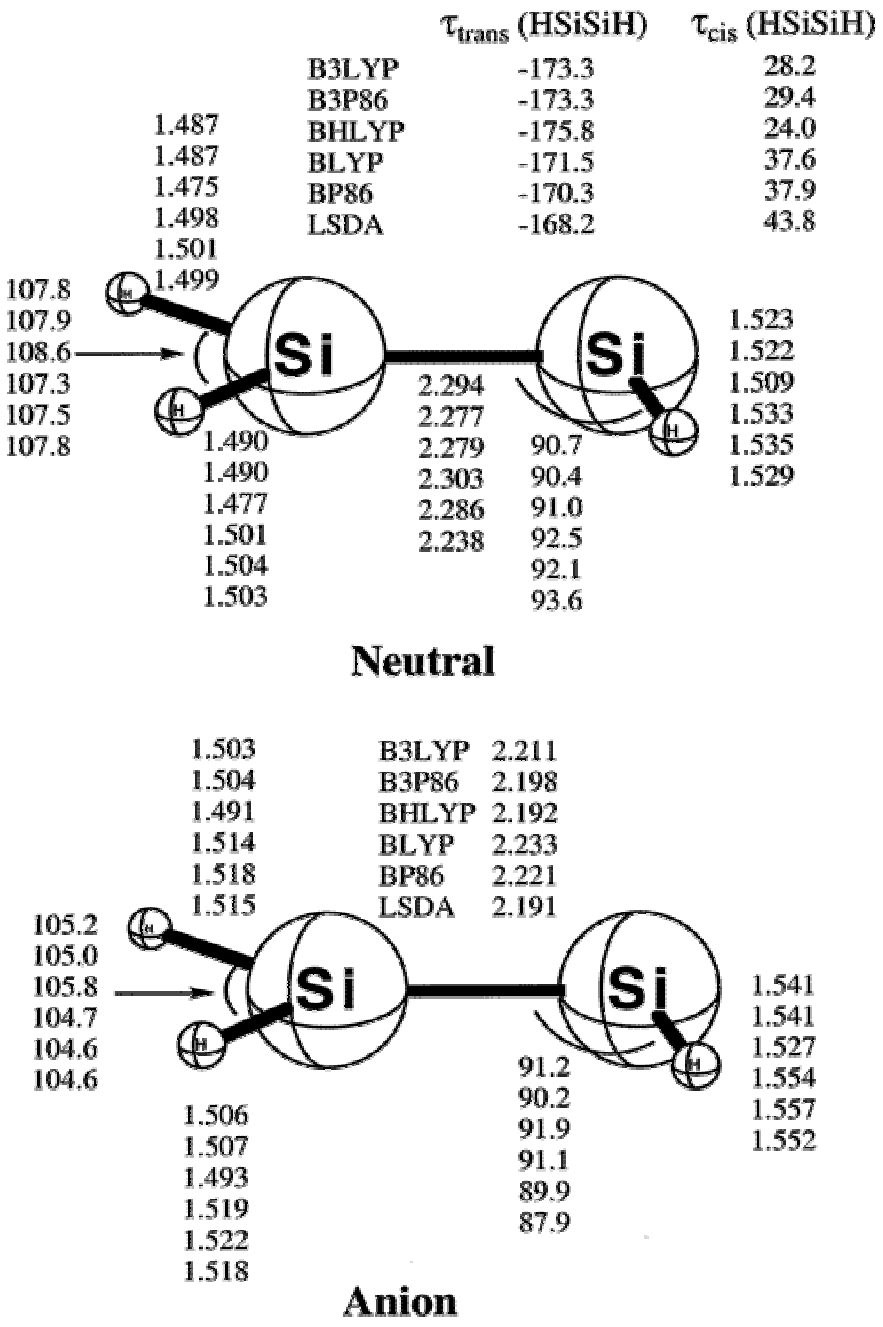

Figure 10 The molecular geometries for the $\tilde{X}^2A$ state of near-planar Si_2H_3 and the $\tilde{X}^1A$ state of planar $Si_2H_3^-$. Bond lengths and bond angles are in angstroms and degrees, respectively. All results were obtained with the DZP^{++} basis set.

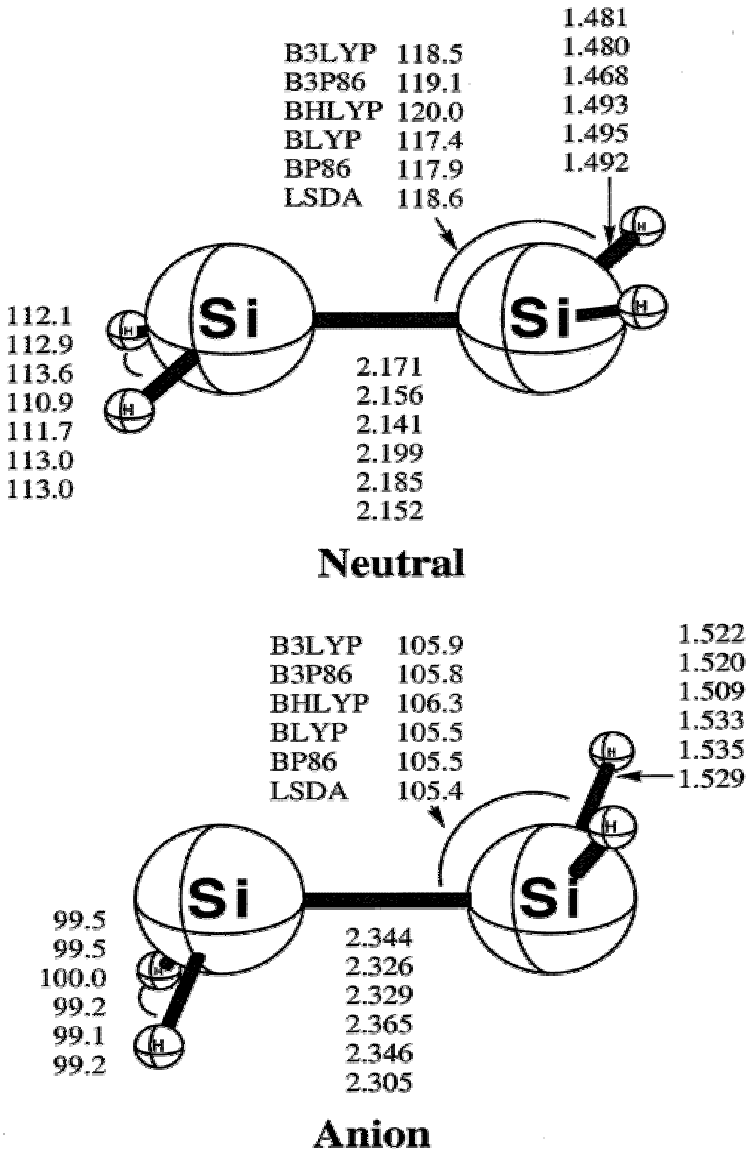

Figure 12 The molecular geometries for the $\tilde{X}^1A_g$ state of Si_2H_4 and the $\tilde{X}^2A_g$ state of $Si_2H_4^-$. Bond lengths and bond angles are in angstroms and degrees, respectively. All results were obtained with the DZP^{++} basis set.

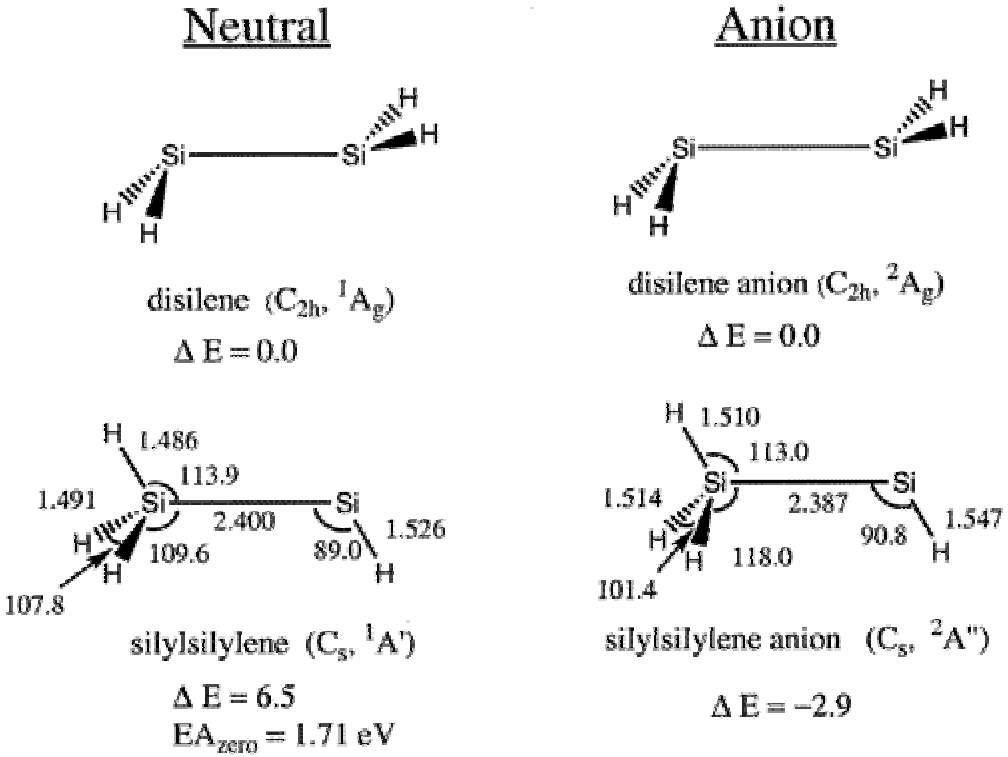

Figure 11 Two structural isomers of each Si_2H_4 and $Si_2H_4^-$. All results depicted are at the B3LYP level. For optimized geometries of the disilene isomers see Figure 12. Relative energies are in kcal/mol and without ZPVE correction. Bond distances are in angstroms and angles in degrees.

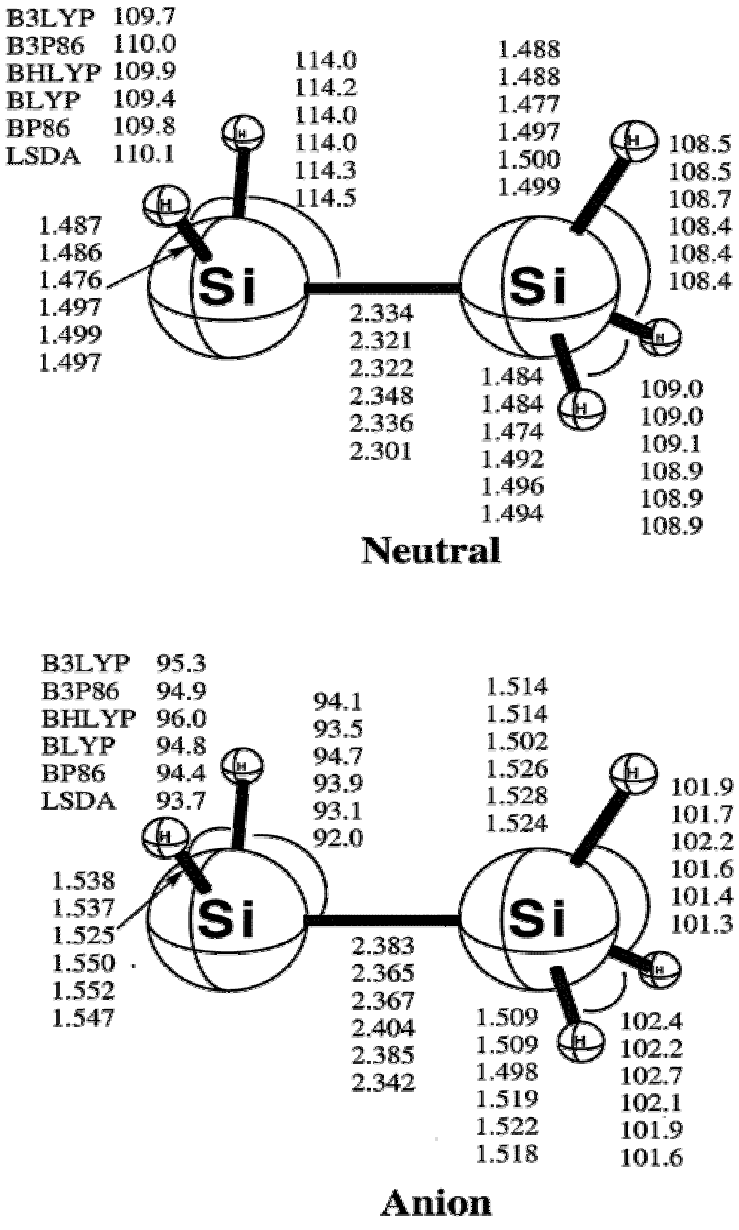

Figure 13 The molecular geometries for the $\tilde{X}^2A'$ state of Si_2H_5 and the $\tilde{X}^1A'$ state of $Si_2H_5^-$. Bond lengths and bond angles are in angstroms and degrees, respectively. All results were obtained with the DZP^{++} basis set.

The best adiabatic electron affinity is expected to be 1.85 eV given by B3LYP, $EA_{zero.}$ Other functionals ranged from 1.61 (BHLYP) to 2.50 eV (LSDA) for EA_{zero}, and 0.96 to 1.84 eV for EA_{vert} and 2.22 to 3.16 eV for the VDE.

L. Si_2H_6 and $Si_2H_6^-$.

The D_{3d} symmetry disilane, Si_2H_6 ($\tilde{X}\ ^1A_{1g}$) and $Si_2H_6^-$ ($\tilde{X}\ ^2A_{2u}$) optimized geometries are shown in Figure 14. All of our gradient functionals overestimate the experimental bond distance extracted from Shotten, Lee, and Jones's Raman spectroscopy results.[17] The Si-Si bond distances with the BHLYP and B3P86 level of theory are only 0.005 Å longer than experiment, 2.327 Å. Our DFT average bond angle of equatorial ∠HSiH was 108.6° compared to the experimental 107.8°. Our results are close to previous UCCSD(T)/aug-cc-pVQZ results,[34] which give $r_{Si\text{-}Si}$ = 2.346 Å, $r_{Si\text{-}H}$ = 1.484 Å, and H-Si-H = 108.7°. The anion displays a similar geometry with a Si-Si distance which is about 0.07 Å longer. It is interesting to note that previous UHF/DZPD results[28] show that D_{3d} $Si_2H_6^-$ has two doubly degenerate imaginary frequencies and a long Si-Si bond of 3.423 Å. In contrast, all our DFT results for the D_{3d} anion show it to be a minimum with a much more reasonable Si-Si length of about 2.4 Å.

Our predicted adiabatic electron affinity for disilane is -0.61 eV (B3LYP), and unbound with each functional (see Table 3). As one might expect, there are no experimental electron affinities available, as is the case for C_2H_6, and the only relevant theoretical results are the EA_{vert}, as with SiH_4.

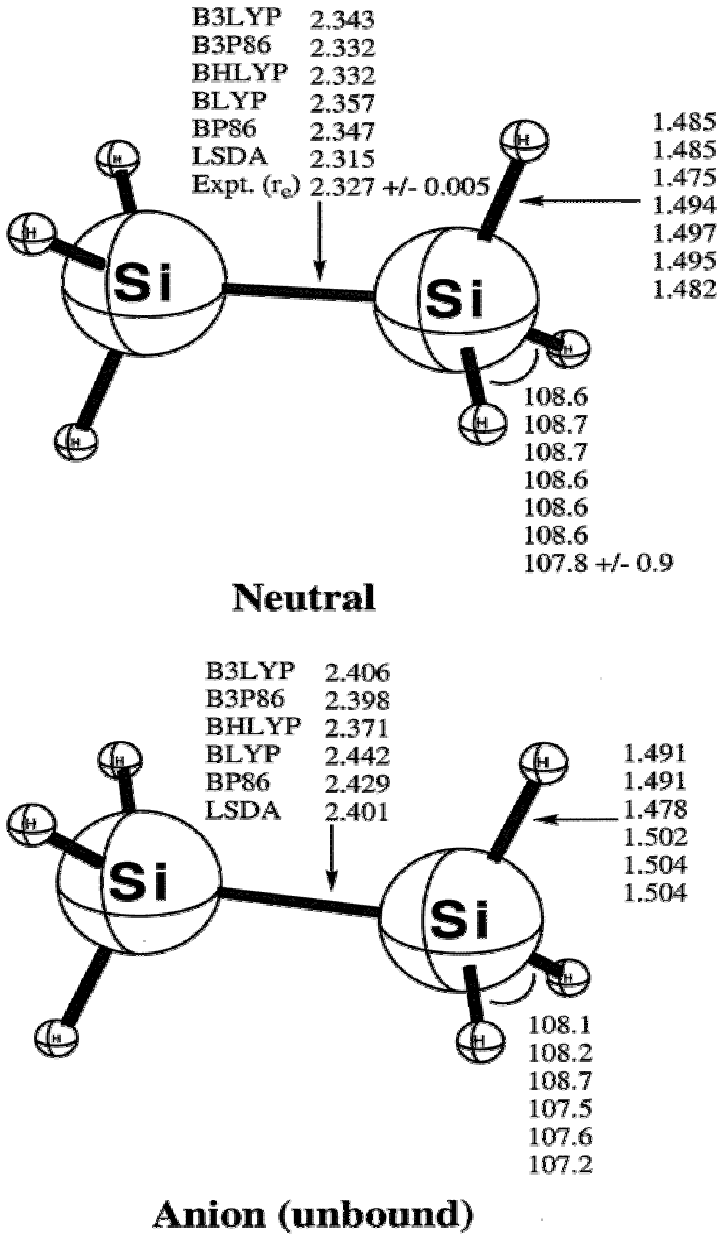

Figure 14 The molecular geometries for the $\tilde{X}^1A_{1g}$ state of Si_2H_6 and the unbound $\tilde{X}^2A_{2u}$ state of $Si_2H_6^-$. Bond lengths and bond angles are in angstroms and degrees, respectively. All results were obtained with the DZP^{++} basis set. Experimental r_0 values are from ref 17, but r_0(Si-H) is an assumed value.

Table 3.2.: The Adiabatic Electron Affinity (EA_{ad}), Zero-Point Corrected EA_{ad} (EA_{zero}), Vertical Electron Affinity (EA_{vert}), and the Vertical Detachment Energy (VDE) for SiH_n (n = 1-4) Species, Presented in eV (kcal/mol in Parentheses)

Species	Method	EA_{ad}	EA_{zero}	EA_{vert}	VDE
SiH	B3LYP	1.28(29.6)	1.30(29.9)	1.28(29.5)	1.29(29.7)
	B3P86	1.89(43.7)	1.90(43.9)	1.89(43.6)	1.90(43.8)
	BHLYP	1.11(25.6)	1.12(25.9)	1.11(25.5)	1.12(25.8)
	BLYP	1.16(26.8)	1.17(27.0)	1.16(26.7)	1.17(26.9)
	BP86	1.48(34.0)	1.49(34.3)	1.47(33.9)	1.48(34.1)
	LSDA	1.89(43.7)	1.90(43.9)	1.89(43.6)	1.90(43.8)
	CCSD(T)	1.248(28.8)	1.259(29.0)		
	exptl[a]		1.277 ± 0.009		1.276 ± 0.006
SiH_2	B3LYP	1.17(27.0)	1.20(27.6)	1.16(26.8)	1.18(27.3)
	B3P86	1.76(40.7)	1.79(41.2)	1.75(40.4)	1.77(40.9)
	BHLYP	1.00(23.2)	1.03(23.8)	0.99(22.9)	1.02(23.5)
	BLYP	1.05(24.3)	1.08(24.8)	1.04(24.0)	1.06(24.5)
	BP86	1.34(31.0)	1.37(31.5)	1.33(30.8)	1.35 (31.2)
	LSDA	1.74(40.1)	1.76(40.6)	1.73(39.9)	1.75(40.3)
	exptl[b]		1.124 ± 0.020		1.124 ± 0.003
SiH_3	B3LYP	1.40(32.2)	1.45(33.4)	0.96(22.0)	1.91(44.0)
	B3P86	1.89(43.5)	1.94(44.7)	1.43(32.9)	2.42(55.9)
	BHLYP	1.17(26.9)	1.22(28.1)	0.72(16.5)	1.68(38.8)
	BLYP	1.31(30.3)	1.37(31.5)	0.84(19.4)	1.81(41.8)
	BP86	1.49(34.5)	1.55(35.7)	1.05(24.3)	2.02(46.6)
	LSDA	2.02(46.5)	2.06(47.6)	1.57(36.3)	2.55(58.7)
	exptl[c]		1.406 ± 0.014		
SiH_4	B3LYP	-0.74(-17.0)	-0.73(-16.8)	-0.74(-17.0)	-0.74(-17.0)
	B3P86	-0.32(-7.3)	-0.30(-7.0)	-0.32(-7.3)	-0.32(-7.3)
	BHLYP	-0.91(-21.1)	-0.91(-21.0)	-0.91(-21.1)	-0.91(-21.1)
	BLYP	-0.80(-18.4)	-0.79(-18.2)	-0.80(-18.4)	-0.80(-18.4)
	BP86	-0.64(-14.7)	-0.62(-14.4)	-0.64(-14.7)	-0.63(-14.6)
	LSDA	-0.28(-6.5)	-0.26(-6.1)	-0.28(-6.5)	-0.28(-6.4)

[a] Reference 4. [b] Reference 4. [c] Reference 7.

Table 3.3.: The Adiabatic Electron Affinity (EA_{ad}), Zero-point Corrected EA_{ad} (EA_{zero}), Vertical Electron Affinity (EA_{vert}), and the Vertical Detachment Energy (VDE) for Si_2H_n (n = 0-6) Species, Presented in eV (kcal/mol in Parentheses)

species	method	EA_{ad}	EA_{zero}	EA_{vert}	VDE
Si_2	B3LYP	2.06(47.5)	2.05(47.4)	1.86(42.9)	2.28(52.6)
	B3P86	2.65(61.2)	2.65(61.1)	2.44(56.4)	2.89(66.6)
	BHLYP	1.79(41.3)	1.78(41.1)	1.60(36.9)	2.00(46.1)
	BLYP	1.98(45.6)	1.97(45.4)	1.77(40.8)	2.08(47.9)
	BP86	2.28(52.6)	2.27(52.4)	2.07(47.6)	2.28(52.7)
	LSDA	2.90(66.8)	2.89(66.7)	2.66(61.3)	3.16(72.8)
	exptl[a]		2.202 ± 0.010		
Si_2H ($^2B_1 \leftarrow {}^2A_1$)	B3LYP	2.27(52.3)	2.26(52.1)	2.22(51.2)	2.31(53.3)
	B3P86	2.86(65.8)	2.85(65.6)	2.81(64.8)	2.90(66.9)
	BHLYP	2.08(48.0)	2.07(47.8)	2.04(47.0)	2.13(49.1)
	BLYP	2.13(49.0)	2.12(48.9)	2.08(48.0)	2.17(50.1)
	BP86	2.42(55.8)	2.41(55.6)	2.37(54.7)	2.46(56.8)
	LSDA	3.00(69.1)	2.99(68.9)	2.95(68.0)	3.05(70.3)
Si_2H ($^2A_1 \leftarrow {}^1A_1$)	B3LYP	2.31(53.2)	2.31(53.3)	2.30(53.1)	2.31(53.3)
	B3P86	2.86(66.0)	2.87(66.1)	2.86(65.8)	2.90(66.9)
	BHLYP	2.20(50.8)	2.21(50.9)	2.20(50.7)	2.13(49.1)
	BLYP	2.13(49.0)	2.13(49.1)	2.12(48.8)	2.17(50.1)
	BP86	2.38(54.8)	2.38(54.9)	2.37(54.6)	2.46(56.8)
	LSDA	2.87(66.2)	2.87(66.2)	2.86(65.9)	3.05(70.3)
	exptl[b]		2.31 ± 0.10		
Si_2H_2 (dibridged)	B3LYP	0.34(7.7)	0.45(10.4)	0.23(5.3)	0.47(10.8)
	B3P86	0.91(21.0)	1.01(23.4)	0.80(18.5)	1.04(24.0)
	BHLYP	0.06(1.4)	0.18(4.1)	-0.04(-0.9)	0.18(4.2)
	BLYP	0.29(6.8)	0.38(8.7)	0.18(4.3)	0.44(10.1)
	BP86	0.57(13.1)	0.65(14.9)	0.46(10.6)	0.70(16.2)
	LSDA	0.93(21.5)	1.00(23.1)	0.83(19.0)	1.07(24.6)
Si_2H_3	B3LYP	2.21(51.0)	2.21(51.0)	2.09(48.2)	2.28(52.7)
	B3P86	2.78(64.1)	2.78(64.1)	2.65(61.1)	3.65(84.3)
	BHLYP	2.00(46.0)	1.99(45.9)	1.88(43.4)	2.91(67.1)
	BLYP	2.09(48.1)	2.09(48.2)	1.93(44.5)	2.16(49.9)
	BP86	2.35(54.3)	2.35(54.3)	2.18(50.3)	2.43(56.1)
	LSDA	2.92(67.4)	2.92(67.3)	2.68(61.9)	3.02(69.7)
Si_2H_4 (disilene)	B3LYP	1.28(29.5)	1.34(31.0)	0.58(13.5)	1.80(41.4)
	B3P86	1.83(42.2)	1.89(43.6)	1.08(24.9)	2.37(54.6)
	BHLYP	1.16(26.8)	1.23(28.4)	0.28(6.4)	1.75(40.3)
	BLYP	1.13(25.9)	1.19(27.4)	0.54(12.5)	1.59(36.7)
	BP86	1.36(31.4)	1.42(32.8)	0.74(17.1)	1.85(42.7)
	LSDA	1.68(38.8)	1.74(40.1)	1.01(23.3)	2.19(50.6)

Si_2H_5 (disylyl radical)	B3LYP	1.80(41.5)	1.85(42.7)	1.20(27.6)	2.46(56.8)
	B3P86	2.32(53.5)	2.37(54.6)	1.70(39.1)	3.01(69.4)
	BHLYP	1.56(36.0)	1.61(37.2)	0.96(22.1)	2.22(51.3)
	BLYP	1.71(39.5)	1.77(40.8)	1.11(25.7)	2.37(54.6)
	BP86	1.92(44.3)	1.97(45.5)	1.30(30.1)	2.60(60.1)
	LSDA	2.46(56.6)	2.50(57.6)	1.84(42.4)	3.16(72.8)
Si_2H_6	B3LYP	-0.61(-14.1)	-0.53(-12.3)	-0.63(-14.5)	-0.59(-13.5)
	B3P86	-0.16(-3.7)	-0.08(-1.8)	-0.18(-4.1)	-0.13(-3.0)
	BHLYP	-0.88(-20.4)	-0.83(-19.2)	-0.89(-20.6)	-0.87(-20.2)
	BLYP	-0.61(-14.0)	-0.50(-11.6)	-0.63(-14.6)	-0.56(-13.0)
	BP86	-0.42(-9.8)	-0.32(-7.4)	-0.49(-10.4)	-0.38(-8.8)
	LSDA	-0.08(-1.8)	0.05(1.0)	-0.11(-2.6)	-0.02(-0.5)

[a] Reference 10.[b] Reference 13.

Conclusions

On the basis of the known experimental geometries (SiH, SiH^-, SiH_2, SiH_3, SiH_4, Si_2, Si_2^-, Si_2H_4, Si_2H_6) of these systems, we conclude that the DZP^{++} BHLYP level of theory predicts the best geometries, as is the case for other inorganic species.[31,39-43] The average bond distance error with BHLYP were less than 0.01 Å, compared to all experimental values. In general, the hybrid functionals gave better results than the pure functionals; pure functionals often overestimated bond lengths, by as much as 0.02 Å in some cases.

For electron affinities, the average absolute error (EA_{zero} vs exptl) with each functional in order is B3LYP (0.06 eV) < BLYP (0.12 eV) < BP86 (0.15 eV) < BHLYP (0.19 eV) < B3P86 (0.57 eV) < LSDA (0.63 eV). The average maximum error for each functional in order is B3LYP (0.15 eV) < BLYP (0.23 eV) < BP86 (0.25 eV) < BHLYP (0.42 eV) < B3P86 (0.67 eV) < LSDA (0.69 eV). For all but BHLYP and BLYP, average absolute errors between experiment and our predicted EA_{ad} are better than those just

given for EA_{zero} by 0.01-0.02 eV. Clearly, B3LYP is a superior choice for examining the electron affinities of silicon hydride systems. Using B3LYP EA_{zero} values, we predict electron affinities for dibridged Si_2H_2 (0.45 eV), Si_2H_3 (2.21 eV), disilene Si_2H_4 (1.34 eV), and the disilyl radical Si_2H_5 (1.85 eV). For disilavinylidene, Si_2H_2, we find an EA_{zero} = 1.87 eV, for silylsilylidyne, H_3SiSi an EA_{zero} = 1.01 eV, and for silylsilylene an EA_{zero} = 1.71 eV. These values are probably within 0.1 eV of the true electron affinities. It is also comforting to see that all of B3LYP, BLYP, BP86, and BHLYP methods have absolute average errors of less than 0.2 eV, despite low-lying excited states encountered in some silicon hydride systems (i.e., Si_2^- and Si_2H). It is not necessarily surprising that BHLYP predicts the best geometries but not the best electron affinities. The BHLYP functional has significant Hartree-Fock exchange which increases the method error in energy predictions, while on the other hand offsetting the density functional tendency to overestimate bond-lengths (as noted in the preceding paragraph).

Comparing the geometries and electron affinities of the silicon hydride systems to corresponding carbon analogues, shows important differences. For example, C_2H_4 and Si_2H_4 have very different bonding characteristics and show different electron affinities. The C_2H_4 has D_{2h} symmetry whereas Si_2H_4 has C_{2h} symmetry, and Si_2H_4 has an electron affinity of 1.34 eV (B3LYP) whereas ethylene has no electron affinity. Furthermore, one can see that Si_2 and C_2 have a rather large electron affinity difference, about one eV. Some analogues are similar in nature in terms of geometry and/or electron affinities: Si vs C, SiH vs CH, SiH_4 vs CH_4, Si_2H_5 vs C_2H_5, Si_2H_6 vs C_2H_6. We hope that these theoretical predictions will provide motivation for the experimental study of the lesser characterized silicon hydride systems, especially in instances such as $Si_2H_2^-$, $Si_2H_3^-$, and $Si_2H_4^-$ where

the anion potential energy surface does not mirror that of the corresponding neutral species. It seems clear that DFT methods would also be useful in predictions of the electron affinities of the larger silicon hydrides, beginning with the Si_3H_x series.

Acknowledgement

This work is supported by the U.S. National Science Foundation Grant CHE-9815397. C.H.P. thanks Brian Hoffman for his help in the beginning stage of this work. J.C.R.K. thanks Christine Rienstra-Kiracofe for research assistance.

BIBLIOGRAPHY

1. Lickiss, P. D. In *Encyclopedia of Inorganic Chemistry*; King, R. B., Ed.; John Wiley & Sons: Chichester, 1994; Vol. 7, 3770.

2. Jasinski, J. M.; Meyerson, B. S.; Scott, B. A. *Annu. Rev. Phys. Chem.* **1987**, *38*, 109.

3. Dubois, I. *Can. J. Phys.* **1968**, *46*, 2485.

4. Kasdan, A.; Herbst, E.; Lineberger, W. C. *J. Chem. Phys.* **1975**, *62*, 541.

5. Brown, J. M.; Robinson, D. *Mol. Phys.* **1984**, *51*, 883.

6. Ohno, K.; Matsuura, H.; Endo, Y.; Hirota, E. *J. Mol. Spectrosc.* **1985**, *111*, 73.

7. Nimlos, M. R.; Ellison, G. B. *J. Am. Chem. Soc.* **1986**, *108*, 6522.

8. Boo, B. H.; Armentrout, P. B. *J. Am. Chem. Soc.* **1987**, *109*, 3549.

9. Berkowitz, J.; Greene, J. P.; Cho, H.; Ruščić, B. *J. Chem. Phys.* **1987**, *86*, 1235.

10. Arnold, C. C.; Kitsopoulos, T. N.; Neumark, D. M. *J. Chem. Phys.* **1993**, *99*, 766.

11. Liu, Z.; Davies, P. B. *Phys. Rev. Lett.* **1996**, *76*, 596.

12. Liu, Z.; Davies, P. B. *J. Chem. Phys.* **1996**, *105*, 3443.

13. Xu, C.; Taylor, T. R.; Burton, G. R.; Neumark, D. M. *J. Chem. Phys.* **1998**, *108*, 7645.

14. Scheer, M.; Bilodeau, R. C.; Brodie, C. A.; Haugen, H. K. *Phys. Rev. A.* **1998**, *58*, 2844.

15. Nimlos, M. R.; Harding, L. B.; Ellison, G. B. *J. Chem. Phys.* **1987**, *87*, 5116.

16. Kitsopoulos, T. N.; Chick, C. J.; Zhao, Y.; Neumark, D. M. *J. Chem. Phys.* **1991**, *95*, 1441.

17. Shotten, K. C.; Lee, A. G.; Jones, W. J. *J. Raman Spectrosc.* **1973**, *1*, 243.

18. Raghavachari, K.; Rohlfing, C. M. *J. Chem. Phys.* **1991**, *94*, 3670.

19. Viswanathan, R.; Thompson, D. L.; Raff, L. M. *J. Chem. Phys.* **1984**, *80*, 4230.

20. Allen, W. D.; Schaefer, H. F. *Chem. Phys.* **1986**, *108*, 243.

21. Colegrove, B. T.; Schaefer, H. F. *J. Phys. Chem.* **1990**, *94*, 5593.

22. Shen, M.; Schaefer, H. F. *Mol. Phys.* **1992**, *76*, 467.

23. Curtiss, L. A.; Raghavachari, K.; Deutsch, P. W.; Pople, J. A. *J. Chem. Phys.* **1991**, *95*, 2433.

24. Kalcher, J.; Sax, A. F. *Chem. Phys. Lett.* **1992**, *192*, 451.

25. Becerra, R.; Walsh, R. *J. Phys. Chem.* **1992**, *96*, 10856.

26. Hühn, M. M.; Amos, R. D.; Kobayashi, R.; Handy, N. C. *J. Chem. Phys.* **1993**, *98*, 7107.

27. Kalcher, J.; Sax, A. F. *Chem. Phys. Lett.* **1993**, *215*, 601.

28. Tada, T.; Yoshimura, R. *J. Phys. Chem.* **1993**, *97*, 1019.

29. Taketsugu, T.; Gordon, M. S. *J. Phys. Chem.* **1995**, *99*, 8462.

30. Ma, B.; Allinger, N. L.; Schaefer, H. F. *J. Chem. Phys.* **1996**, *105*, 5731.

31. King, R. A.; Mastryukov, V. S.; Schaefer, H. F. *J. Chem. Phys.* **1996**, *105*, 6880.

32. Yamaguchi, Y.; Van Huis, T. J.; Sherrill, C. D.; Schaefer, H. F. *Theor. Chem. Acc.* **1997**, *97*, 341.

33. Gong, X. G.; Guenzburger, D.; Saitovitch, E. B. *Chem. Phys. Lett.* **1997**, *275*, 392.

34. Feller, D.; Dixon, D. A. *J. Phys. Chem.* **1999**, *103*, 6413.

35. Jursic, B. S. *J. Mol. Struct.* (*THEOCHEM*) **2000**, *497*, 65.

36. Aarset, K.; Császár, A. G.; Sibert, E. L.; Allen, W. D.; Schaefer, H. F.; Klopper, W.; Noga, J. *J. Chem. Phys.* **2000**, *112*, 4053.

37. Kutzelnigg, W. *Angew. Chem.*, *Int. Ed. Engl.* **1984**, *23*, 272.

38. Sannigrahi, A. B.; Nandi, P. K. **1992**, *188*, 575.

39. King, R. A.; Galbraith, J. M.; Schaefer, H. F. *J. Phys. Chem.* **1996**, *100*, 6061.

40. Tschumper, G. S.; Fermann, J. T.; Schaefer, H. F. *J. Chem. Phys.* **1996**, *104*, 3676.

41. Van Huis, T. J.; Galbraith, J. M.; Schaefer, H. F. *Mol. Phys.* **1996**, *89*, 607.

42. King, R. A.; Pettigrew, N. D.; Schaefer, H. F. *J. Chem. Phys.* **1997**, *107*, 8536.

43. Pak, C.; Xie, Y.; Van Huis, T. J.; Schaefer, H. F. *J. Am. Chem. Soc.* **1998**, *120*, 11115.

44. Brinkmann, N. R.; Tschumper, G. S.; Schaefer, H. F. *J. Chem. Phys.* **1999**, *110*, 6240.

45. Brown, S. T.; Rienstra-Kiracofe, J. C.; Schaefer, H. F. *J. Phys. Chem. A.* **1999**, *103*, 4065.

46. Rienstra-Kiracofe, J. C.; Graham, D. D.; Schaefer, H. F. *Mol. Phys.* **1998**, *94*, 767.

47. Tschumper, G. S.; Schaefer, H. F. *J. Chem. Phys.* **1997**, *107*, 2529.

48. Becke, A. D. *Phys. Rev. A.* **1988**, *38*, 3098.

49. Lee, C.; Yang, W.; Parr, R. G. *Phys. Rev. B*. **1988**, *37*, 785.

50. Becke, A. D. *J. Chem. Phys.* **1993**, *98*, 1372.

51. Becke, A. D. *J. Chem. Phys.* **1993**, *98*, 5648.

52. Perdew, J. P. *Phys. Rev. B.* **1986**, *33*, 8822; *34*, 7046.

53. Vosko, S. H.; Wilk, L.; Nusair, M. *Can. J. Phys.* **1980**, *58*, 1200.

54. Slater, J. C. *Quantum Theory of Molecular and Solids: The Self-Consistent Field for Molecular and Solids*; McGraw-Hill: New York, 1974; Vol. IV.

55. Kohn, W.; Sham, L. J. *Phys. Rev A.* **1965**, *140*, 1133.

56. Frisch, M. J.; Trucks, G. W.; Schlegel, H. B.; Gill, P. M. W.; Johnson, B. G.; Robb, M. A.; Cheeseman, J. R.; Keith, T. A.; Petersson, G. A.; Montgomery, J. A.; Raghavachari, K.; Al-Laham, M. A.; Zakrzewski, V. G.; Ortiz, J. V.; Foresman, J. B.; Cioslowski, J.; Stefanov, B. B.; Nanayakkara, A.; Challacombe, M.; Peng, C. Y.; Ayala, P. Y.; Chen, W.; Wong, M. W.; Andres, J. L.; Replogle, E. S.; Gomperts, R.; Martin, R. L.; Fox, D. J.; Binkley, J. S.; Defrees, D. J.; Baker, J.; Stewart, J. P.; Head-Gordon, M.; Gonzalez, C.; Pople, J. A. GAUSSIAN 94, Revision C.3, Gaussian, Inc.: Pittsburgh, PA, 1995.

57. Huzinaga, S. *J. Chem. Phys.* **1965**, *42*, 1293. Dunning, T. H. *J. Chem. Phys.* **1970**, *53*, 2823; *Approximate Atomic Wave functions II*, Department of Chemistry Report; University of Alberta: Edmonton, Alberta, Canada, 1971. Dunning, T. H.; Hay, P. J.

Modern Theoretical Chemistry; Schaefer, H. F., Ed.; Plenum: New York, 1977; Vol. 3, pp 1-27.

58. Lee, T. J.; Schaefer, H. F. *J. Chem. Phys.* **1985**, *83*, 1784.

59. Rittby, M.; Bartlett, R. J. *J. Phys. Chem.* **1988**, *92*, 3033.

60. Watts, J. D.; Gauss, J.; Barlett, R. J. *J. Chem. Phys. Lett.* **1992**, *200*, 1.

61. Watts, J. D.; Gauss, J.; Barlett, R. J. *J. Chem. Phys.* **1993**, *98*, 8718.

62. Dunning, T. H. *J. Chem. Phys.* **1989**, *90*, 1007.

63. Woon, D. E.; Dunning, T. H. *J. Chem. Phys.* **1993**, *98*, 1358.

64. ACES II is a program product of the Quantum Theory Project, University of Florida. Stanton, J. F.; Gauss, J.; Watts, J. D.; Nooijen, M.; Oliphant, N.; Perera, S. A.; Szalay, P. G.; Lauderdale, W. J.; Gwaltney, S. R.; Beck, S.; Balkova, A.; Bernholdt, D. E.; Baeck, K.-K.; Rozyczko, P.; Sekino, H.; Hober, C.; Barlett, R. J. Integral packages included are VMOL (Almlof, J.; Taylor, P. R.); VPROPS (Taylor, P.); ABACUS (Helgaker, T.; Jensen, H. J. Aa.; Jorgensen, P.; Olsen, J.; Taylor, P. R.).

65. Huber, K. P.; Herzberg, G. *Molecular Spectra and Molecular Structure, Constants of Diatomic Molecules*; Van Nostrand Reinhold: New York, 1979; Vol. IV.

66. Rosmus, P.; Meyer, W. *J. Chem. Phys.* **1978**, *69*, 2745.

67. Lewerenz, M.; Bruna, P. J.; Peyerimhoff, S. D.; Buenker, R. J. *J. Phys. B.* **1983**, *16*, 4511.

68. Kalcher, J. *Chem. Phys.* **1987**, *118*, 273.

69. Kasdan, A.; Herbst, E.; Lineberger, W. C. *Chem. Phys. Lett.* **1975**, *31*, 78.

70. Yamada, C.; Kanamori, H.; Hirota, E.; Nishiwaki, N.; Itabashi, N.; Kato, K.; Goto, T. *J. Chem. Phys.* **1989**, *91*, 4582.

71. Leopold, D. G.; Murray, K. K.; Miller, A. E. S.; Lineberger, W. C. *J. Chem. Phys.* **1985**, *83*, 4849.

72. Yamada, C.; Hirota, E. *Phys. Rev. Lett.* **1986**, *56*, 923.

73. Ellison, G. B.; Engelking, P. C.; Lineberger, W. C. *J. Am. Chem. Soc.* **1978**, *100*, 2556.

74. Tschumper, G. S.; Rienstra-Kiracofe, J. C.; Barden, C. J.; Brown, S. T.; Schaefer, H. F. Work in progress.

75. Hutter, J.; Lüthi, H. P.; Diederich, F. *J. Am. Chem. Soc.* **1994**, *116*, 750.

76. Curtiss, L. A.; Redfern, P. C.; Raghavachari, K.; Pople, J. A. *J. Chem. Phys.* **1998**, *109*, 42.

77. Miller, T. F.; Hall, M. B. *J. Am. Chem. Soc.* **1999**, *121*, 7389.

78. Tschumper, G. S. Unpublished results.

79. Ervin, K. M.; Lineberger, W. C. *J. Phys. Chem.* **1991**, *95*, 1167.

80. Lischka, H.; Köhler, H. *J. Am. Chem. Soc.* **1983**, *105*, 6646.

81. Grev, R. S.; Schaefer, H. F. *J. Chem. Phys.* **1992**, *97*, 7990.

82. Bogey, M.; Bolvin, H.; Demuynck, C.; Destombes, J. L. *Phys. Rev. Lett.* **1991**, *66*, 413.

83. Sherrill, C. D.; Lee, M. S.; Head-Gordon, M. *Chem. Phys. Lett.* **1999**, *302*, 425.

84. Ernst, M. C.; Sax, A. F.; Kalcher, J. *Chem. Phys. Lett.* **1993**, *216*, 189.

85. Sax, A. F.; Kalcher, J. *J. Mol. Struct.* (*THEOCHEM*) **1990**, *208*, 123.

86. Ervin, K. M.; Gronert, S.; Barlow, S. E.; Gilles, M. K.; Harrison, A. G.; Bierbaum, V. M.; DePuy, C. H.; Linegerger, W. C.; Ellison, G. B. *J. Am. Chem. Soc.* **1990**, *112*, 5750.

87. Burrow, P. D.; Jordan, K. D. *Chem. Phys. Lett.* **1975**, *36*, 594.

88. Wong, M. W.; Baker, J.; Nobes, R. H.; Radom, L. *J. Am. Chem. Soc.* **1987**, *109*, 2245.

CHAPTER 4

DO SNARE PROTEINS COMMUNICATE BY A SOLITON MECHANISM? LOCAL ELECTRON AFFINITIES OF THE "ZERO-LAYER" ARGININE AND GLUTAMINE[1]

[1]Pak, C.H., H.F. Schaefer. to be submitted to Biochemistry.

Abstract:

The electrostatic interactions in proteins are important due to their profound structure and function relationships. This property in the amino acids arginine and glutamine is perhaps a crucial piece of information in understanding the function of the "zero-layer" in SNARE proteins. The SNARE protein complex (bundle) is comprised of four alpha helices which contain arginine and glutamine at the "zero-layer," in a three glutamine to one arginine ratio, which forms the strongest side chain bonding. Here we propose that t- and v-SNARE proteins may communicate by a soliton (electron transfer) mechanism through the "zero-layer." In order to see how much energy is required to lose an electron from arginine and glutamine, we determined four different types of local neutral-anion energy differences: the local electron affinity (LEA_{lo}), zero-point corrected local electron affinity (LEA_{zero}), the vertical electron affinity (EA_{vert}), and vertical detachment energy (VDE). We adopted density functional theory (DFT, B3LYP), and a basis set of double-ζ plus polarization quality with additional *s*- and *p*-type diffuse functions, denoted DZP^{++}. Both arginine and glutamine seem to have LEAs of about -5 kcal/mol, which correlates well with the energy of the soliton.

Abbreviations: SNARE, soluble N-ethylmaleimide-sensitive factor attachment protein receptor; SNAP-25, synaptosomal protein of 25 kDa.

Introduction

The t- and v-SNARE proteins function as molecular "zip-codes" in cells[1]. They ensure that the right package (vesicle) is delivered to the right place (membrane). Only when they have correct t- (alpha helical proteins that are attached to the membrane) and v-SNARE (an alpha helical protein that is attached to the vesicle) protein pairs, can the vesicles embed themselves in the membrane. The actual mechanism explaining how the vesicle recognizes its target place, how it is transported to the right membrane, and the fusion process is rather complicated, unclear, and involves multiple steps. But the function of t- and v-SNARE proteins has been well studied and defined[2-13].

The first SNARE proteins were discovered in late 1980s, independently on yeast cells and neurons (reviews[14-15]). Since then, there have been many studies of these proteins, and many more SNARE proteins have been isolated or are expected. Currently there are more than 60 known SNARE proteins, and they are also characterized as Q (t-SNARE) or R (v-SNARE) proteins. The symbol Q denotes glutamine, and R denotes arginine. The reason for this grouping is that all the SNARE proteins have Q and R amino acids at the center of the SNARE motif (also called the "zero-layer"), and they form the strongest side chain bonding in the SNARE protein complex, which is composed of four alpha helical strands (Syntaxin, SNAP-25, and VAMP).

How one protein recognizes the other is a fundamental problem in biology, and there are many experiments and theories available, but no clear answer to this question. One of the intriguing theories in molecular recognition involves the concept of the soliton, also known as the Davydov soliton. The soliton was first observed by John Scott Russell[16] in 1834. Then in 1973, A.S. Davydov suggested that solitons may be

created in alpha helices[17]. His work proposed a mechanism for the localization and transport of vibrational energy in proteins. Since then, there have been many related experiments, and considerable theoretical work has been done on this topic. According to Scott[18], "Vibrational energy of the CO stretching (or Amide-I) oscillators that is localized on the helix acts — through a phonon coupling effect — to distort the structure of the helix. The helical distortion reacts — again through phonon coupling — to trap the Amide-I oscillation energy and prevent its dispersion. This effect is called self-localization or self-trapping"[18]. One quantum of this Amide-I vibration or C=O stretch has a vibrational energy of about 4.7 kcal/mol of energy, which is about the same energy as the GTP hydrolysis (4.6 kcal/mol) and about half the energy of the ATP hydrolysis (10 kcal/mol)[19]. This soliton or solitary wave, which can preserve its shape and velocity, may be sent off to far distances through myosin to a particular place[17].

SNARE proteins are alpha helical (three alpha helices comprise a t-SNARE, and one alpha helix per v-SNARE); they give the specificity of the vesicle transport, and there are microtubules in between. In order for a specific recognition to take place, there has to be a specific long-range interaction between the proteins. Representing the gas phase local electron affinity or LEA (the LEA is the difference between the energy of a particular conformation of a neutral system and the energy of the anion with the same conformation) of the isolated arginine and glutamine does not necessarily mean much when considering the complexity of the system and the number of proteins involved. However, if the energy of the soliton and LEA_{zero} match for the arginine and glutamine, this may be the place ("zero-layer") where solitons (electrons) might be exchanged.

Arginine and glutamine are also known for their importance in the recognition of DNA and RNA[20-30]. Not surprisingly, most of the arginine and glutamine are found in neuronal cells, and the lack of these nonsynthesized amino acids can be highly detrimental to vertebrates, causing mental retardation. Similarly, supplements of arginine and glutamine, known as "immunonutrients," are often used for HIV patients, cancer patients, and patients undergoing major surgeries, due to their known effects in boosting the immune system. Furthermore, these "immunonutrients" are known to provide some benefits with respect to impotence, wound healing and endurance for athletes[31-32].

Despite this importance and the ensuing potential benefits, there exists a very small amount of theoretical work available on these two amino acids, and most of the other twenty amino acids. Therefore, the main purpose of this project is to explore possible conformations of the neutrals and anions of arginine (R) and glutamine (Q), then to see if the energy of losing an electron might correspond to the soliton's energy, which is known to be about 4.7 kcal/mol.

When predicting molecular structures and energies, there are many theoretical approaches. Considering both the size of the molecule and the reliability of different methods, gradient corrected density functional theory (DFT) has been used here. In recent years, we have examined electron affinities for more than 200 atoms and molecules using DFT with a standard DZP^{++} basis set, and have concluded that several DFT methods are effective and reliable in predicting electron affinities. For a comprehensive recent review on theoretical and experimental electron affinities, one is referred to the recent paper in Chemical Reviews by Rienstra-Kiracofe *et. al.*[33].

At this point, it is appropriate to mention more about the new term "local" we are using in the context of electron affinities. When determining the electron affinities for inorganic or organic molecules, we study the energy difference between the global minima of the neutral and the anion, because they are thermodynamically pertinent. However, for this particular study, where we are interested in the kinetically pertinent dynamics of losing an electron, we desire to study the energy differences between similar local minima (conformations) of the neutral and anion (LEA).

Methods

Eight low-lying conformations of neutral arginine have been structurally optimized here, plus six low-lying conformers of glutamine, with the idea that the two amino acids will be fully stretched. The stretched amino acids have been edited in such a way that they will have different orientations of the groups on each end of the amino acid. All the anions were independently structurally optimized, beginning from the appropriate neutral equilibrium structures. During the optimization, structure R7N gave rise to both R7A and R2A (Figure 1). Therefore, two different local electron affinities are given for the pairs R7N and R7A and R7N and R2A, with R7A and R2A being neighbors in potential energy hyper surface. All 28 conformations were found to be minima after determining the harmonic vibrational frequencies via analytic second derivatives for the B3LYP functional. All computations were carried out using the Gaussian 94 program suite[34].

A standard double-ζ plus polarization (DZP) basis set with the addition of diffuse functions was utilized. The DZP^{++} basis sets were constructed from the Huzinaga-

Dunning[35-36] sets of contracted Gaussian functions with one set of *p*-type polarization functions for each H atom, and one set of five *d*-type polarization functions for each C, N, and O atom [α_p(H)=0.75, α_d(C)=0.75, α_d(N)=0.80, α_d(O)=0.85]. The DZP basis was augmented with diffuse functions; the C, N, and O atoms received one additional *s*-type and one additional set of *p*-type functions, while H received one additional *s*-type function. The diffuse function orbital exponents were determined in an "even-tempered sense" as a mathematical extension of the primitive set, according to the formula of Lee and Schaefer[37]. The final contraction scheme for this basis is C, N, O (10s6p1d/5s3p1d) and H (5s1p/3s1p).

Neutral-anion energy separations were evaluated as differences in total energies in the following manner: the classical local electron affinities are determined by,

$$EA_{lo} = E_{(optimized\ neutral)} - E_{(optimized\ anion)}$$

zero-point corrected local electron affinities are determined by,

$$EA_{zero} = E_{(zero\text{-}point\ corrected\ neutral)} - E_{(zero\text{-}point\ corrected\ anion)}$$

the vertical electron affinities by,

$$EA_{vert} = E_{(optimized\ neutral)} - E_{(anion\ at\ neutral\ equilibrium\ geometry)}$$

and the vertical detachment energies by,

$$VDE = E_{(neutral\ at\ anion\ equilibrium\ geometry)} - E_{(optimized\ anion)}$$

Results

The four types of predicted local neutral-anion energy differences for the arginine (R) and glutamine (Q) conformers are reported in Table I. Relative energies and dipole moments for the different conformations are given in Table II, and structures in Figures 1 and 2. Unless otherwise indicated, zero-point corrected electron affinities (LEA_{zero}) will the quantities discussed herein.

A. Arginine (R)

There has been some theoretical work done on this amino acid, mostly in regard to stability of the zwitterionic vs. nonionic forms[38-43]. The conclusion of these earlier studies is that isolated arginine, and perhaps most of the other amino acids, exist in the zwitterionic form in solution, and in a nonionic form in the gas phase. For the purpose of this study, to determine the small energy differences between the neutrals and the anions (LEAs), and to eliminate outside influences on these small energy differences, nonionic structures are considered.

a. Electron Affinities

The first three (R1,R2,R3) conformations of arginine have roughly zero LEAs. The next three (R4,R5,R6) conformations are predicted to have LEAs of approximately -4.5 kcal/mol. The last three conformations (R7,R8,R7N-R2A) have positive theoretical LEAs ranging from 2.1 to 5.1 kcal/mol. R4, R5 and R6 are of particular interest not only because they have LEA_{zero} values of about -5 kcal/mol, but because the VDEs are also about -5 kcal/mol. The largest structural changes (between neutral and anion) we

predict for these conformations involve the peptide bond (see Table III). It seems that orientation of the guanidinium group is not important in determining the LEAs. These neutral-anion structural changes in the peptide bond area may correspond to Xu's[44] "asymmetric kink group" in his alpha helix where the solitons may be able to leave. The kink groups are also often found in DNA and RNA, and also in the Rhodopsin protein, where the retinal goes through a cis-trans transformation as it accepts a photon.

b. Relative Energies

All the neutral conformations of arginine are close in energy, except for R7N and R8N, which are predicted to lie about 5 kcal/mol higher. For the anions, except for R1A, R2A, and R3A, the structures are all higher in energy, again by about 5 kcal/mol. The lowest energy conformations for arginine are R1N and R3A, which have the same orientation of the peptide bond area and different orientation of the guanidinium group. R5A and R7A have essentially the same conformational energy.

c. Charge Distributions

Weinhold Natural Population Analyses (NPA) have been performed, and some interesting patterns have been discovered. The main difference was noted in hydrogen atom (26); R1, R2, and R3 display no significant charge difference between the anion and the neutral, whereas R4, R5, and R6 have large neutral-anion charge differences. For R7 and R8, the main charge difference is noted for H(5), H(7) and H(26). Overall, most of the charge differences were found in the peptide bond area, and most of the charges were well distributed over the molecule.

d. Dipole Moments

We predict very large dipole moments, especially for the anions. The anion conformers all have dipole moments of about 4.5 debye, whereas neutral dipole moments range from 1.9 to 5.2 debye. The theoretical dipole moments do not seem to have a clear correlation with the electron affinities or the relative energies.

B. Glutamine (Q)

There have been some experimental[45-48] and theoretical studies[47-48] of the neutral zwitterionic forms of glutamine. However, it seems that there has been no experimental or theoretical work done on the conventional forms of either the neutrals or anions.

a. Electron Affinities

The first four conformations (Q1, Q2, Q3, Q4) have very similar predicted electron affinities; the average LEA_{zero} and LVDE were -5 kcal/mol and -5.4 kcal/mol respectively. Q5 and Q6 have electron affinities LEA_{zero} of -7.1 kcal/mol and 3 kcal/mol respectively. It seems that the position of the carbonyl group is important in determining the LEAs. Q6, in which the carbonyl group is farthest from the peptide bond end, has a local electron affinity of 3 kcal/mol, but Q5, for which the carbonyl group is closest to the peptide bond end, has an LEA_{zero} of -7.1 kcal/mol.

b. Relative Energies

All of the neutral and anion glutamine conformers have similar conformational energies, ranging from 0.0 to 1.9 kcal/mol for the neutrals, and 5.3 to 8.0 kcal/mol for the

anions (except for Q6A which is about 5kcal/mol lower in energy than the other anion conformers). In average, anions are about 6 kcal/mol or higher in energy than the neutrals and Q6A. Q6A seems to be the lowest lying energetically, due to hydrogen bonding between O(4) and H(18).

c. Charge Distributions

NPA analysis reveals some differences in electron distribution as a function of the conformation of the molecule. For the stretched forms of glutamine (Q1, Q2, Q3, and Q4), which have local electron affinities of about -5 kcal/mol, the main charge difference was found for atoms H(18) and H(20). However, the neutral-anion electron distribution differences for the bent Q5 and Q6 were less obvious: for Q5, the main charge differences were from atoms H(18) and H(14), but the main charge differences for the Q6 were found in the peptide bond area.

d. Dipole Moments

Both the neutrals and anions of glutamine have large dipole moments, but on average, the neutrals have larger dipole moments than the anion conformations. Like arginine, the dipole moments do not seem to have an obvious relationship to the electron affinities or relative energies.

Discussion

In nature, there are only twenty different amino acids, and they are known to be important in human life. Yet, there exist only a very small number of theoretical studies

of these critical systems. Each amino acid has its own unique properties. For example, Nuclear Localization Signal (NLS) sequence often contains proline residue upstream of the basic amino acid residues to break the alpha helix formation (to have a "kink"); aromatic side chains such as phenylalanine, tyrosine, and tryptophan are known to be important in cation-pi interactions, which are often found in the active sites of proteins; and basic residues like arginine and lysine are known to be important in biological recognition processes. Considering many of the experimental studies, which confirm the importance of arginine and glutamine in biological recognition processes, and based on our results, we suggest the recognition or specific interactions between t- and v-SNARE proteins may be possible by a soliton mechanism. This idea is partially supported by the recent mutagenesis work done on "zero-layer" by Scales[11] who showed that the "zero-layer" arginine and glutamines are needed for proper dissociation of the SNARE protein complex. If the vesicles and target membrane cannot recognize that they are at the right place, the vesicles will not fuse into the membrane, and therefore cannot properly dissociate themselves. This may be due to inefficient exchange of information (solitons) between the four alpha helices through the "zero-layer."

Acknowledgements

C.H.P. would like to thank Catherine Li, Dr.Yukio Yamaguchi, Dr. Yaoming Xie, Lubos Horny, Nancy Richardson, Levant Sari, Professor Yun dong Wu, for their useful discussions and help. This work is supported by the U.S. National Science Foundation Grant CHE-0136186.

TABLE 4.1.: The Local adiabatic electron affinity (LEAad), zero-point corrected LEAad (LEAzero), vertical electron affinity (LEAvert), and the vertical detachment energy (LVDE) for the different conformations of the Arginine (R) and Glutamine (Q) species presented in eV (kcal/mol in parentheses).

Species	Conformations	LEA_{ad}	LEA_{zero}	LEA_{vert}	LVDE
Arginine	R1	-0.07(-1.7)	0.00(0.0)	-0.14(-3.3)	0.01(0.3)
	R2	-0.05(-1.1)	0.02(0.4)	-0.10(-2.3)	0.01(0.2)
	R3	-0.04(-0.9)	0.02(0.5)	-0.08(-1.9)	0.01(0.2)
	R4	-0.26(-6.0)	-0.18(-4.1)	-0.28(-6.5)	-0.24(-5.5)
	R5	-0.27(-6.3)	-0.19(-4.5)	-0.30(-7.0)	-0.24(-5.5)
	R6	-0.29(-6.6)	-0.21(-4.9)	-0.32(-7.3)	-0.25(-5.8)
	R7	0.01(0.2)	0.09(2.1)	-0.05(-1.3)	0.14(3.2)
	R8	0.06(1.3)	0.13(3.0)	-0.13(-2.9)	0.06(1.4)
	R7N-R2A	0.21(4.8)	0.22(5.1)	-0.05(-1.2)	0.01(0.2)
Glutamine	Q1	-0.25(-5.7)	-0.18(-4.1)	-0.29(-6.6)	-0.21(-4.8)
	Q2	-0.27(-6.2)	-0.20(-4.7)	-0.35(-8.1)	-0.17(-4.0)
	Q3	-0.32(-7.4)	-0.24(-5.6)	-0.35(-8.0)	-0.29(-6.6)
	Q4	-0.32(-7.4)	-0.25(-5.7)	-0.44(-10.1)	-0.28(-6.5)
	Q5	-0.39(-9.0)	-0.31(-7.1)	-0.42(-9.7)	-0.35(-8.2)
	Q6	0.01(0.2)	0.13(3.0)	-0.28(-6.4)	1.10(25.4)

TABLE 4.2.: Relative energies (R.E.) and total dipole moments (Dipole) for different conformations of Arginine (R) and Glutamine (Q) presented in eV (kcal/mol in parentheses) and Debye. The anion dipole moments were evaluated relative to the center of mass.

Species	Conformations	Neutral R.E.	Neutral Dipole	Anion R.E.	Anion Diplole
Arginine	R1	0.00(0.0)	5.2	0.03(0.6)	4.4
	R2	0.07(1.6)	4.1	0.07(1.6)	4.5
	R3	0.01(0.2)	4.4	0.00(0.0)	4.4
	R4	0.11(2.5)	3.7	0.32(7.5)	4.1
	R5	0.05(1.1)	4.2	0.27(6.3)	4.1
	R6	0.09(2.0)	1.9	0.33(7.6)	4.3
	R7	0.33(7.5)	4.8	0.27(6.3)	4.1
	R8	0.36(8.4)	2.5	0.26(6.1)	6.6
Glutamine	Q1	0.08(1.9)	5.0	0.28(6.4)	3.1
	Q2	0.01(0.2)	4.1	0.23(5.3)	3.0
	Q3	0.00(0.0)	2.8	0.27(6.2)	1.5
	Q4	0.03(0.7)	2.1	0.30(6.9)	2.2
	Q5	0.01(0.2)	2.3	0.35(8.0)	5.4
	Q6	0.06(1.4)	5.6	0.00(0.0)	0.1

TABLE 4.3.: Critical geometrical parameters for different conformations of the neutral (N) and anion (A) of Arginine (R) and Glutamine (Q), given in angstroms and degrees.

	R1N	R1A	R2N	R2A	R3N	R3A	R4N	R4A	R5N	R5A
N(1)-C(2)	1.48	1.48	1.47	1.48	1.48	1.48	1.46	1.47	1.46	1.46
C(2)-C(3)	1.55	1.54	1.55	1.55	1.55	1.55	1.54	1.54	1.54	1.54
C(3)-O(6)	1.34	1.35	1.34	1.34	1.34	1.34	1.36	1.35	1.36	1.35
τ (1-2-3-6)	11.7°	10.7°	345.1°	1.9°	11.1°	9.8°	348.8°	355.3°	167.7°	175.4°
C(2)-C(9)	1.54	1.54	1.54	1.54	1.54	1.54	1.55	1.54	1.55	1.54
C(9)-C(12)	1.54	1.54	1.55	1.55	1.53	1.53	1.54	1.54	1.54	1.54
C(12)-C(15)	1.54	1.54	1.54	1.54	1.54	1.54	1.53	1.53	1.54	1.54
τ (2-9-12-15)	175.9°	187.8°	95.7°	109.3°	182.8°	166.2°	178.5°	184.4°	178.9°	172.9°
N(17)-C(19)	1.40	1.39	1.42	1.40	1.40	1.39	1.40	1.39	1.40	1.39
C(19)-N(22)	1.40	1.39	1.39	1.41	1.40	1.40	1.40	1.40	1.40	1.40
C(19)-N(21)	1.29	1.30	1.29	1.29	1.29	1.30	1.29	1.30	1.29	1.29
τ (17-19-22-21)	180.4°	179.5°	180.9°	181.9°	180.3°	180.7°	180.3°	180.3°	180.6°	180.2°
C(15)-N(17)	1.47	1.47	1.48	1.48	1.47	1.47	1.47	1.47	1.47	1.46
N(17)-C(19)	1.40	1.39	1.42	1.40	1.40	1.39	1.40	1.39	1.40	1.39
C(19)-N(22)	1.40	1.39	1.39	1.41	1.40	1.40	1.40	1.40	1.40	1.40
τ (15-17-19-22)	323.2°	341.9°	313.1°	317.5°	324.5°	330.3°	324.9°	330.8°	323.0°	334.1°

Table 4.3 continued

	R6N	R6A	R7N	R7A	R8N	R8A	R7N	R2A
N(1)-C(2)	1.46	1.46	1.46	1.47	1.47	1.46	1.46	1.48
C(2)-C(3)	1.54	1.54	1.55	1.54	1.54	1.55	1.55	1.55
C(3)-O(6)	1.36	1.35	1.36	1.36	1.37	1.35	1.36	1.34
τ (1-2-3-6)	355.6°	334.7°	359.1°	44.0°	271.0°	331.0°	359.0°	1.9°
C(2)-C(9)	1.55	1.55	1.54	1.54	1.54	1.55	1.54	1.54
C(9)-C(12)	1.54	1.54	1.54	1.53	1.54	1.54	1.54	1.55
C(12)-C(15)	1.54	1.54	1.53	1.53	1.53	1.53	1.53	1.53
τ (2-9-12-15)	179.8°	171.1°	175.2°	182.3°	174.3°	174.6°	175.2°	109.3°
N(17)-C(19)	1.40	1.39	1.40	1.38	1.40	1.39	1.40	1.40
C(19)-N(22)	1.40	1.40	1.40	1.40	1.40	1.40	1.40	1.41
C(19)-N(21)	1.29	1.30	1.29	1.30	1.29	1.30	1.29	1.29
τ (17-19-22-21)	180.0°	180.5°	180.5°	180.0°	180.3°	180.1°	180.5°	181.9°
C(15)-N(17)	1.47	1.47	1.47	1.47	1.47	1.47	1.47	1.48
N(17)-C(19)	1.40	1.39	1.40	1.38	1.40	1.39	1.40	1.40
C(19)-N(22)	1.40	1.40	1.40	1.40	1.40	1.40	1.40	1.41
τ (15-17-19-22)	323.8°	330.0°	321.8°	338.0°	323.5°	334.3°	321.8°	317.5°

Table 4.3 continued

	Q1N	Q1A	Q2N	Q2A	Q3N	Q3A	Q4N	Q4A	Q5N	Q5A
N(1)-C(2)	1.465	1.465	1.467	1.466	1.463	1.468	1.464	1.472	1.462	1.465
C(2)-C(3)	1.537	1.540	1.533	1.539	1.534	1.537	1.535	1.535	1.543	1.538
C(3)-O(6)	1.364	1.353	1.362	1.353	1.361	1.358	1.360	1.357	1.357	1.363
τ (1-2-3-6)	327.4°	340.5°	312.2°	323.2°	324.3°	315.3 °	319.4°	303.4°	33.2°	25.1°
C(2)-C(9)	1.547	1.546	1.542	1.545	1.545	1.543	1.545	1.541	1.543	1.543
C(9)-C(12)	1.537	1.537	1.532	1.542	1.533	1.539	1.534	1.541	1.547	1.542
C(12)-C(15)	1.530	1.530	1.529	1.528	1.529	1.528	1.530	1.527	1.525	1.524
τ (2-9-12-15)	174.7°	181.3°	179.9°	175.8°	167.7°	173.5°	186.9°	175.6°	54.0°	58°
C(15)-O(16)	1.2275	1.2337	1.228	1.234	1.228	1.234	1.228	1.235	1.2336	1.241
C(12)-C(15)	1.5301	1.530	1.529	1.528	1.529	1.528	1.530	1.527	1.525	1.524
C(15)-N(17)	1.3724	1.370	1.374	1.372	1.374	1.369	1.373	1.368	1.369	1.361
∠C(12)C(15)N(17)	115.6°	115.0°	115.0°	115.2°	115.3°	115.7°	115.2°	115.5°	116.6°	115.9°
τ (12-15-17-16)	178.4°	179.9°	180.6°	180.5°	179.3°	179.2°	180.7°	179.0°	178.7°	180.0°

Table 4.3 continued

	Q6N	Q6A
N(1)-C(2)	1.466	1.486
C(2)-C(3)	1.543	1.525
C(3)-O(6)	1.356	1.434
τ (1-2-3-6)	48.2°	51.0°
C(2)-C(9)	1.534	1.540
C(9)-C(12)	1.553	1.558
C(12)-C(15)	1.531	1.532
τ (2-9-12-15)	142.3°	118.4°
C(15)-O(16)	1.229	1.245
C(12)-C(15)	1.531	1.532
C(15)-N(17)	1.371	1.356
∠C(12)C(15)N(17)	114.1°	115.0°
τ (12-15-17-16)	180.3°	181.4°

Figure Captions

Figures 4.1. DZP^{++} DFT local minimum conformations R1-R9 of the neutral (^1A state) and anionic (^2A state) arginine species with atomic charges indicated. Critical geometrical parameters for the equilibrium structures are reported in Table III.

Figures 4.2. DZP^{++} DFT local minimum conformations Q1-Q6 of the neutral (^1A state) and anionic (^2A state) glutamine species with atomic charges indicated. Critical geometrical parameters for the equilibrium structures are reported in Table III.

R1

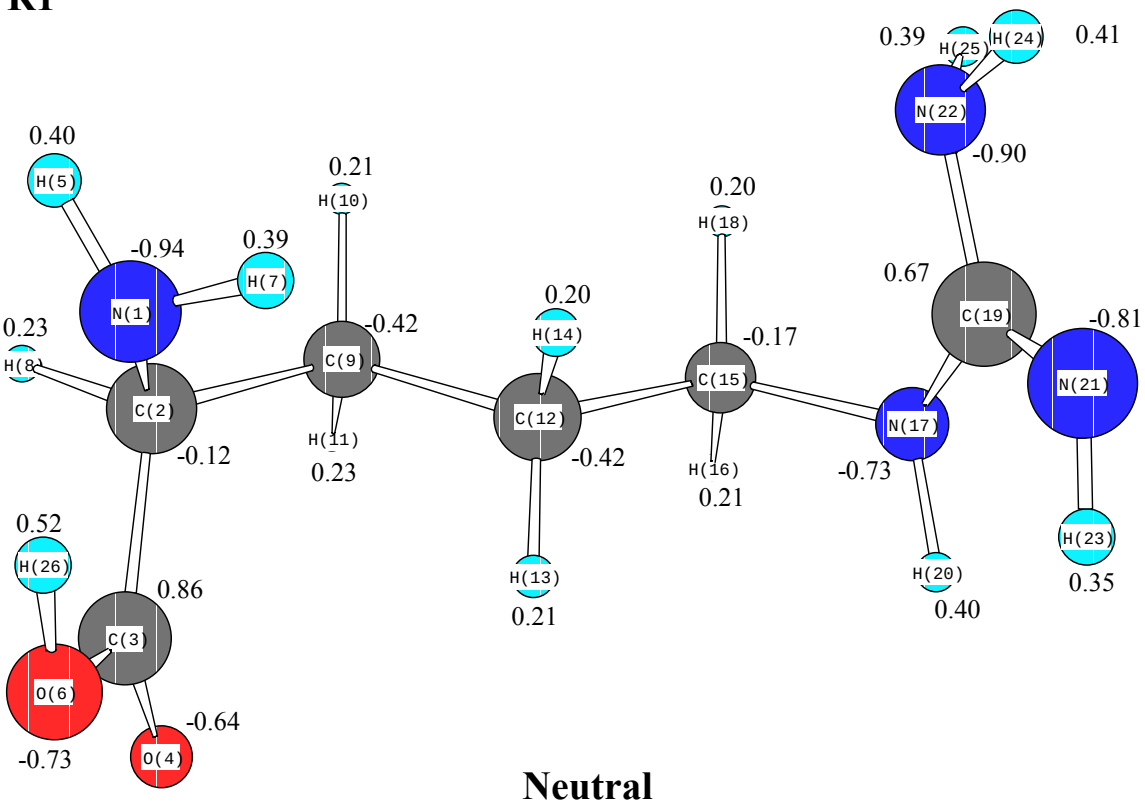

Neutral

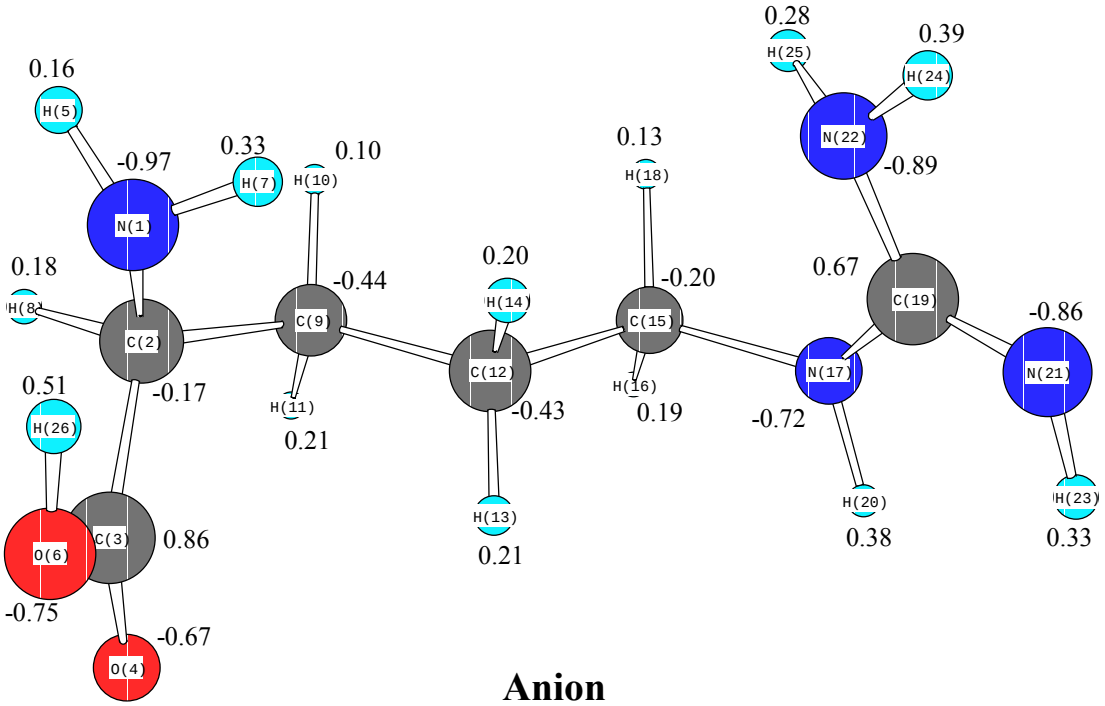

Anion

R2

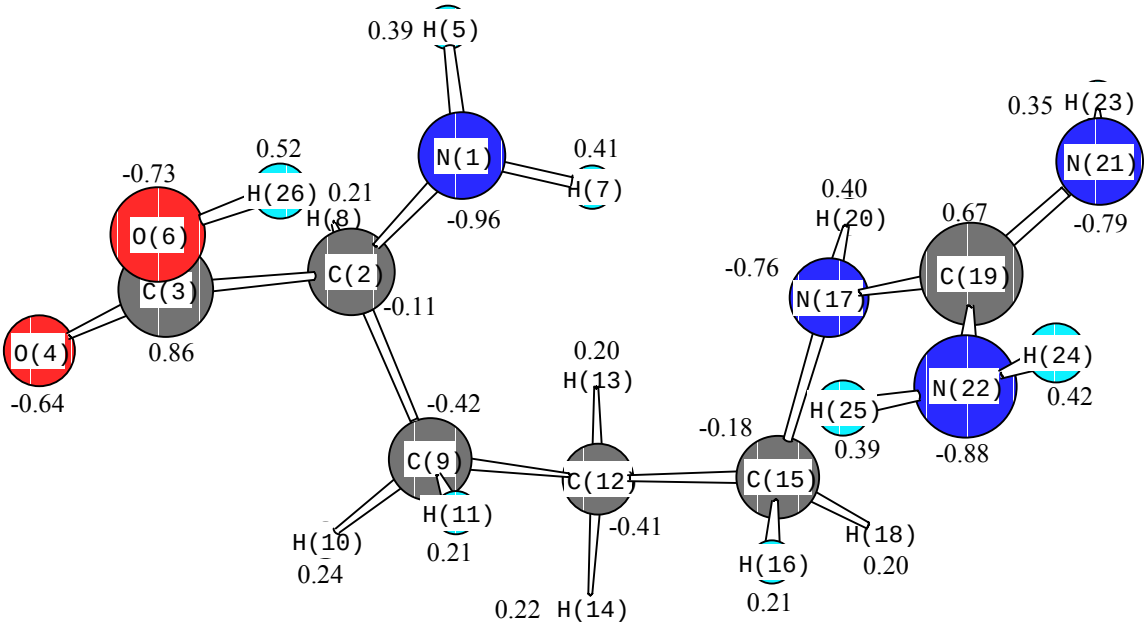

Neutral

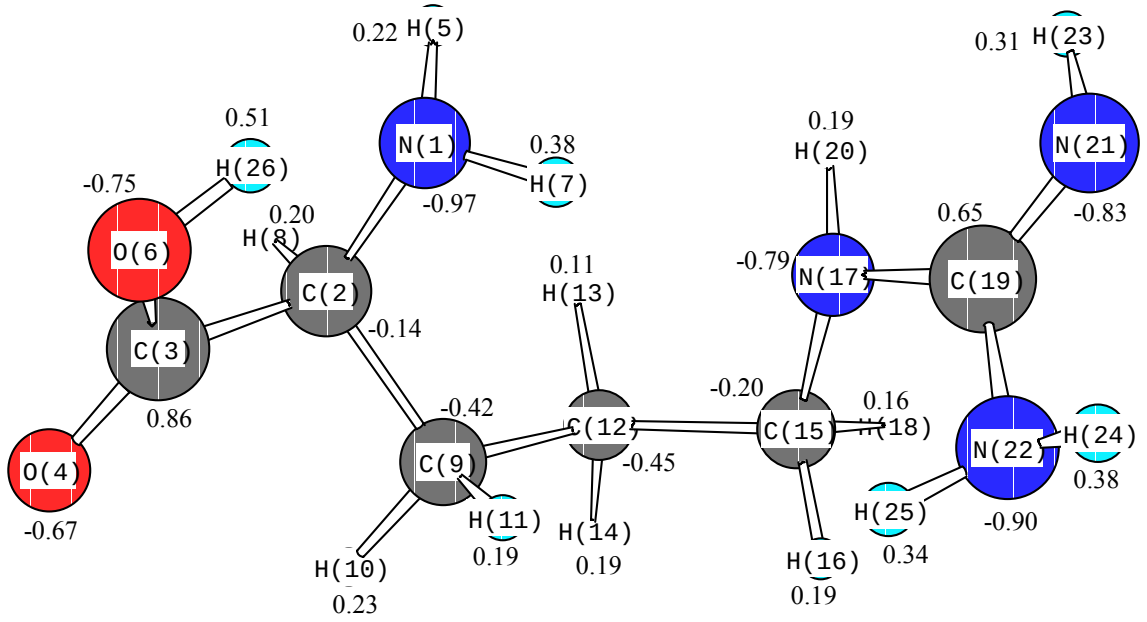

Anion

R3

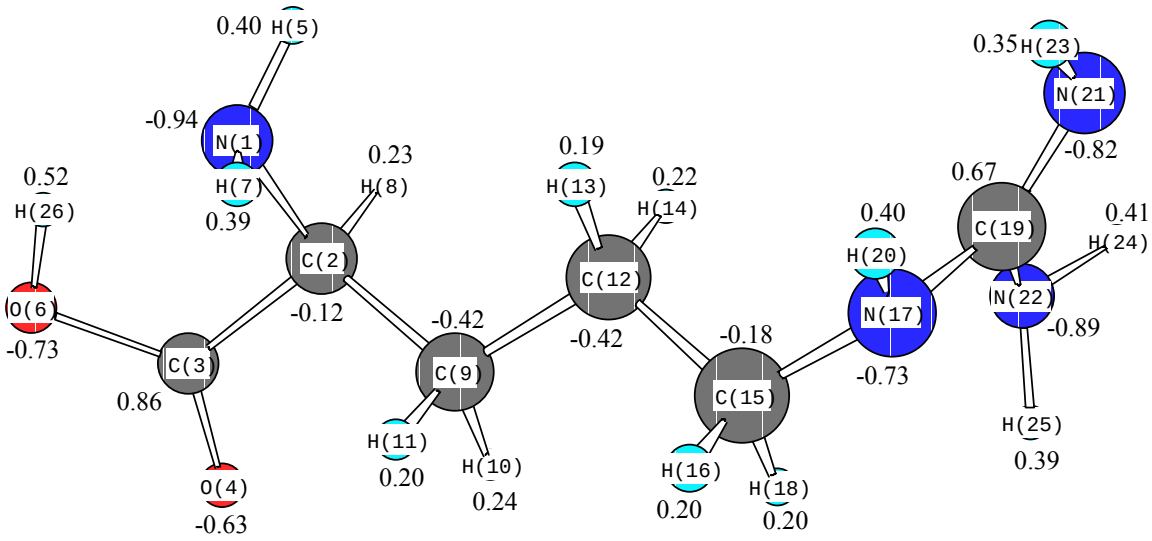

Neutral

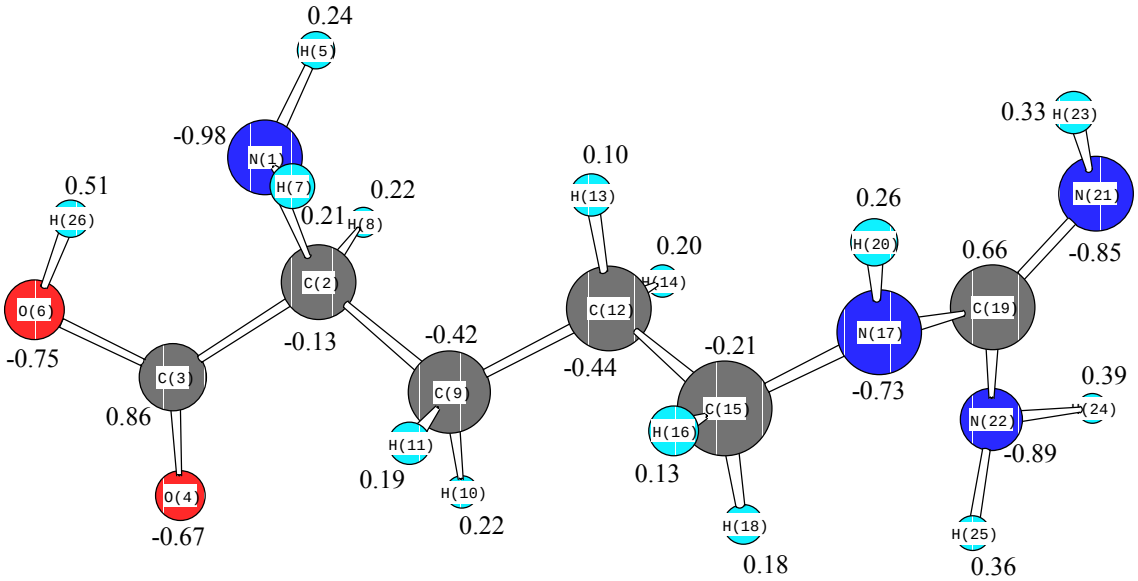

Anion

R4

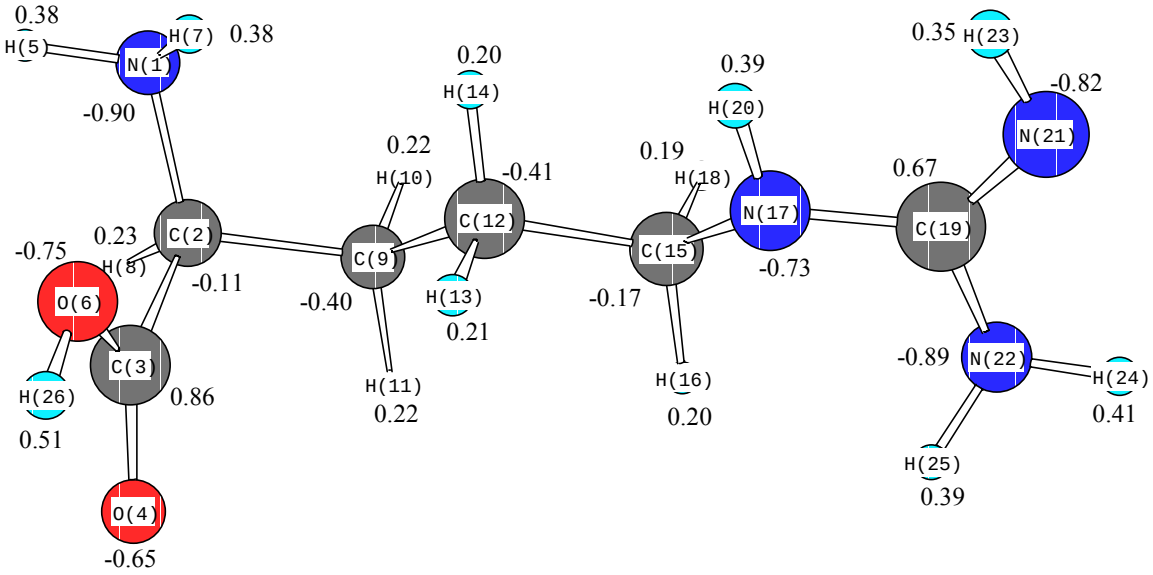

Neutral

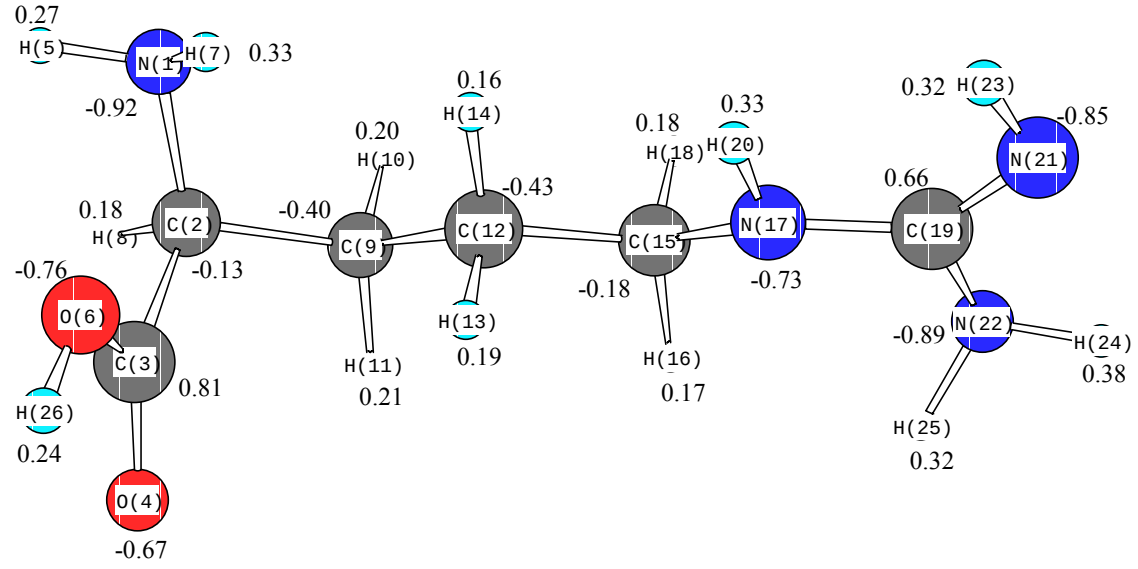

Anion

R5

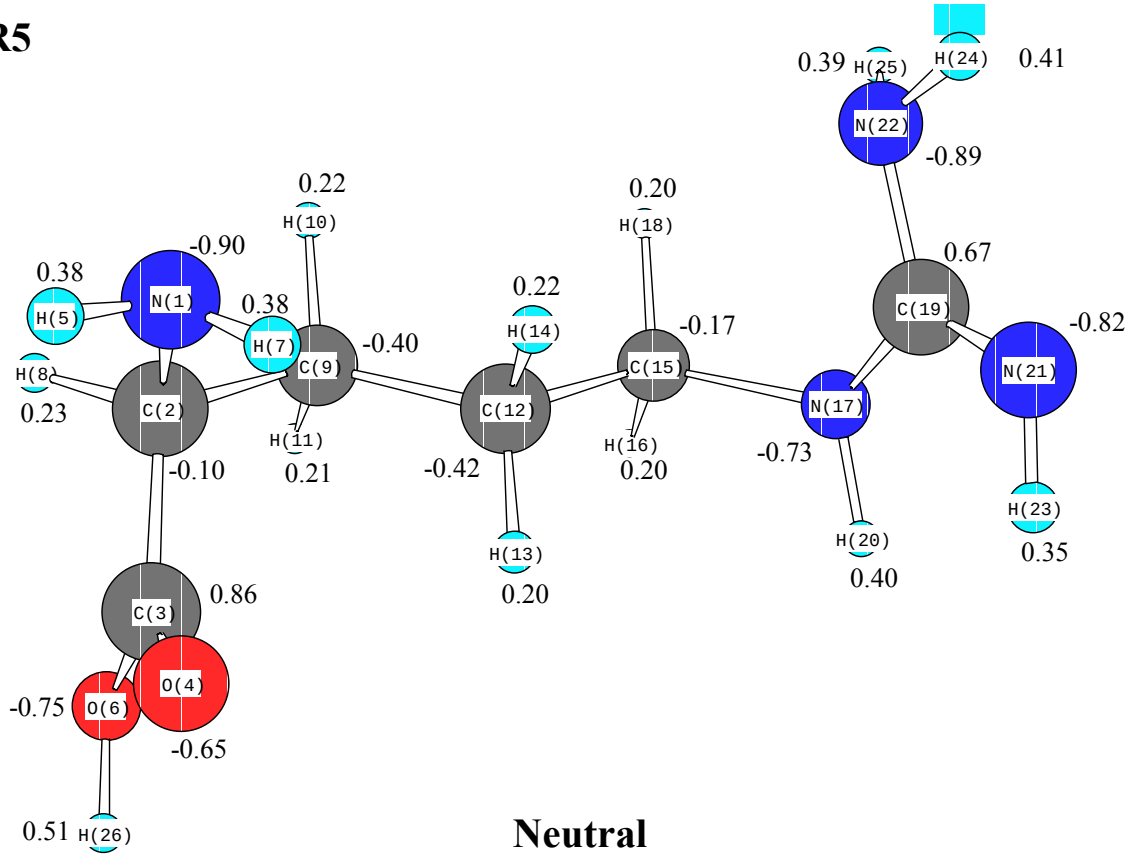

Neutral

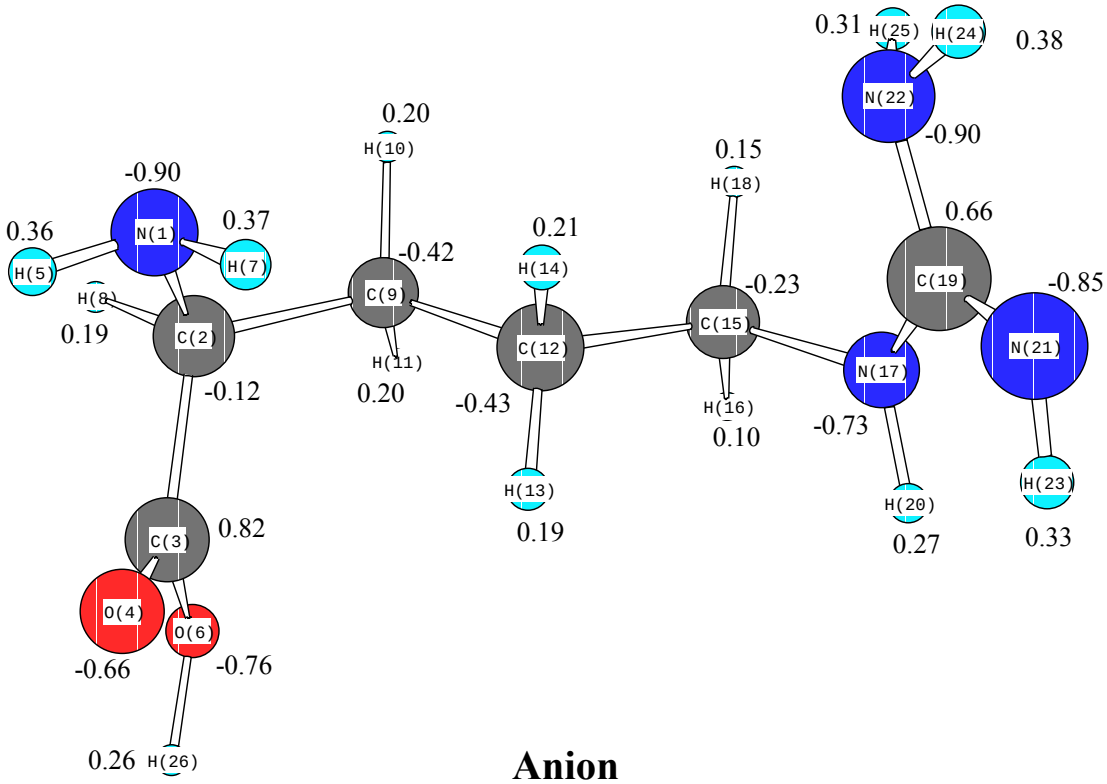

Anion

R6

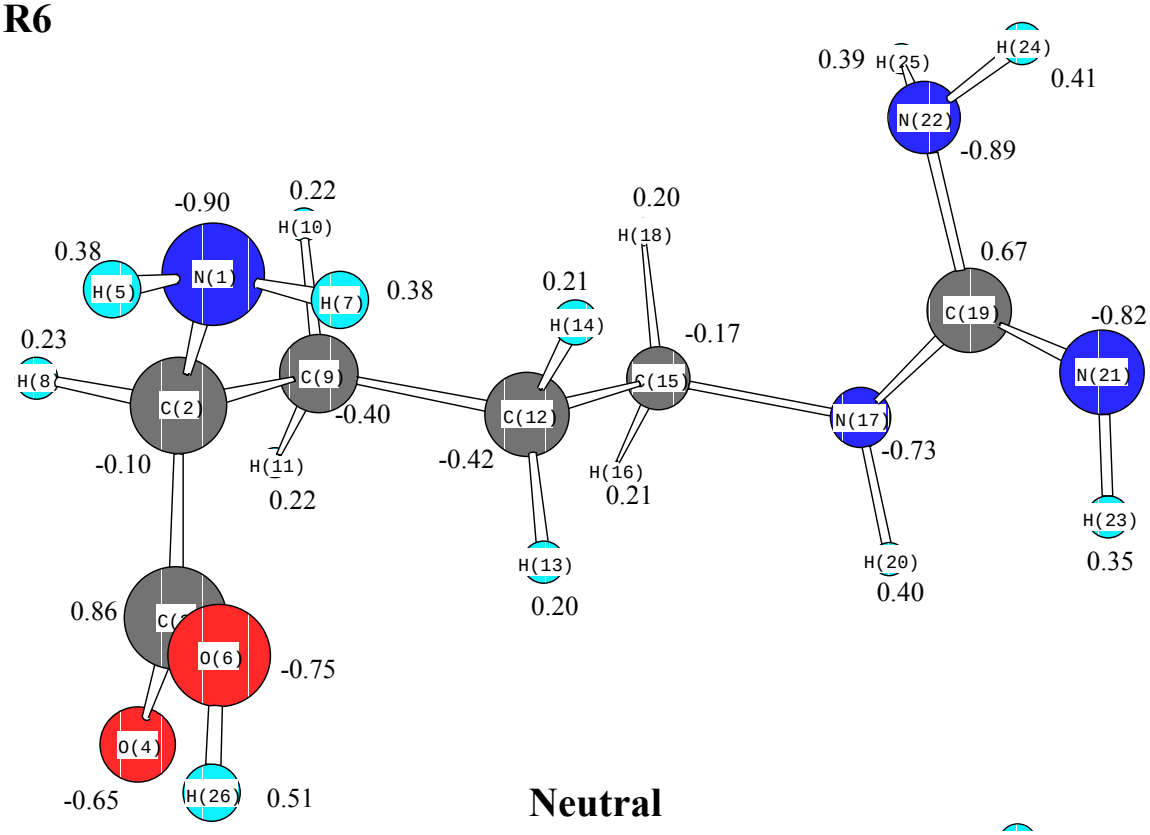

Neutral

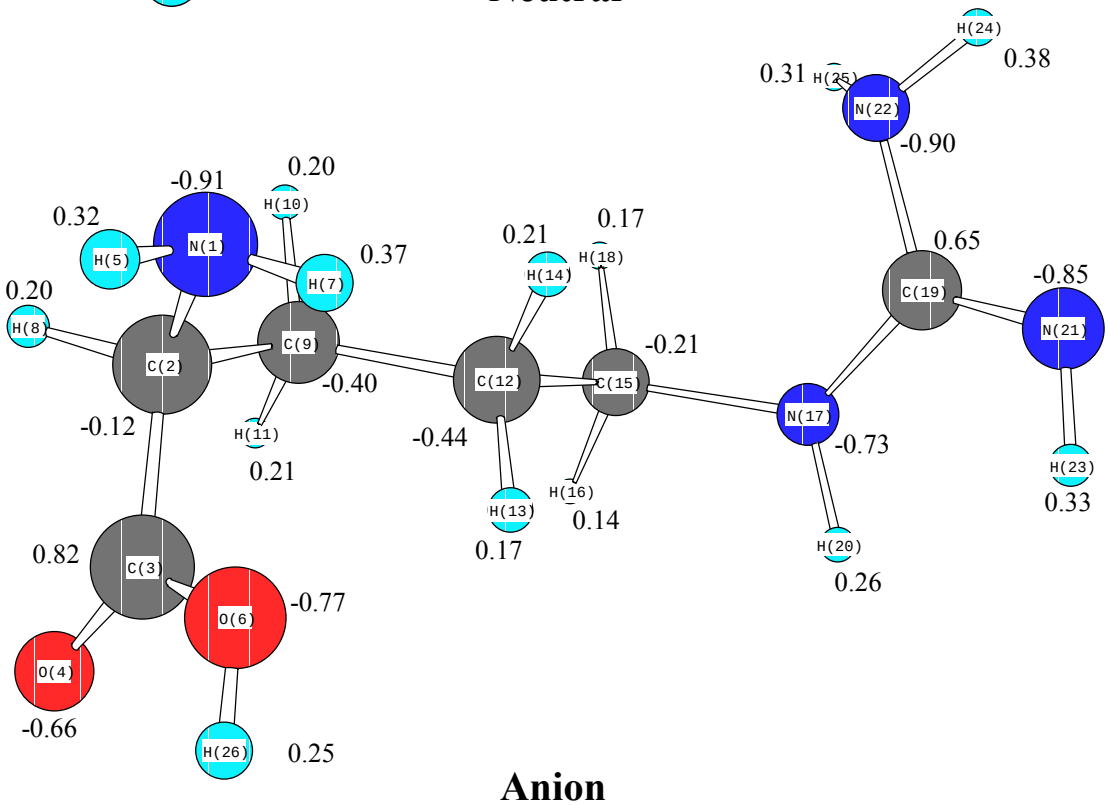

Anion

R7

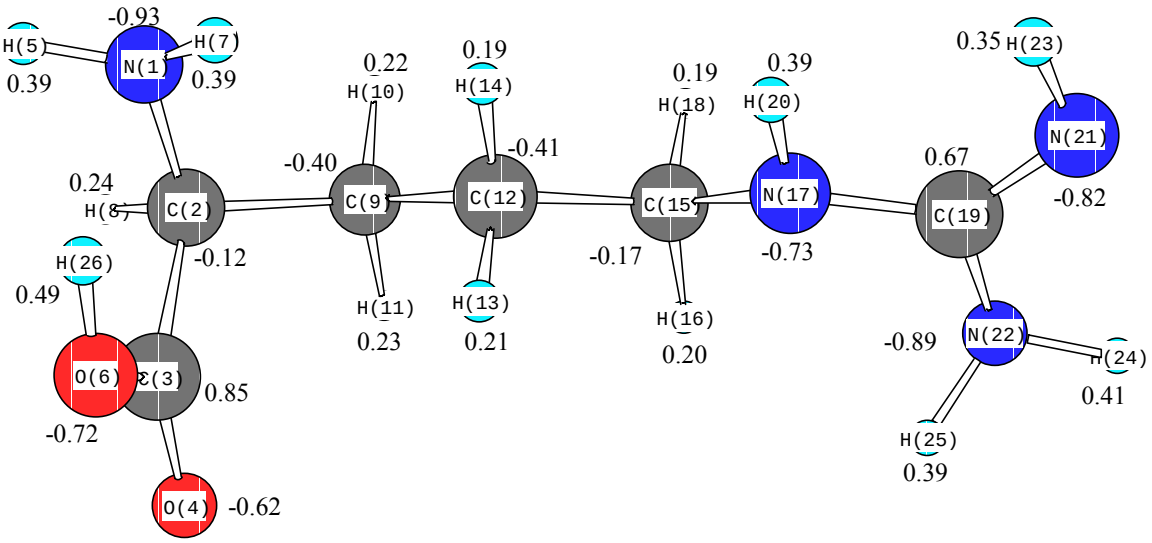

Neutral

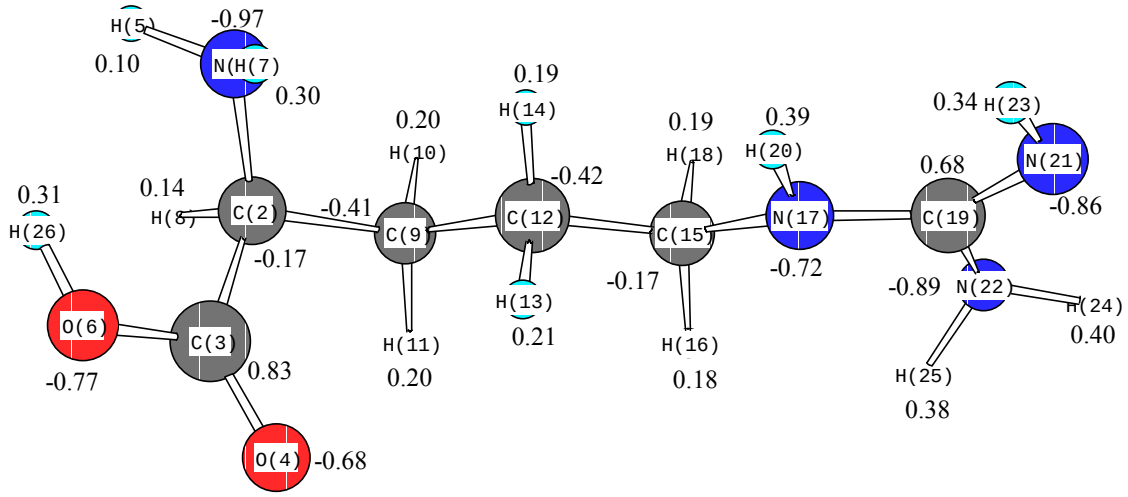

Anion

R8

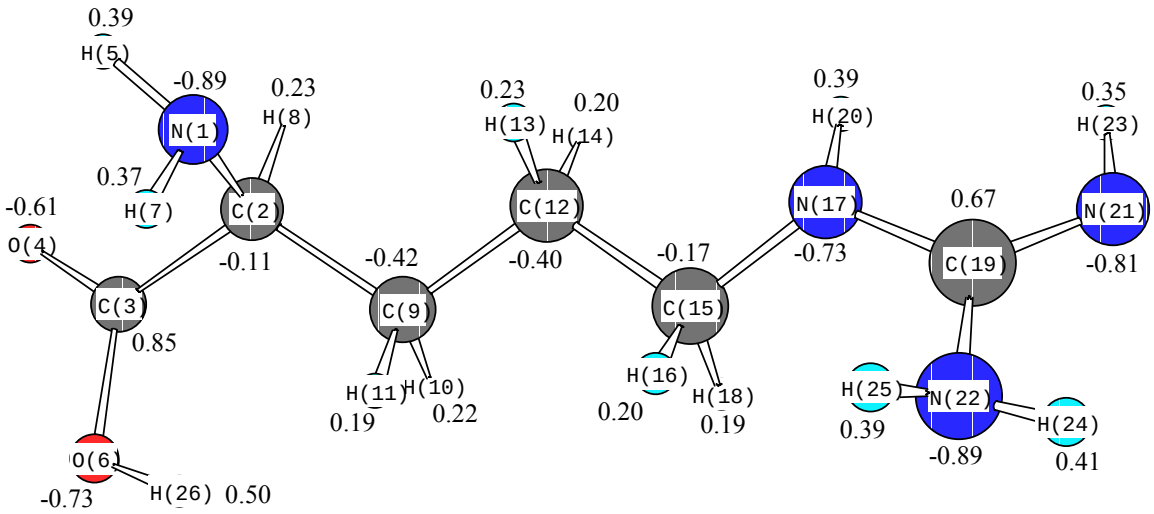

Neutral

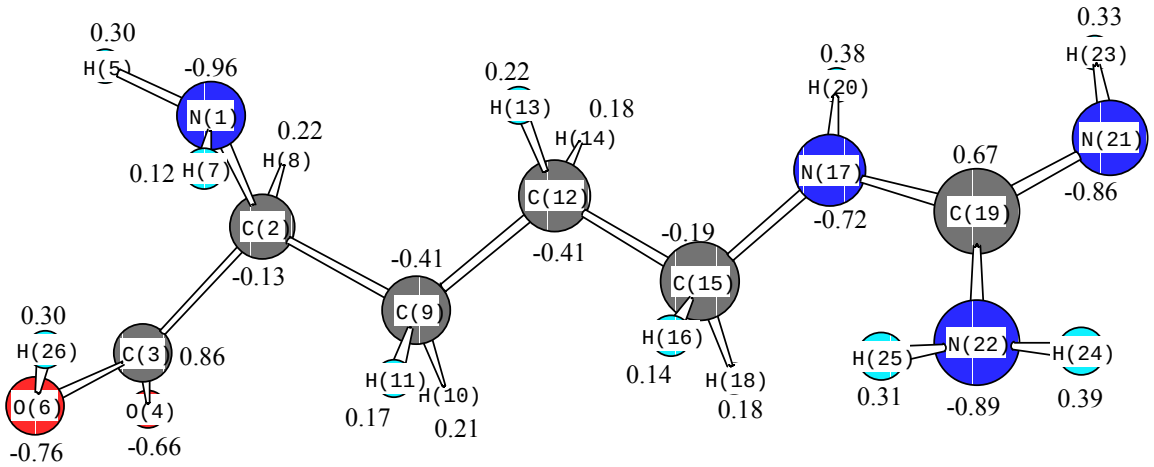

Anion

R9

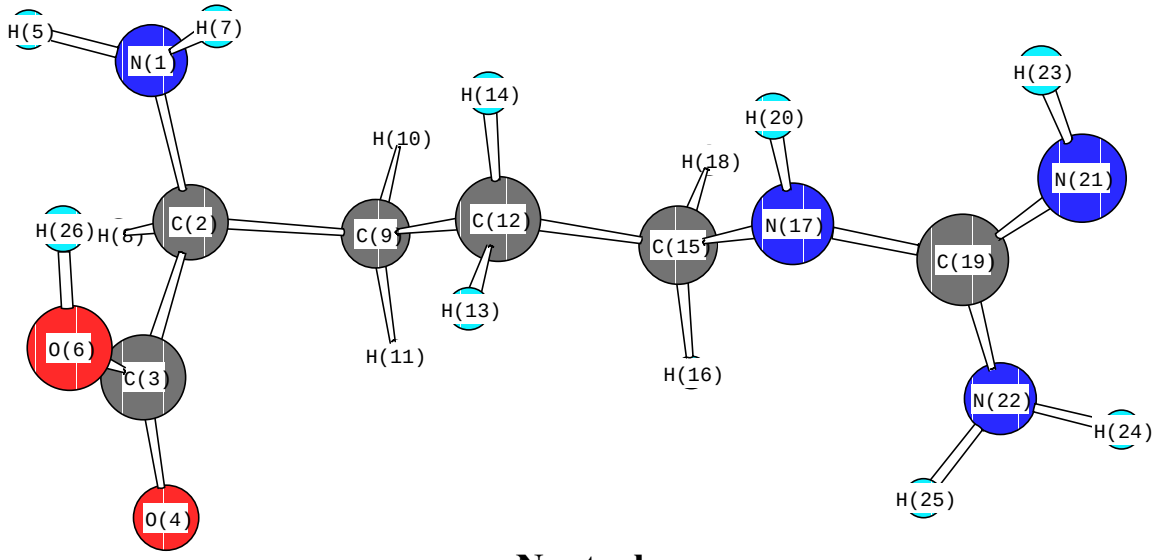

Neutral

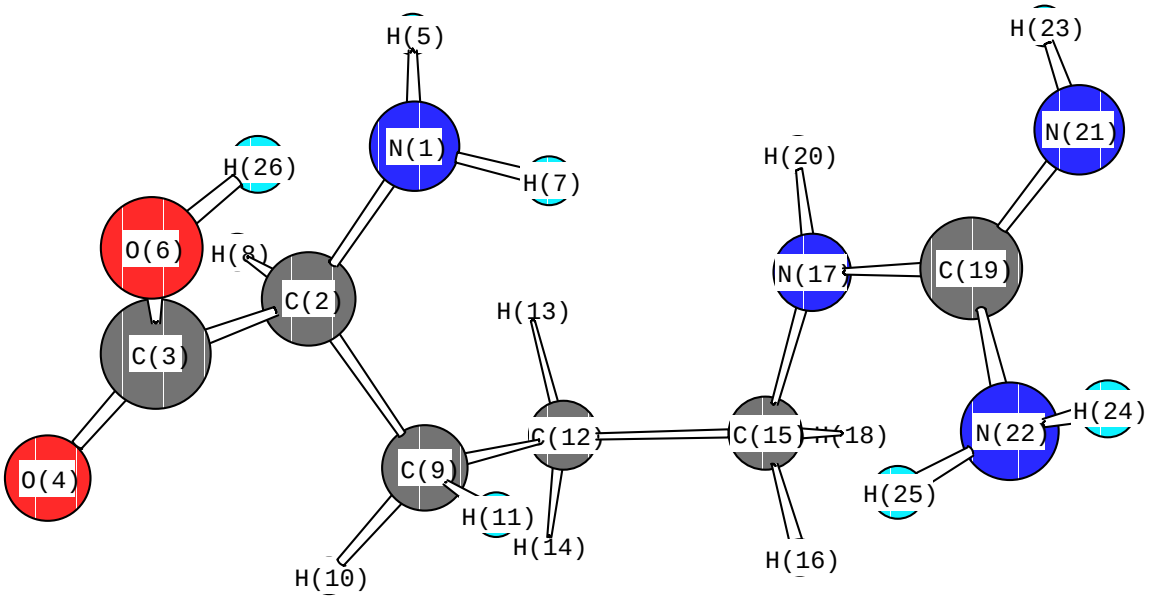

Anion

Q1

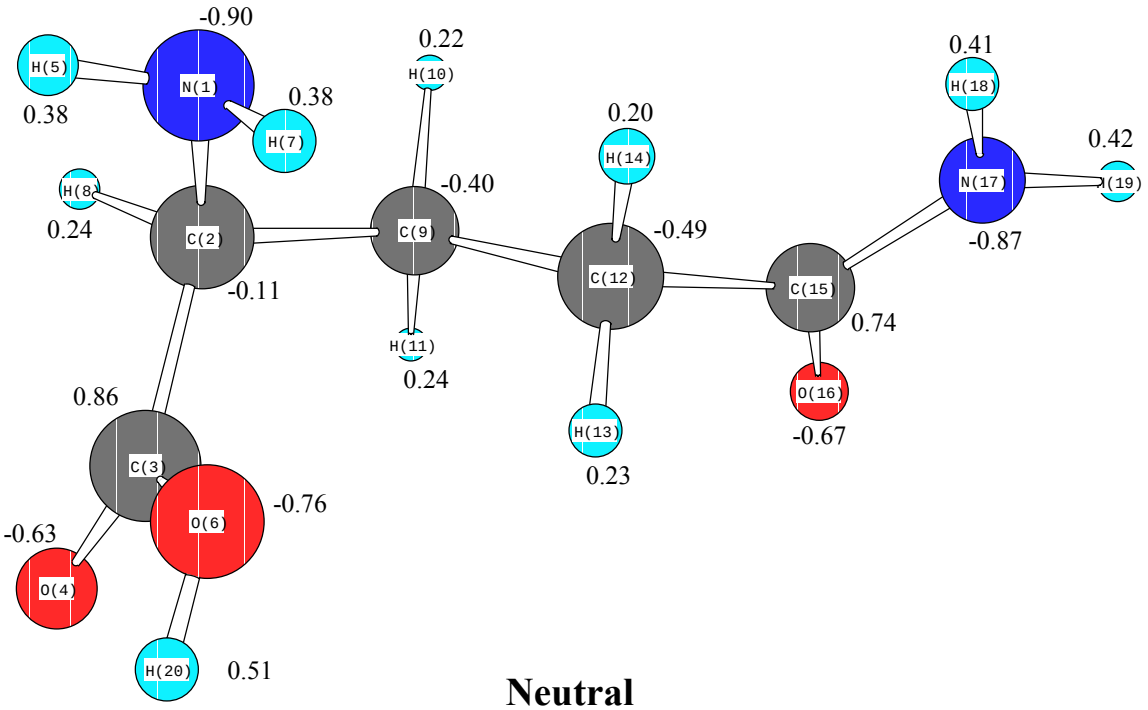

Neutral

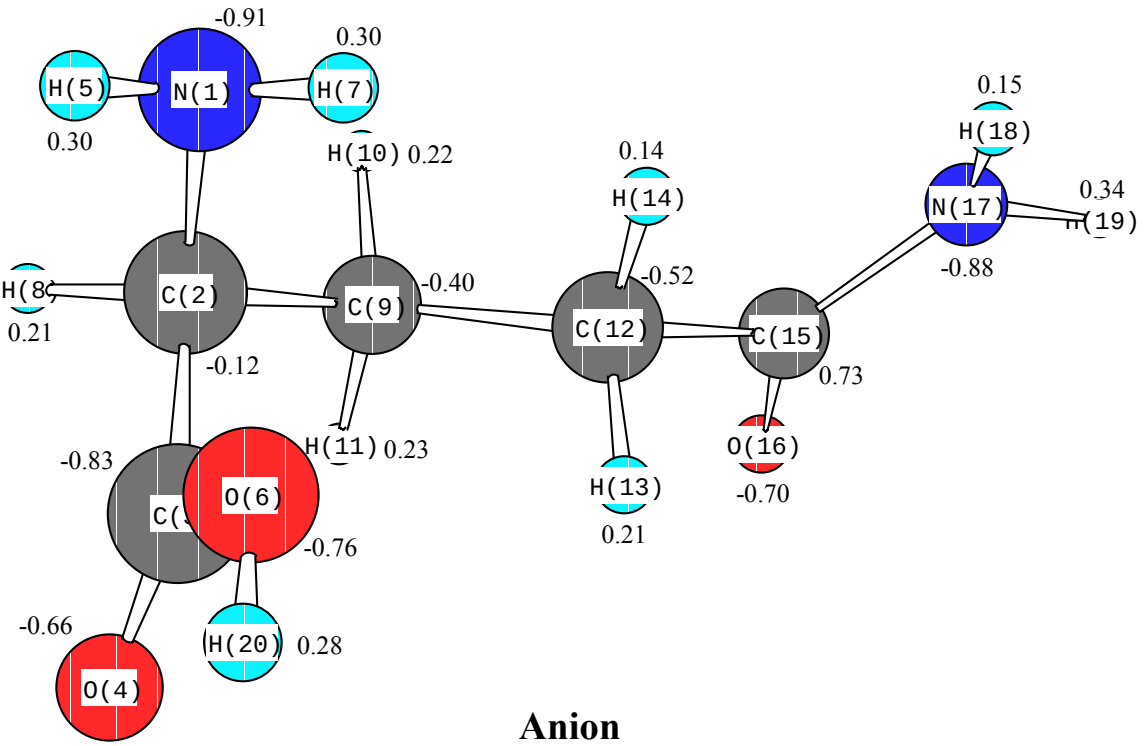

Anion

Q2

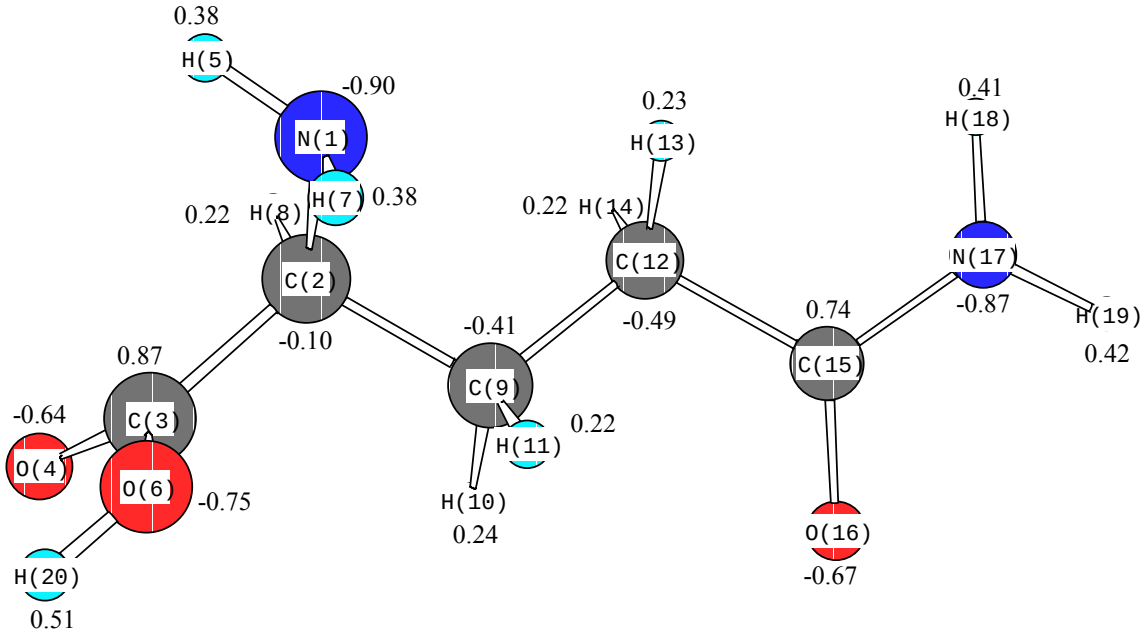

Neutral

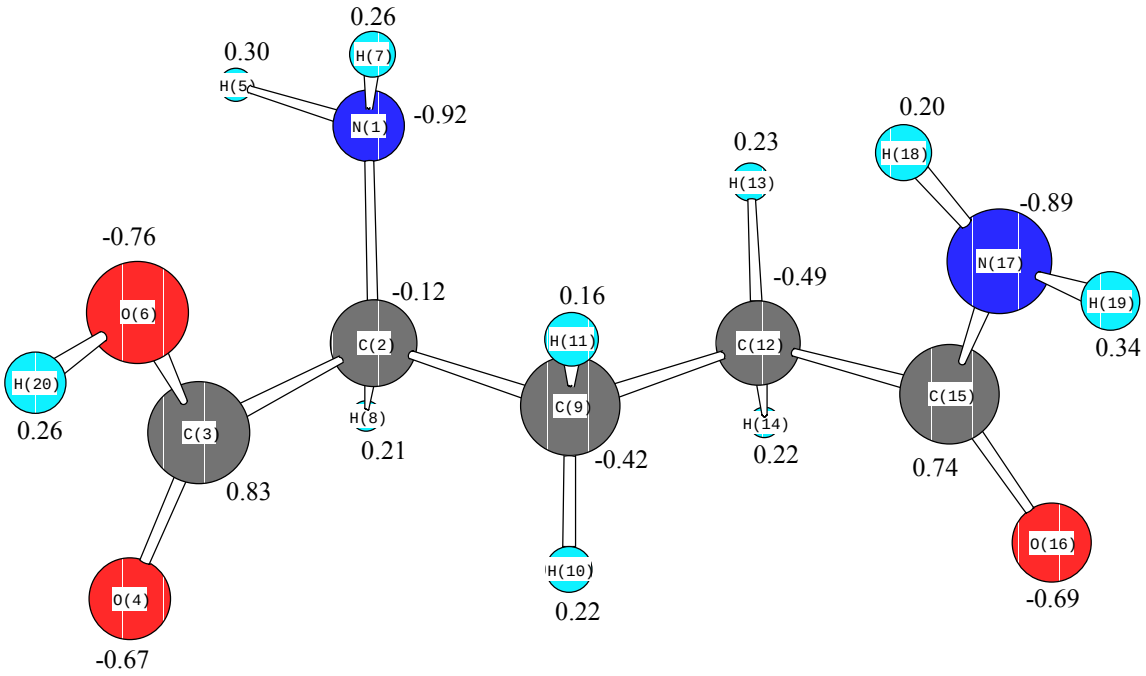

Anion

Q3

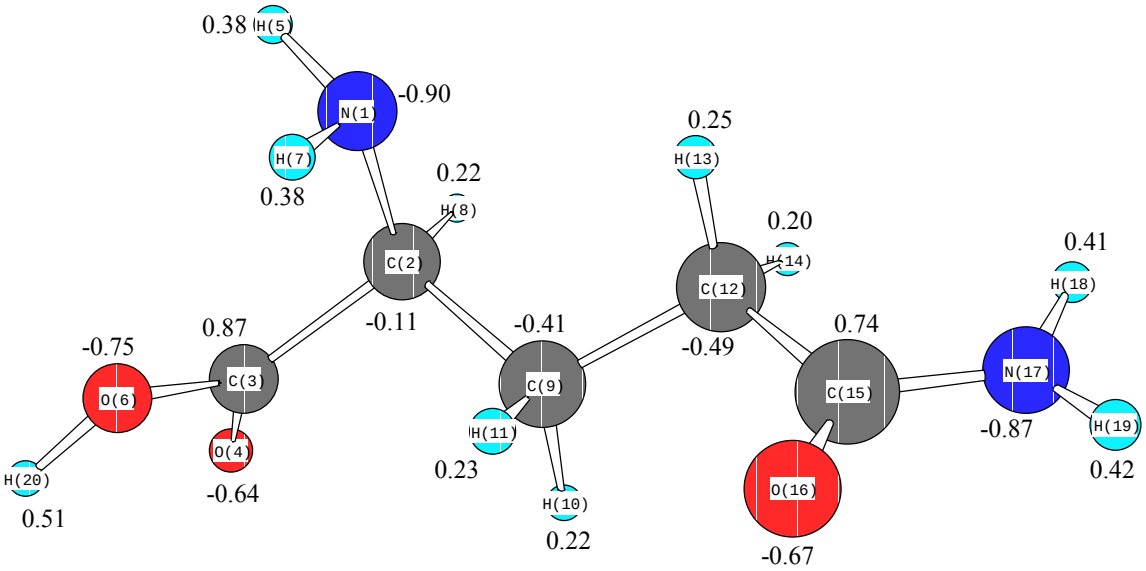

Neutral

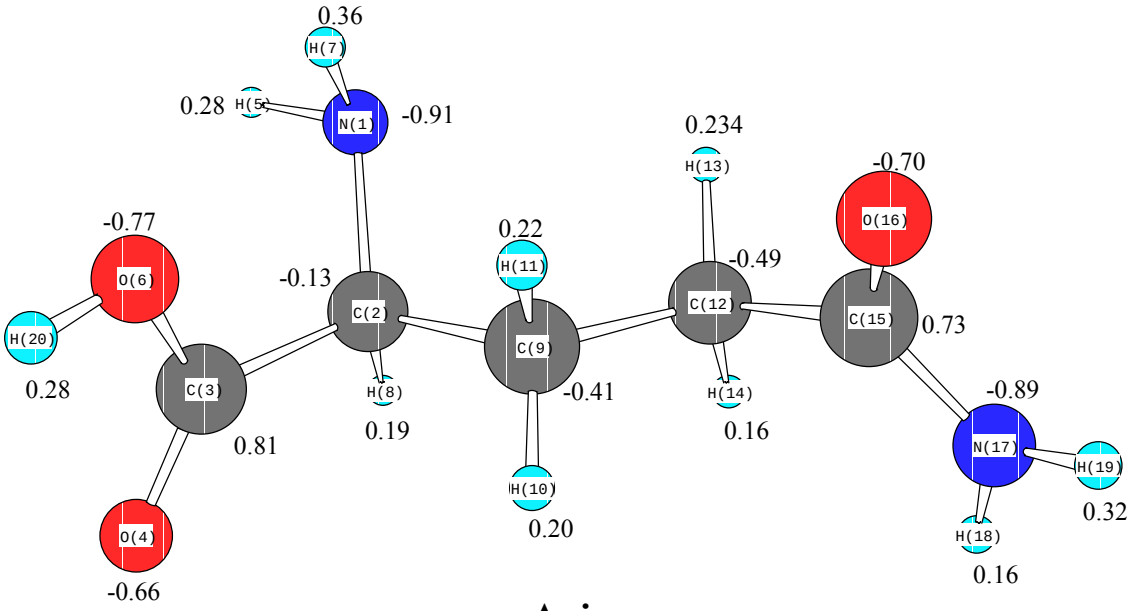

Anion

Q4

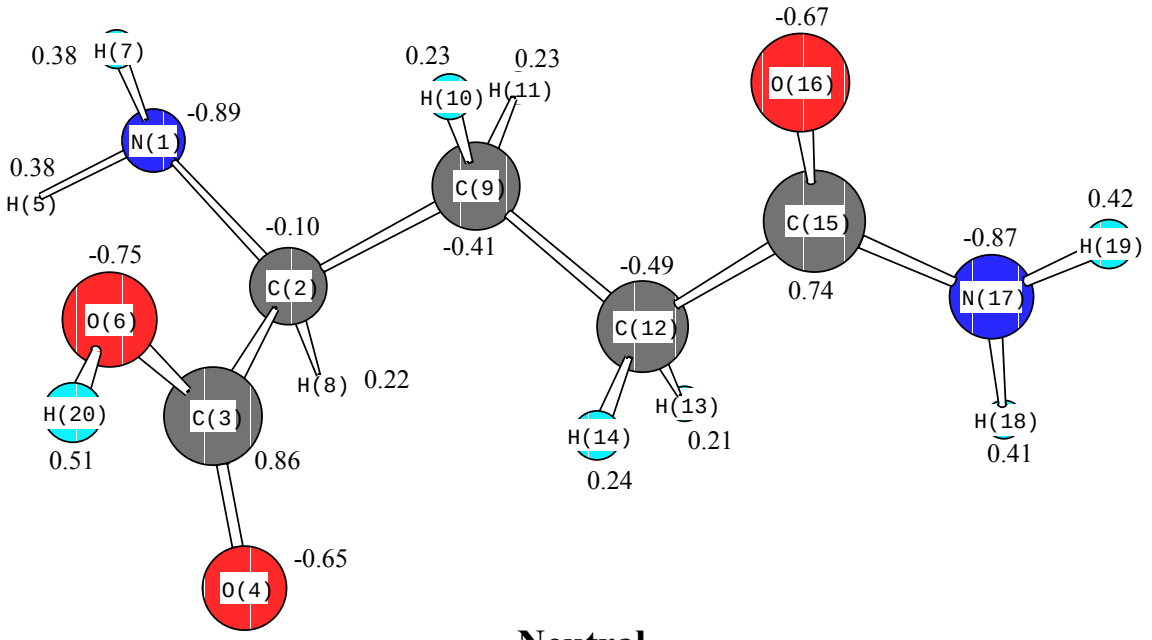

Neutral

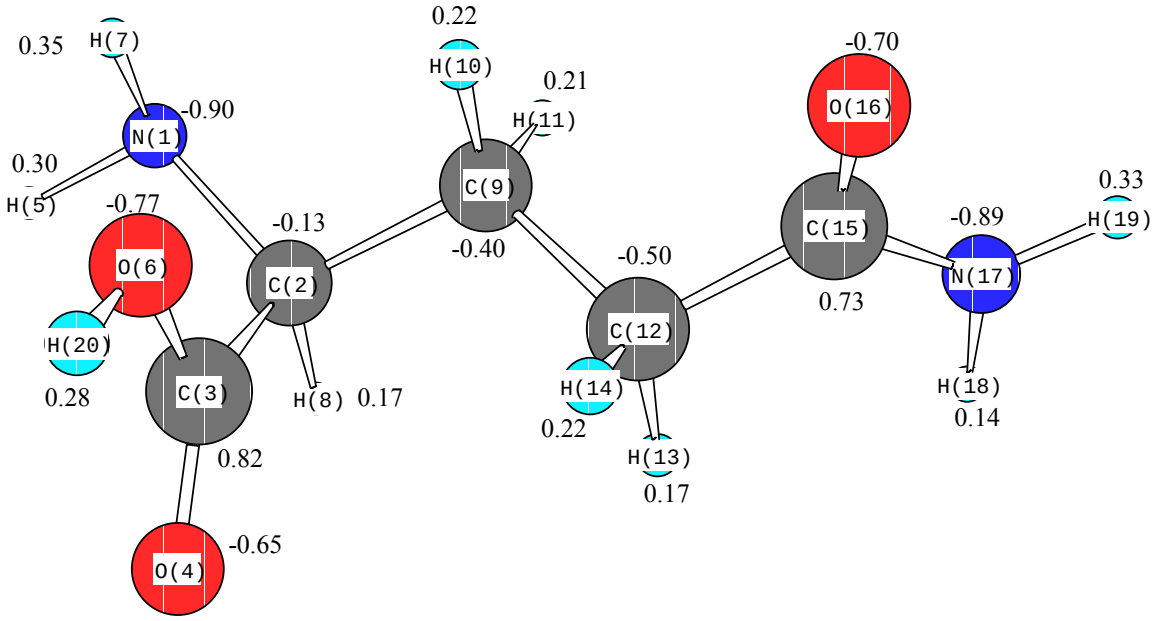

Anion

Q5

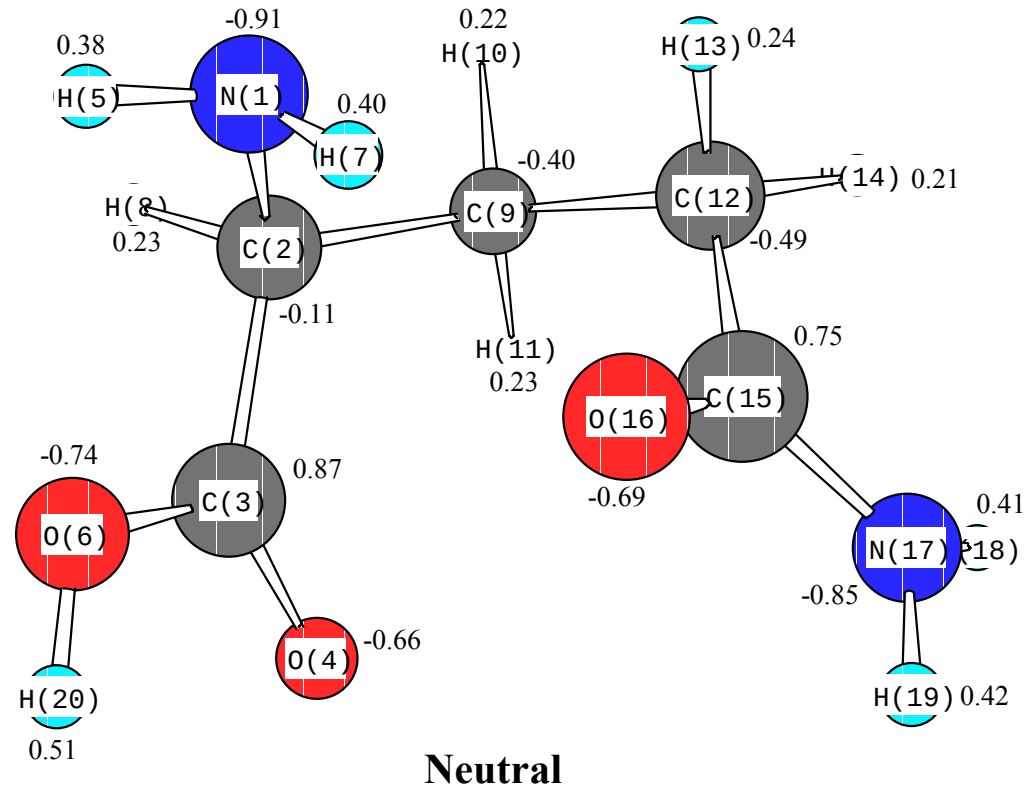

Neutral

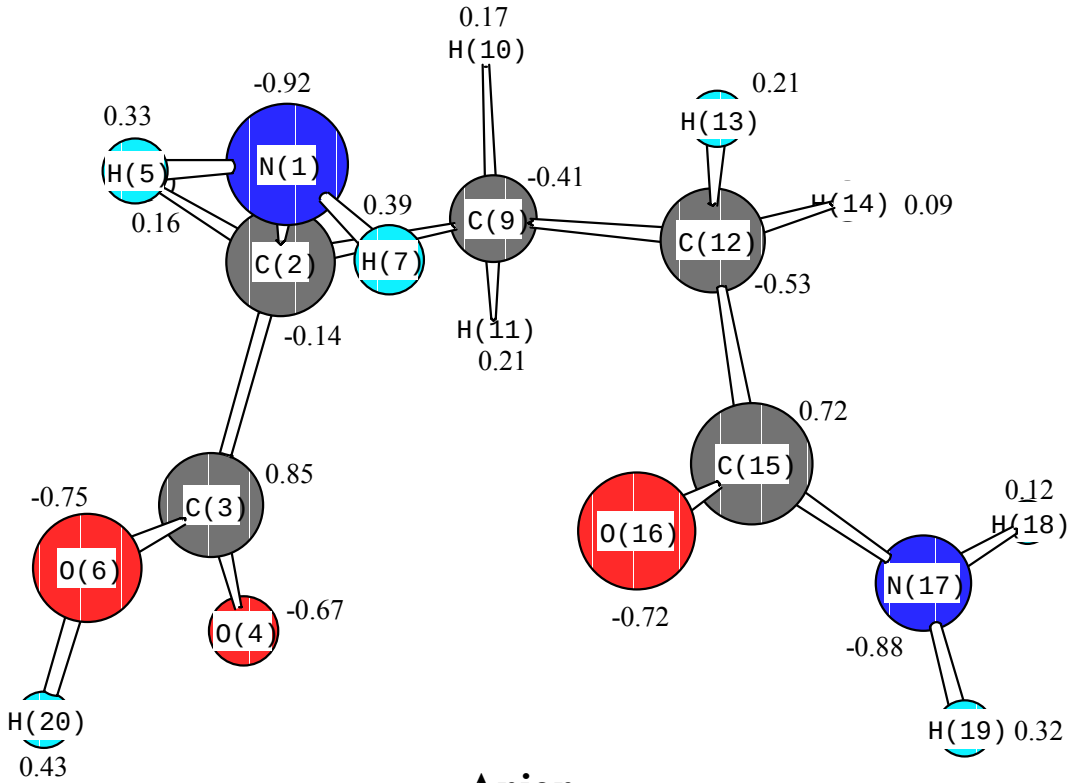

Anion

Q6

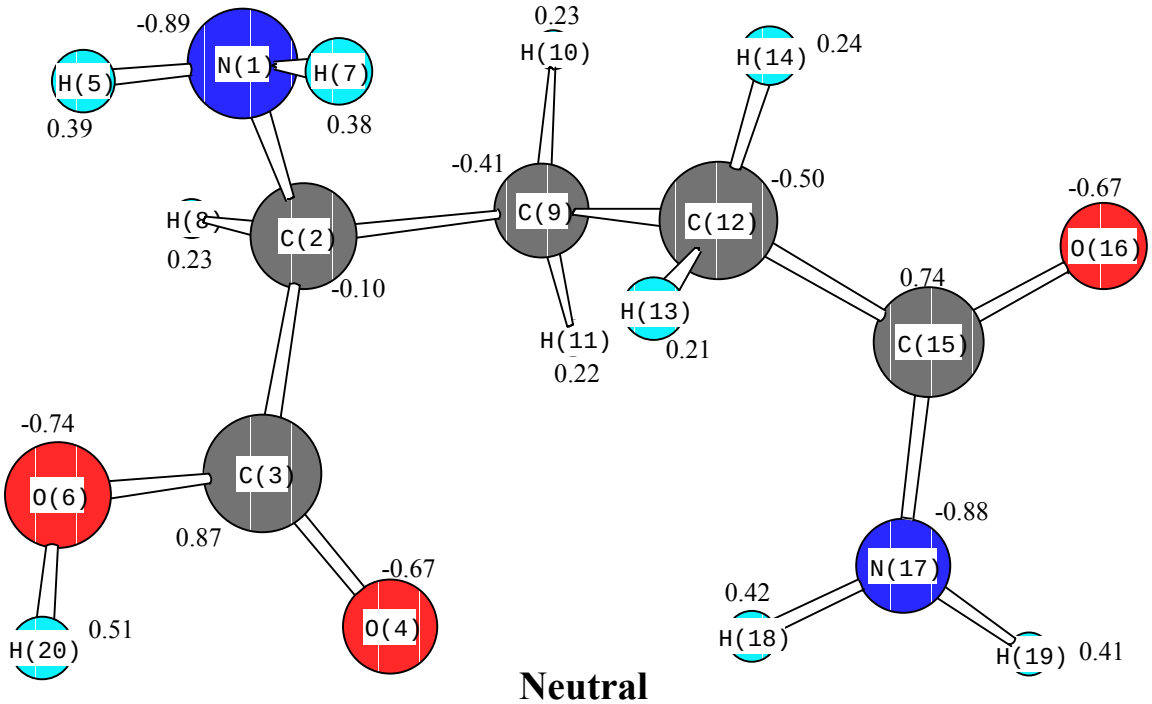

Neutral

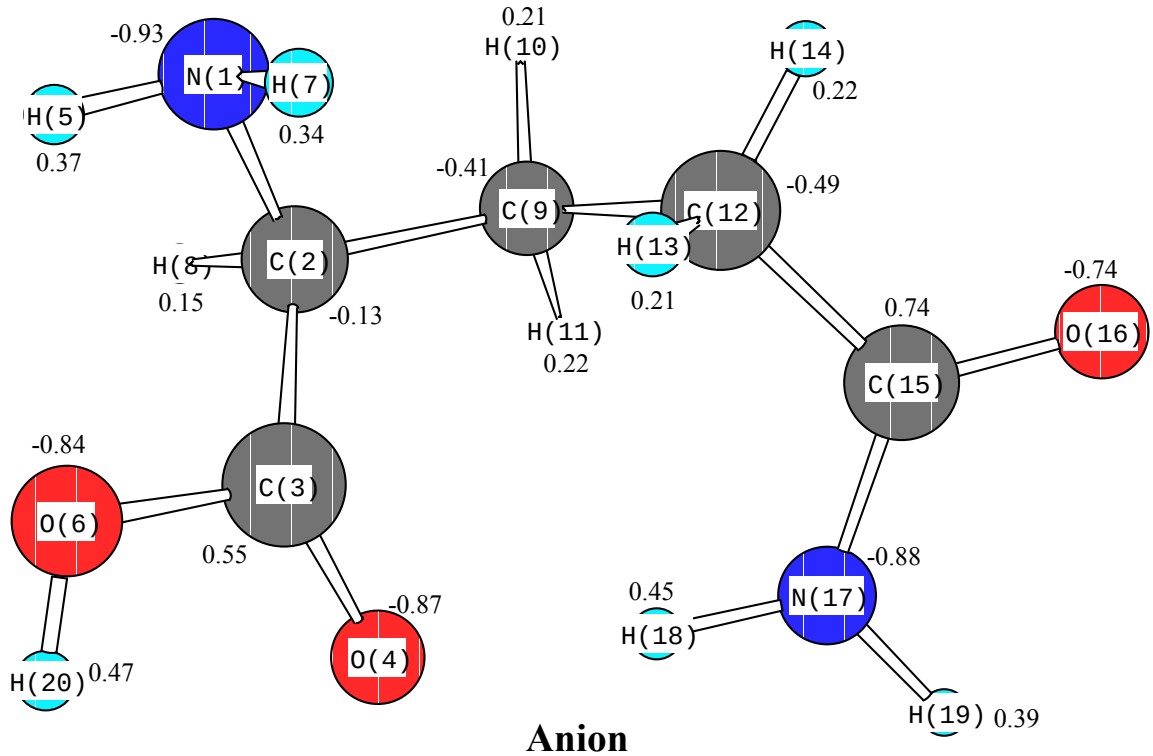

Anion

REFERENCES:

1. Alberts, B.; Bray, D.; Lewis, J.; Raff, M.; Roberts, K. & Watson, J.D. "Molecular Biology of the Cell" (Third Edition, Garland Publishing, New York & London, 1994).
2. Jahn, R., Südhof, T.C. *Annu. Rev. Biochem.* **68,** 863-911 (1999).
3. McNew, J.A., Parlati, F., Fukuda, R., Johnston, R.J., Paz, K., Paumet, F., Sollner, T.H. & Rothman, J.E. *Nature* **407,** 153-159 (2000).
4. Parlati, F. McNew, J.A., Fukuda, R., Miller, R. Sollner, T.H. & Rothman, J.E. *Nature* **407,** 194-197 (2000).
5. Fukuda, R., McNew, J.A., Weber, T., Parlati, F., Engel, T., Nickel, W., Rothman, J.E. & Sollner, T.H. *Nature* **407,** 198-202 (2000).
6. Ryan, T.A., Smith, S.J., & Reuter, H. *Proc. Natl. Acad. Sci. USA*. **93,** 5567-5571.
7. Ryan, T.A., J. *Neuroscience* **19,** 1317-1323 (1999).
8. Connor, V.O., Heuss, C., De Bello, W.M., Dresbach, T., Charlton, M.P., Hunt, J.H., Pellegrini, L.L., Hodel, A., Burger, M.M., Betz, H., Augustine, G.J., & Schafer, T. *Proc. Natl. Acad. Sci. USA* **94**, 12186-12191 (1997).
9. Rowe, J., Corradi, N., Malosio, M.L., Taverna, E., Halban, P., Meldolesi, J., & Rosa, P. *Journal of Cell Science* **112,** 1865-1877 (1999).
10. Huang, X., Wheeler, M.B., Kang, Y.H., Sheu, L., Lukacs, G.L., Trimble, W.S., & Gaisano, H.Y. *Molecular Endocrinology* **12**, 1060-1070 (1998)
11. Scales, S.J.; Yoo, B.Y. & Scheller, R.H. *Proc. Natl. Acad. Sci. USA* **98,** 14262-14267 (2001).
12. Pfeffer, S.R. *Nature Cell Biology* **1,** E17-E22 (1999).
13. Langley, K. & Grant, N.J. *Neurochem. Int.* **31,** 739-757 (1997).
14. Bennett, M.K. & Scheller, R.H. *Proc. Natl. Acad. Sci. USA* **90,** 2559-63 (1993).
15. Ferro-Novick, S. & Jahn, R. *Nature* **370,** 191-93 (1994).
16. Russell, J.S., "Report on Waves", report of the XlVth meeting of the British Association for the Advancement of Science, York, Sept. 1844 (London, 1845), pp.311-390.
17. Davydov, A.S. *J. Theor. Biol.* **66,** 559-569 (1973).
18. Scott, A., *Physics Reports-Review Section of Physics Letters* **217,** 1-67 (1992).

19. Forner, W. *J. Mol. Model.* **3**, 78-116 (1997).
20. Tao J.S. & Frankel A.D. *Biochemistry* **35**, 2229-2238 (1996).
21. Galetich, I., Stepanian, S.G., Shelkovsky, V., Kosevich, M., Blagoi, Y.P. & Adamowicz, L. *J. Phys. Chem. A*. **104**, 8965-8971 (2000).
22. Escher, D., Bodmer-Glavas, M., Barberis, A. & Schaffner, W. *Molecular and Cellular Biology* **20**, 2774-2782 (2000).
23. Guha Thakurta, D. & Draper, D.E. *Journal of Molecular Biology* **295**, 569-580 (2000).
24. Matsushita, K. & Sugiura, Y. *Bioorganic & Medical Chemistry* **9**, 2259-2267 (2001).
25. Terreux, R., Pairot, S., Cabrol-Bass, D., Patino, N. & Condom, R. *Journal of Molecular Graphics & Modelling* **19**, 579 (2001).
26. Jones, S., Daley, D.T.A., Luscombe, N.M., Berman, H.M. & Thornton, J.M. *Nucleic Acids Research* **29**, 943-954 (2001).
27. Aboul-ela, F. & Varani, G. *Theochem-Journal of Molecular Structure* **423**, 29-39 (1998).
28. Nadassy, K., Wodak, S.J. & Janin, J. *Biochemistry* **38**, 1999-2017 (1999).
29. Allers, J. & Shamoo, Y. *Journal of Molecular Biology* **311**, 75-86 (2001).
30. Stickeler, E., Fraser, S.D., Honig, A., Chen, A.L., Berget, S.M. & Cooper, T.A. *Embo Journal* **20**, 3821-3830 (2001).
31. Field, C.J., Johnson, I. & Pratt, V.C. *Med. Sci. Sports. Exerc* **32**, 377-388 (2000).
32. Grimble, R.F. *Proceedings of the Nutrition Society* **60**, 389-397 (2001).
33. Rienstra-Kiracofe, J.C.; Tschumper, G.S.; Schaefer, H.F.; Nandi, S.; Ellison, G.B. *Chem. Rev.* **102**, 231 (2002).
34. Frisch, M.J.; Trucks, G.W.; Schlegel, H.B.; Gill, P.M.W.; Johnson, B.G.; Robb, M.A.; Cheeseman, J.R.; Keith, T.A.; Petersson, G.A.; Montgomery, J.A.; Raghavachari, K.; Al-Laham, M.A.; Zakrzewski, V.G.; Ortiz, J.V.; Foresman, J.B.; Cioslowski, J.; Stefanov, B.B.; Nanayakkara, A.; Challacombe, M.; Peng, C.Y.; Ayala, P.Y.; Chen, W.; Wong, M.W.; Andres, J.L.; Replogle, E.S.; Gomperts, R.; Martin, R.L.; Fox, D.J.; Binkley, J.S.; Defrees, D.J.; Baker, J.;

Stewart, J.P.; Head-Gordon, M.; Gonzalez, C.; Pople, J.A., GAUSSIAN 94, Revision C.3, Gaussian, Inc., Pittsburgh, PA, 1995.

35. Huzinaga, S. *J. Chem. Phys.* **42**, 1293 (1965).
36. Dunning, T.H. *J. Chem. Phys.* **55**, 2823 (1970).
37. Lee, T.J.; Schaefer, H.F., *J. Chem. Phys.* **83**, 1784 (1985)
38. Julian, R.R.; Beauchamp, J.L. & Goddard, W.A., *J. Phys. Chem. A* **106**, 32-34 (2002).
39. Skurski, P.; Gutowski, M.; Barrios, R. & Simons, *J., Chem. Phys. Lett.* **337**, 143-150 (2001).
40. Jockusch, R.A.; Price, W.D. & Williams, E.R., *J. Phys. Chem. A* **103**, 9266-9274 (1999).
41. Chapo, C.J.; Paul, J.B.; Provencal, R.A; Roth, K. & Saykally, R.J., *J. Am. Chem. Soc.* **120**, 12956-12957 (1998).
42. Price, W.D.; Jockusch, R.A. & Williams, E.R., *J. Am. Chem. Soc.* **119**, 11988-11989 (1997).
43. Aida, M., *Theochem.* **311**, 45-53 (1994).
44. Xu, J.Z., *Chaos, Solitons and Fractals*. **11**, 779-790 (2000).
45. Koetzle, T.F.; Frey, M.N.; Lehmann, M.S.; Hamilton, W.C., *Acta Crystallogr., Sect. B* **29** 2571 (1973).
46. Cochran, W.; Penfold, B.R., *Acta Crystallogr.* **5**, 644 (1952).
47. Ramirez, F.J.; Tunon, I.; Silla, E., *J. Phys. Chem. B* **102**, 6290-6298 (1998).
48. Wagner, A.; Luger, P., *J. Mol. Struc.* **595**, 39-46 (2001).

CHAPTER 5

CONCLUSIONS

As my work demonstrates, the DFT methods, when used in conjunction with conventional *ab-initio* methods, can be very powerful tool in predicting molecular structures and energies. For example, our DFT method predicts the experimental results within an absolute error of only 0.01 Å bond distance and 0.06 eV in electron affinity with silicon hydrides where many of the experimental data are available (Si, SiH, SiH^-, SiH_2, SiH_3, SiH_4, Si_2, Si_2^-, Si_2H_4, Si_2H_6). For other molecules that contain Halogens like Bromine Fluorides and Dibromine Oxides, the theoretical methods is a great way to understand and perhaps guide the experimentalists because experimental data are scarce due to the compounds' volatility.

There are many interesting chemical problems to be solved, and the tools for solving them are getting better each day. Although current DFT methods, and conventional *ab-initio* methods cannot study large molecular systems that are significant to biology, the development of computational chemistry along with advancements in the computer industry are quite promising.